Stratocumulus Clouds

Robert Wood *

University of Washington, Seattle, WA, USA

ABSTRACT

This paper reviews the structural, organizational and climatological aspects of stratocumulus clouds and the physical processes controlling them. More of the Earth's surface is covered by stratocumulus clouds than by any other cloud type making them extremely important for Earth's energy balance, primarily through their reflection of solar radiation. They are generally thin clouds, typically occupying the upper few hundred meters of the planetary boundary layer (PBL), and they preferably occur in shallow PBLs that are readily coupled by turbulent mixing to the surface moisture supply. Thus, stratocumuli favor conditions of strong lower tropospheric static stability, large-scale subsidence, and a ready supply of surface moisture, and are therefore common over the cooler regions of subtropical and midlatitude oceans where their coverage can exceed 50% in the annual mean. The primary driver of turbulence in stratocumulus clouds is convective instability driven by the emission of thermal infrared radiation from near the cloud tops. Turbulence and evaporative cooling drives entrainment at the top of the stratocumulus-topped boundary layer (STBL) which is stronger than it would be in the absence of cloud, and this tends to result in a deepening of the STBL over time, which leads to thicker clouds. Although most stratocumulus clouds produce some drizzle through the collision-coalescence process, thicker clouds drizzle more readily, which can lead to changes in the dynamics of the STBL that favor increased mesoscale variability, stratification of the STBL, and in some cases cloud breakup. Most marine stratocumulus cloud systems are driven by a tight interplay between radiative cooling, precipitation formation, turbulence and entrainment. Non-drizzling stratocumulus clouds also break up as the STBL deepens and it becomes more difficult to maintain buoyant production of turbulence through the entire depth of the STBL. Stratocumulus cloud properties are also sensitive to the concentration of aerosol particles, which is the primarily determinant of the cloud droplet concentration. For a given cloud thickness, more polluted clouds tend to produce smaller cloud droplets which results in increased cloud albedo, reduced collision-coalescence rates and a suppression of drizzle. In addition, cloud droplet size also affects the timescale for evaporation-entrainment interactions and sedimentation rate, both of which can affect entrainment and therefore cloud dynamics. Aerosols are themselves also strongly modified by physical and chemical processes in stratocumuli, and these two-way interactions may be a key driver of aerosol concentrations over the remote oceans. Aerosol-stratocumulus interactions is therefore one of the most challenging frontiers in cloud-climate research. Low cloud feedbacks are also a primary driver of uncertainty in future climate prediction because even small changes in cloud coverage and thickness have a significant impact on the radiation budget. A better understing of stratocumulus dynamics, particularly entrainment processes and mesoscale variability, will be required to contrain these feedbacks.

1. Introduction

Stratocumulus, from the latin *stratus* meaning "layer", and *cumulus* meaning "heap", is a genus of low clouds comprised of an ensemble of individual convective elements that together assume a layered form. The layering is typically achieved through capping by a temperature inversion that is often strong and only tens of meters thick.

Stratocumulus clouds swathe enormous regions of the earth's surface and exhibit a multitudinous variety of structure on a wide range of spatial scales (Fig. 1). Stratocumulus clouds cover a approximately one fifth of the Earth's surface (23% of the ocean surface and 12% of the land surface), making them the dominant cloud type in terms of total area covered (Warren et al. 1986, 1988; Hahn and Warren 2007). Because of this, and because of their significant optical thickness (Hahn et al. 2001) stratocumuli reflect a considerable amount of incoming solar radiation (Chen et al. 2000). Because they reside close to the earth's surface they exert a relatively small effect upon the top of atmosphere longwave radiation, with the result being a strong overall net radiative effect and a significant impact upon the Earth's radiative balance (e.g. Stephens and Greenwald 1991; Hartmann et al. 1992). Thus, only small changes in the coverage and thickness of stratocumulus clouds would be required to produce a radiative effect comparable to those associated with increasing greenhouse gases (Ran-

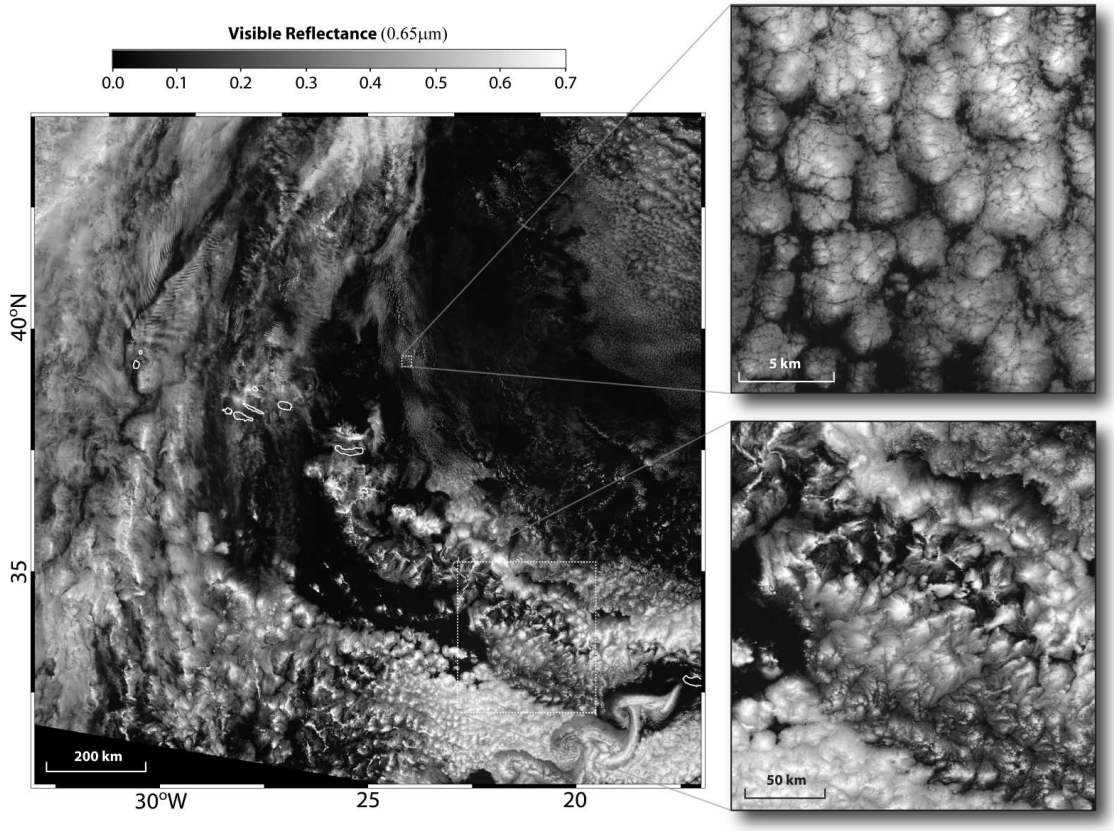

FIG. 1. Satellite imagery demonstrating the tremendous wealth of form for stratocumulus clouds on the mesoscale. This main panel shows a 250 m resolution visible reflectance image ($\lambda = 0.65$ μm) taken on April 7th 2001 at 12:35 UTC using the Moderate Resolution Imaging Spectroradiometer (MODIS) over the northeast Atlantic Ocean (note the Azores and Canary Islands). The inset to the upper right shows a higher resolution (15 m) visible image ($\lambda = 0.8$ μm) taken at approximately the same time using the Advanced Spaceborne Thermal Emission and Reflection Radiometer (ASTER) which has a resolution of 15 m. The inset to the lower right shows detail from the main image.

dall et al. 1984; Slingo 1990). Understanding why, where, when, and how stratocumuli form therefore constitutes a basal problem in the atmospheric sciences.

Stratocumuli occur beneath layers of the atmosphere with strong static stability (Klein and Hartmann 1993). The clouds themselves, through strong longwave cooling at the cloud top, help to enhance, maintain, and sharpen the stability profile locally with the result that in regions of persistent stratocumulus the temperature jump across the inversion can be as strong as 10-20 K in just a few vertical meters (Riehl et al. 1951; Riehl and Malkus 1957; Neiburger et al. 1961; Roach et al. 1982). The longwave cooling also serves to generate instability within the cloud layer and is the primary driver of the overturning convective circulations which constitute the key dynamical elements of these clouds (Lilly 1968; Nicholls 1989). This convection helps to homogenize the cloud-containing layer, frequently couples this layer to the surface which is the source of moisture that maintains the cloud layer (e.g. Nicholls 1984; Bretherton and Wyant 1997), and controls the development of mesoscale organization (Shao and Randall 1996; Atkinson and Zhang 1996). The condensing moisture in the upward branches of the convective elements provides additional energy to the dynamic motions in the cloud (e.g Moeng et al. 1992). Thus, stratocumulus clouds are a key component of the planetary boundary layer and frequently exert first order effects upon its structure and evolution (Stevens 2005; Atkinson and Zhang 1996). Fig. 2 shows the key processes occurring in the stratocumulus-topped boundary layer.

The strong link between static stability and the formation of stratocumuli implies that there are strong large-scale meteorological controls upon these clouds, that is, they are tightly coupled with the general circulation in which they exist (Bretherton and Hartmann 2008). As demonstrated in Fig. 3, stratocumuli exist in abundance over the oceans in the downward branches of large scale atmospheric circulations such as the Hadley and Walker circulations (Schubert 1976; Randall 1980; Klein and Hartmann 1993), in the subsiding regions of midlatitude baroclinic systems (Norris et al. 1998; Norris and Klein 2000; Lau and Crane 1997; Klein and Jakob 1999; Field and Wood 2007), over the undisturbed polar regions (see e.g.

Hermann and Goody 1976; Warren et al. 1988; Klein and Hartmann 1993; Curry et al. 1996, and references therein), and over the oceans during cold-air outbreaks (Agee 1987; Klein and Hartmann 1993; Atkinson and Zhang 1996). Stratocumulus cloud radiative properties also depend upon their microphysical properties (Hansen and Travis 1974) which are impacted by variability in atmospheric aerosol (e.g. Twomey 1974, 1977; Brenguier et al. 2000b). This control of stratocumulus radiative properties by processes on scales ranging from the planetary scale to the droplet scale explains why these clouds are such a challenge to understand and to predict (Siebesma et al. 2004; Zhang and coauthors 2005). Indeed, uncertainties surrounding their behavior thwarts accurate prediction of future climate change (e.g. Wyant et al. 2006; Bony et al. 2006; IPCC 2007).

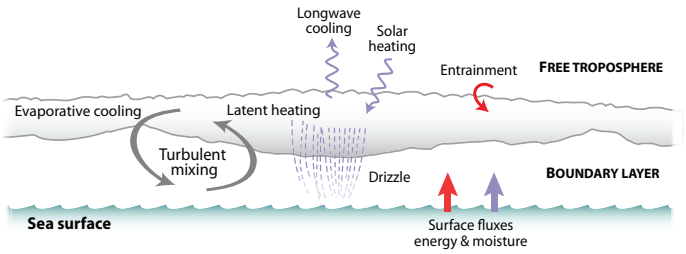

FIG. 2. Schematic showing the key processes occurring in the stratocumulus-topped boundary layer.

As Fig. 1 visually demonstrates, it is rather meaningless, and certainly not practically useful, to conceive of a single stratocumulus cloud. Instead, these clouds must be treated, both in the imagination and for practical purposes, as an ensemble of interacting convective elements which together form a *stratocumulus cloud system*. The convection is turbulent in nature; as we shall see, the variety of structural forms that stratocumuli exhibit (particularly on mesoscales) betrays the key processes that organize the turbulent dynamics of these clouds.

Our current knowledge of stratocumulus clouds has been built up from critical observational studies which have informed theory and allowed us to build a hierarchy of models to explain their behavior and to present new hypotheses for observational studies to test. Many studies have focused upon clouds over the ocean as 80% of the world's stratocumulus clouds are located there (Warren et al. 1986, 1988). Increasingly, the focus of both observational and modeling research into stratocumulus clouds has centered upon their role in the climate system and how these clouds may change in response to increases in greenhouse gases (e.g. Bony and Dufresne 2005) and changes in the anthropogenic contribution to aerosol loading (see Lohmann and Feichter 2005, for a recent review). This increasingly necessitates observational programs that can couple the small scale processes critical to cloud formation with the large scale meteorology associated with the atmospheric general circulation. This review seeks to summarize our current state of knowledge about stratocumulus clouds with a focus upon the challenges that we face in understanding their role in the climate system.

This review is organized as follows. Section 2 considers the scales of organization of stratocumulus. Section 3 describes the nature of the stratocumulus-topped boundary layer (STBL) including its vertical structure, dynamics, and entrainment. Section 4 discusses the formation, maintenance and dissipation of stratocumulus clouds. Section 5 gives an overview of the climatology of stratocumulus, including its variability on seasonal, synoptic, interannual and diurnal timescales. Section 6 discusses the key processes controlling stratocumulus. Section 7 details some of the key microphysical properties and processes in stratocumulus.

2. Scales of organization

As Fig. 1 clearly shows, and as one might argue is behavior becoming of high Reynolds number flows, the range of spatial scales that stratocumulus cloud systems span is dramatic. Although not always the case, scalar conserved variables and other scalar fields in the subtropical marine STBL exhibit power law scaling extending from the smallest measureable scales (the "inner" scale, typically on the order of millimeters) out to scales that are generally in the range 5-100 km (Nucciarone and Young 1991; Wood et al. 2002b) or timescales of several hours or more (Wood and Taylor 2001) for stationary observations (the "outer" scale). Such scalar signatures are imprinted on the cloud liquid water or cloud optical thickness field which shows consistent scaling (Cahalan and Snider 1989; Cahalan et al. 1994; Davis et al. 1996, 1999; Wood and Taylor 2001; Wood et al. 2002b; Wood and Hartmann 2006). In general, over the scaling range the variance increases with increasing spatial scale as $\sigma_{scalar} \approx \alpha L^{\beta}$ with β equal to roughly 1/3 and α being larger for deeper STBLs Wood et al. (2002b). This is consistent with Kolmogorov scaling of the scalar field, which is remarkable given that this scaling law was derived for homogeneous isotropic turbulence which clearly is not the case for scales larger than around 1 km in the STBL.

a. *Large eddy scale*

While the generally increasing variance with increasing scale for scalars in the STBL is also found in the horizontal wind components (Nucciarone and Young 1991), there is relatively little variance in the vertical wind component at scales significantly longer than the depth z_i of the STBL (Rothermel and Agee 1980; Nucciarone and Young 1991; de Roode et al. 2004). This dominant horizontal scale of the vertical motion field is generally referred to as the *large*

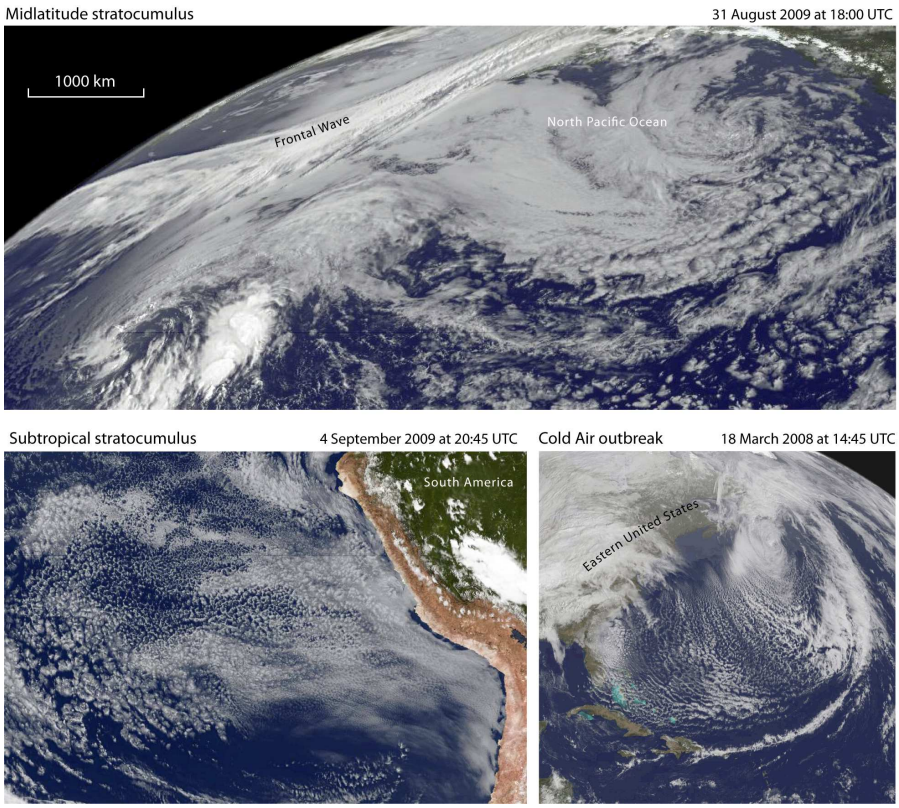

FIG. 3. Visible satellite imagery showing stratocumulus clouds in the midlatitudes, subtropics, and associated with a cold air outbreak. Data are from the Geostationary Operational Environmental Satellites (GOES), with times shown on the images. The scale is approximately the same in each of the images.

eddy scale, or sometimes the *energy-containing scale*, since much of the turbulent kinetic energy is concentrated here. For the STBL, it is useful to define those scales between the large eddy and the outer scale as the *mesoscale*.

One might imagine that with weak TKE variance in the mesoscale, the vertical transport of energy, moisture and momentum would be also confined to the large eddy scale, as appears to be the case for the clear convective boundary layer (de Roode et al. 2004). In the STBL, however, a signficiant fraction of the vertical transport can occur at mesoscales (de Roode et al. 2004; Faloona et al. 2005; Tjernstrom and Rune 2003). Problems with aircraft wind measurement drift and the high-pass filtering (the removal of information on scales longer than around 2-3 km is common) designed to remove these problems may have missed the mesoscale contribution to vertical transports in many studies. Clearly more work is needed to assess these contributions.

b. Mesoscale structure and organization

Because the outer scale is frequently similar to the typical lengths of aircraft flight legs used in research flights, it can be determined unequivocally in most cases only by using satellite data (e.g. Wood and Hartmann 2006), although there is some evidence from aircraft data that the outer scale is greater for deeper boundary layers (Davis et al. 1996; Wood and Hartmann 2006). This outer (or *characteristic*) scale is often associated with a clearly definable mesoscale cellular pattern in the cloud fields (see Wood and Hartmann 2006, for a discussion). For example, the visible radiance power spectrum (not shown) from the lower right panel in Fig. 1 has an outer scale of approximately 30 km, and visual inspection shows that this corresponds to the approximate diameters of the mesoscale cellular convective cells (see e.g. Atkinson and Zhang 1996, for a recent review of mesoscale cellular convection, or MCC).

Stratocumulus over the oceans may be grouped into four general mesoscale morphological types: (i) no cellularity on the mesoscale; (ii) organized closed cellular MCC; (iii) organized open cellular MCC; (iv) unorganized mesoscale cells. Figure 4 shows examples of these prevailing types. Broadly speaking, these types represent different stages of an airmass transition from shallow marine stratus to trade cumulus over the subtropical-tropical eastern oceans (Agee et al. 1973; Wood and Hartmann 2006). In many cases, the organization of marine stratocumulus may resemble a hybrid of these canonical mesoscale forms, e.g. actinoform clouds (Garay et al. 2004). There are no detailed studies

of stratocumulus mesoscale morphology over land, and visual inspection of satellite images suggests that well-defined mesoscale cellularity is not a common feature of terrestrial stratocumulus.

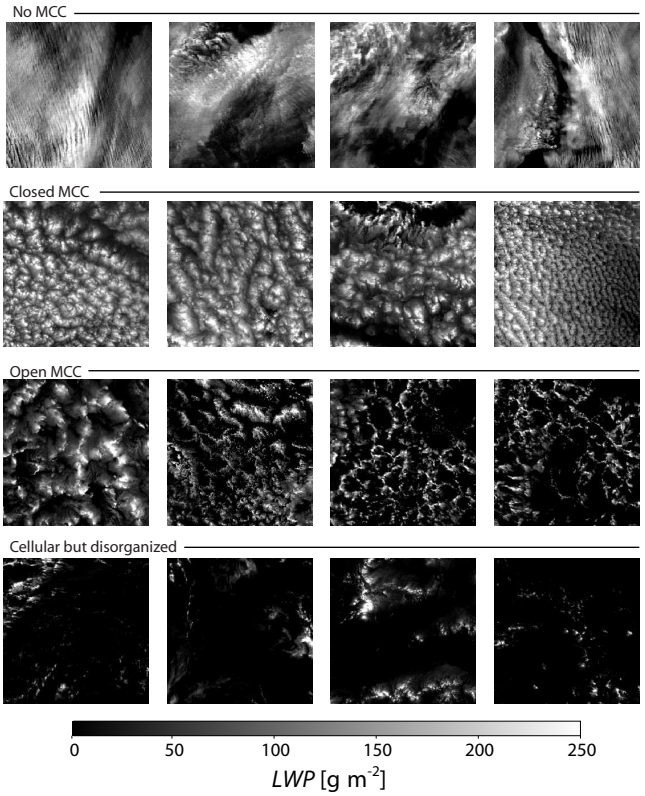

FIG. 4. Examples of different mesoscale structure types occurring in marine stratocumulus. Each image is 256×256 km in size and shows liquid water path estimated using the Moderate Resolution Imaging Spectroradiometer (MODIS). Note that visible reflectance imagery would look almost identical. Reproduced from Wood and Hartmann (2006), (c)American Meteorological Society. Reprinted with permission.

Horizontal cell diameters for standard Bénard-Rayleigh convection are typically of order the depth of the convecting layer. Aspect ratios for STBL cells are typically much larger (Agee et al. 1973; Agee 1987; Rothermel and Agee 1980; Moyer and Young 1994) with values from 3-40 reported in the literature (see review by Atkinson and Zhang 1996). Such "closed" MCC seems to be found primarily over oceans (Atkinson and Zhang 1996). Statistically, the outer scale for closed subtropical marine STBL cells scales well with the boundary layer depth (Wood and Hartmann 2006), although it is not yet clear whether such scaling is the case for STBLs in other meteorological regimes, or what the fundamental physics behind the scaling is.

Stratocumulus may also organize into roll-like structures on the large eddy-scale and particularly on the mesoscale (Atkinson and Zhang 1996), especially in cold-air outbreaks over lakes and oceans (Agee 1987). Roll formation in these cases often occurs prior to the formation of open and closed

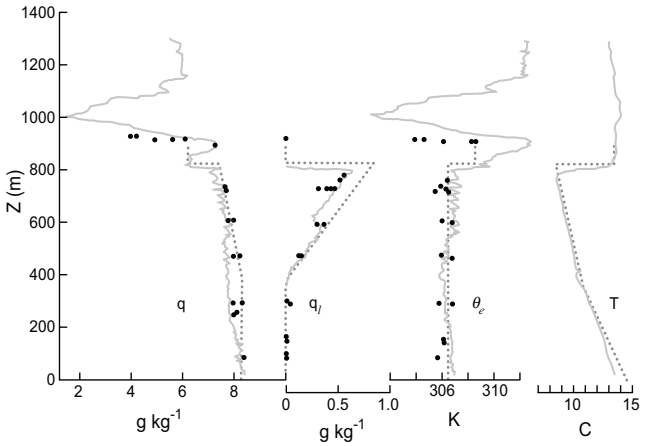

FIG. 5. Vertical profiles of water vapor q and liquid water q_l mixing ratios, equivalent potential temperature θ_e and temperature T for a summertime STBL observed over the North Sea to the east of a ridge. Means from horizontal legs are denoted by dots. The dotted lines in each case show the values expected for a well-mixed layer. Adapted from Nicholls (1984).

cellular structures that are more prevalent further downstream after the boundary layer has deepened (Walter 1980; Agee 1987; Young and Sikora 2003). Stratocumulus rolls generally form in cases with significant wind shear across the STBL (Atkinson and Zhang 1996). STBL rolls or bands in cold air outbreaks may have aspect ratios significantly larger than those typically found in clear boundary layers (Agee 1987). Rolls are not a particularly common feature of stratocumulus over the remote parts of the ocean other than to the north of the equatorial Pacific cold tongue.

For the marine STBL, the majority of the mesoscale variance in cloud liquid water path can be attributable to fluctuations in cloud base height, with cloud top height contributing only weakly (consistent with the visual picture we take away from Fig. 7) and only at scales larger than the typical characteristic scale (Wood and Taylor 2001). For continental stratocumulus, both cloud top and cloud base variations have been found to be important at regulating the cloud thickness on the mesoscale (Kim et al. 2005), which may reflect the typically weaker capping inversion associated with continental stratocumulus.

3. The stratocumulus-topped boundary layer (STBL)

Because stratocumulus clouds strongly modify the layer in which they reside, and because this layer is frequently connected to the earth's surface, our understanding of stratocumulus demands a corresponding understanding the processes governing boundary layer structure. Observational work carried out over the last half century or more has led to an understanding that the vertical and horizontal structure of stratocumulus clouds is very strongly coupled with the vertical thermodynamic structure of the boundary

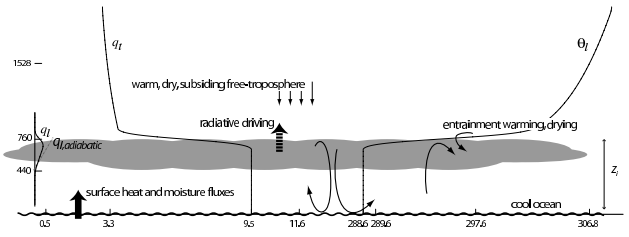

FIG. 6. Sketch showing the mean thermodyanmic structure observed during July 2001 over the subtropical northeast Pacific Ocean at 30°S,120°W. Liquid potential temperature, total water and liquid water mixing ratio profiles are shown, together with mean values immediately adjacent to the surface, within the STBL, and in the free-troposphere at 850 hPa. From Stevens et al. (2007). (c)American Meteorological Society. Reprinted with permission.

layer, particularly its depth (typically diagnosed as the inversion base height z_i) and vertical stratification (Albrecht et al. 1995b; Wood and Bretherton 2004; Wood and Hartmann 2006; Bretherton et al. 2010).

a. Mean vertical structure of the STBL

1) THERMODYNAMICS AND MEAN WINDS

In general the fractional coverage of low clouds is greatest when the boundary layer is moderately shallow ($0.5 < z_i < 1$ km), particularly over the subtropical and tropical oceans (Albrecht et al. 1995b; Wood and Hartmann 2006). Figure 5 shows an example of the vertical structure (Nicholls 1984) of a typical marine STBL that is 800 m deep and contains a thick layer (400 m) of unbroken stratocumulus. As is often the case with shallow STBLs, the layer is fairly well-mixed[1], with near-constant equivalent potential temperature θ_e through the STBL, a near dry adiabatic lapse rate below cloud, a moist adiabatic layer above cloud base, and a strong capping inversion that acts to spatially homogenize the cloud top height.

Other than very close to the ocean surface, horizontal winds in the well-mixed STBL are often close to constant with height, and sometimes significant jumps in the winds may occur across the inversion (Garratt 1992).

Figure 6 shows typical mean profiles for the STBL observed during the summertime in a region of persistent subtropical marine low cloud, which paint a very similar picture to that shown in Fig. 5. Figure 7 shows a photograph taken above this type of STBL which demonstrates the both the large scale horizontal homogeneity in the inversion/cloud top height and also the small-scale convective eddies that are responsible for much of the mixing in the well-mixed STBL.

As the STBL deepens beyond 1 km, which often occurs

[1]In this paper, the term *well-mixed* is used to refer to a boundary layer in which the turbulent mixing is sufficiently strong to maintain height-independent conserved variables

FIG. 7. Photograph of stratocumulus cloud top taken on a research flight over the subtropical northeast Pacific (30.4°N,122°W) on July 20, 2001. The photograph was taken shortly after noon from an altitude of 5 km, with the cloud tops at a height of 800 m. For reference, the horizontal distance across the base of the image is approximately 5 km. Photo courtesy of Gabor Vali.

FIG. 8. Photograph of stratocumulus with cumulus below within a decoupled STBL taken from a research ship over the tropical southeastern Pacific (20°S,85°W) on October 21, 2001. The photograph was taken two hours after sunrise. Photo courtesy of Sandra Yuter.

through the entrainment of free tropospheric air into the STBL, it becomes increasingly difficult for longwave and evaporative cooling at the top of the cloud to sustain mixing of the positively buoyant entrained air over the entire depth of the STBL (Bretherton and Wyant 1997). The STBL then begins to separate into two layers (Albrecht et al. 1995a; Bretherton and Pincus 1995; Bretherton et al. 1995; Wyant et al. 1997; Miller et al. 1998) with the upper (cloud) layer becoming somewhat decoupled from the surface moisture supply by a weakly stable interface. An example of a deeper STBL that has undergone decoupling is shown in Fig. 9. Within a decoupled STBL, the stratocumulus layer itself often exists within a mixed layer but the negatively buoyant eddies generated by longwave cooling are not able to reach the surface in this case. Meanwhile the layer immediately adjacent to the can be mixed

by buoyancy- and/or shear-generated mixing. Such a layer is termed the *surface mixed layer* (SML). Between the SML and the mixed layer there is often a layer which is conditionally unstable (see Fig. 9). Cumulus clouds often form at the top of the SML and act to intermittently and locally couple the stratocumulus layer with the surface, the stratocumulus deck can show breaks, and there is a greater degree of mesoscale variability, as illustrated in Fig. 8.

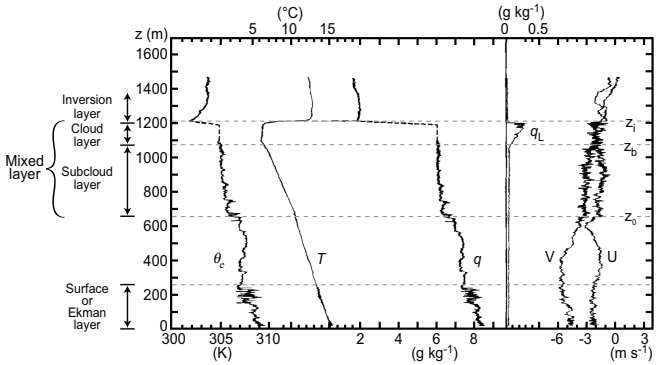

FIG. 9. Vertical profiles of water vapor q and liquid water q_l mixing ratios, equivalent potential temperature θ_e, temperature T, and easterly/northerly wind components (u and v) for a summertime STBL observed over the North Sea. Adapted from Nicholls and Leighton (1986).

Composite vertical profiles from different locations (Fig. 10) representative of different stages of the transition from a shallow well-mixed STBL to a deep, largely trade cumulus dominated boundary layer show increased stratification in conserved variables, and decreased cloud cover, as the boundary layer deepens. The decreased cloud cover is achieved through an increased frequency of cumulus clouds and a decreased frequency of stratocumulus clouds, although even for the regions with the deepest marine trade wind boundary layers low stratiform clouds constitute a significant fraction of the total cloud cover (Warren et al. 1988) (see also Section 5 below). Figure 11 shows a schematic of the vertical cloud and boundary layer structure associated with the different stages of this transition.

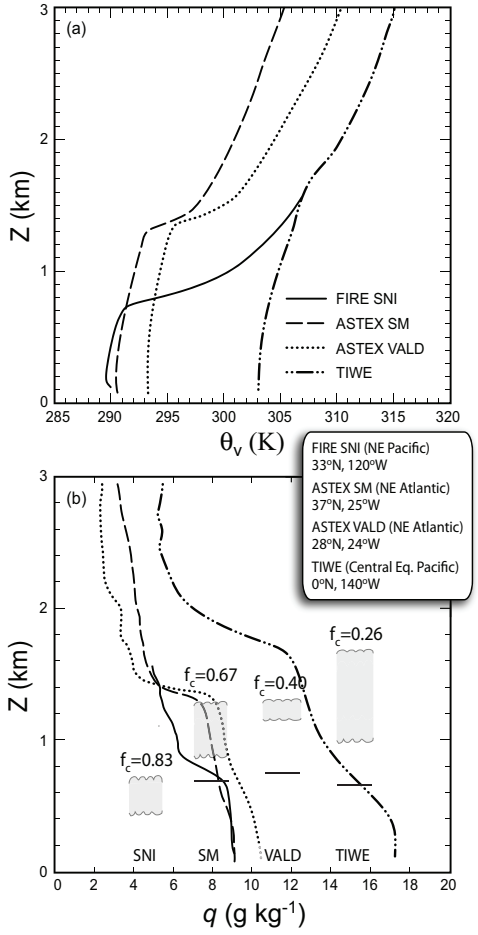

FIG. 10. Composite mean profiles of (a) virtual potential temperature θ_v; (b) water vapor mixing ratio from four marine field studies located in regions with distinctly different marine boundary layer characteristics: just off the Californian coast (San Nicholas Island, SNI); the subtropical/midlatitude eastern Atlantic (Santa Maria Island in the Azores, SM); the subtropical Atlantic (R/V *Valdivia*, VALD); the equatorial central Pacific (Tropical Instability and Waves Experiment, TIWE). See Albrecht et al. (1995b) for details of the locations. On panel (b) is indicated mean inversion base heights and cloud bases (indicated with cloud extent), lifting condensation levels (horizontal lines), and cloud cover f_c. Figure adapted from Fig. 2 and Table 2 of Albrecht et al. (1995b). Reproduced/modified by permission of American Geophysical Union.

2) LIQUID WATER

Because a cloud's liquid water content is a primary determinant of its optical properties (e.g. Stephens 1978a), it is a critical link between the cloud dynamics and the climate (see also Eqn. 9 and discussion in Section 6b below). The vertically integrated liquid water content (the liquid water *path*) is the product of the cloud thickness h and the mean liquid water content within the cloud. The latter is dependent upon the nature of the liquid water profile within the cloud layer. The rate at which liquid water increases with height is frequently quasi-linear and can approach that consistent with well-mixed conserved variables (Figs. 5 and 6). The well-mixed rate is often referred to as the *adiabatic* liquid water profile but would be more appropriately termed the *moist adiabatic* or *pseudo adiabatic* profile since latent heat release is fundamental in determining it. The moist adiabatic rate of increase of q_l with height is a function of the temperature and pressure only, with the dependence upon temperature dominant (see Albrecht et al. 1990, for the complete expression).

Observations from aircraft (Nicholls and Leighton 1986; Gerber 1996; Miles et al. 2000; Wood 2005a) and from surface-based remote sensing (Albrecht et al. 1990; Zuidema et al. 2005) suggest that stratiform boundary layer cloud

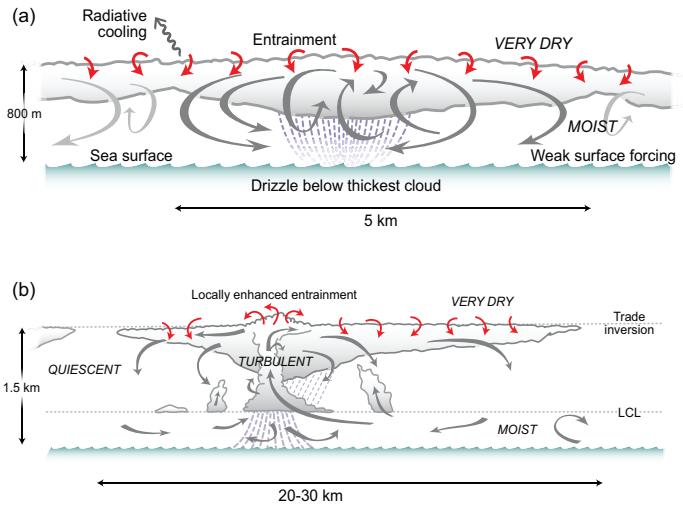

FIG. 11. Schematic showing structure of marine stratocumulus in (a) the shallow, well-mixed boundary layer; (b) deeper, cumulus-coupled boundary layers. Gray arrows indicate the primary motions on the scale of the boundary layer, while smaller red arrows indicate the small-scale entrainment mixing taking place at the inversion atop the layer. Vertical thermodynamic profiles associated with the two schematics are roughly represented by the (a) the FIRE SNI and (b) the ASTEX VALD profiles shown in Fig. 10.

layers frequently approach moist adiabatic. The degree of adiabaticity in a cloud layer can be quantified using the *adiabaticity* F_{ad}, defined as the ratio of the vertical integral of the liquid water content (i.e. the liquid water path) to that expected for a moist adiabatic layer with the equivalent cloud base and top (Slingo et al. 1982b; Albrecht et al. 1990; Wood 2005a). Given the sensitive nature of aircraft and surface remote sensing measurements of liquid water, it is often easier to detect stratification in the vertical thermodynamic profile using the adiabaticity than by examination of temperature or moisture profiles (Nicholls and Leighton 1986).

Significant deviations from the moist adiabatic liquid water profile are found close to the top of the cloud layer, where entrainment can play a significant role in evaporating droplets (e.g. Nicholls and Leighton 1986). In addition, several studies have found that during periods where the stratocumulus is precipitating (see Section XX) the cloud layer can become subadiabatic in nature (Austin et al. 1995; Gerber 1996; Miller et al. 1998; Wood 2005a; Zuidema et al. 2005), and when the drizzle is heavy the profile may exhibit no linearity at all (Nicholls and Leighton 1986; Gerber 1996).

Theory to quantify the effects of boundary fluxes (cloud base and entrainment) and precipitation on the adiabaticity is needed but is incomplete; an expression was presented in Nicholls and Leighton (1986) that adapted dry surface-driven boundary layer theory (Wyngaard and Brost 1984) in an attempt to relate deviations from $F_{ad} = 1$ to the entrainment rate, the jump in total water mixing ratio across the cloud top, and a mixing efficiency parameter. Nicholls and Leighton (1986) hypothesized that entrainment might explain the deviations of around 20% from F_{ad} seen in their observations. However, the mixing efficiency parameter is expected to depend upon the nature of the turbulent mixing process (Wyngaard and Brost 1984) which is still poorly understood in stratocumulus (see below), and so the hypothesis has not yet been tested. A more recent study (Wood 2005a) finds evidence that substantial departures of F_{ad} from unity appear to scale with the ratio of the timescales for moisture replenishment by turbulent fluxes to that for precipitation removal. Further, passive microwave radiometry also suggests that strongly-drizzling stratocumulus is subadiabatic (Zuidema et al. 2005). This adds additional complexity to the factors controlling liquid water path but is qualitatively consistent with the findings that in strongly precipitating stratocumulus the precipitation flux can significantly exceed the replenishment moisture flux (Austin et al. 1995).

b. *Turbulence and Dynamics*

The mean state of the STBL is determined by fluxes of energy, water (both vapor and liquid), and, more indirectly by other atmospheric constituents (e.g. aerosols). These fluxes are predominantly turbulent[2], which calls for analysis methods and theory that address this fundamental characteristic. The amount of energy associated with the turbulent components of the flow field, particularly in the vertical wind component, is critical for determining the rate of entrainment of free-tropospheric air into the cloud top from above, which plays a leading role in determining key aspects of the stratocumulus climatology (Lilly 1968; Bretherton and Wyant 1997; Stevens 2002).

For clear neutral boundary layers, similarity theory provides well-characterized scaling relations for turbulent kinetic energy (TKE) and turbulent fluxes as a function of the mean state. This is not the case for the STBL (Garratt 1992; Nieuwstadt and Duynkerke 1996) because of the complexity of the diabatic processes that shape it, and its often intermittently coupled nature (which is clearly evident even in composite profiles of mean values in Fig. 10). Thus, the existence of simple nondimensional scaling relationships for fluxes and variances within the STBL is not guaranteed in general (Nieuwstadt and Duynkerke 1996). Nevertheless, progress has been made towards understanding some of the most important statistical properties of the turbulent vertical motion field, and some useful approximate scaling relationships and useful nondimension-

[2]By turbulent, we are implying a flow that is inherently irreversible, diffusive, stochastic and multiscale in nature. An accessible primer on the general properties of turbulent flows is found in Tennekes and Lumley (1972). Useful reviews of STBL turbulent structure are found in Driedonks and Duynkerke (1989); Moeng et al. (1992).

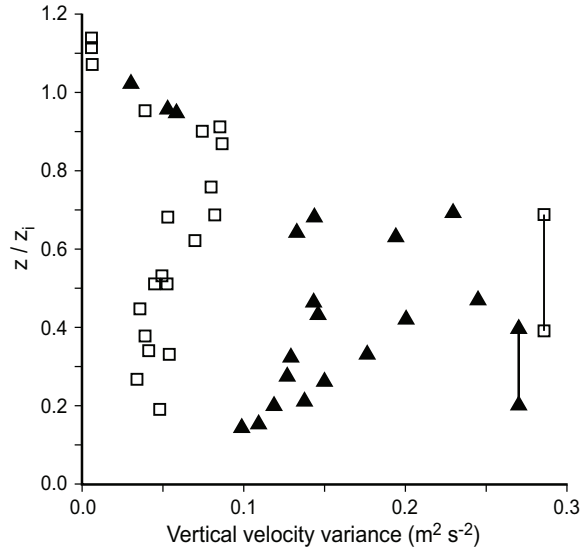

FIG. 12. Variance of the vertical wind against height normalized by the STBL depth around local noon (open squares) and for 9:30-midnight (filled triangles). Measurements were made from a tethered ballon at San Nicholas Island in unbroken Californian marine stratocumulus sheet during July 1987. The range of cloud base height for the two periods is denoted by the vertical lines. Reproduced from Hignett (1991). (c)American Meteorological Society. Reprinted with permission.

alizing variables have been found to be useful for relatively well-mixed STBLs. Many observations suggest that stratocumulus layers are often relatively well-mixed (Nicholls 1984; Nicholls and Leighton 1986; Caldwell et al. 2005), even though at times these layers may be only intermittently coupled with the underlying surface (Nicholls and Leighton 1986; Turton and Nicholls 1987).

1) Turbulent fluxes

The vertical structures of the vertical turbulent fluxes of energy and moisture are important for determining stratocumulus cloud thickness and therefore radiative properties (e.g. Schubert et al. 1979a; Bretherton and Wyant 1997). The most elegant description of the boundary layer fluxes that can be applied to the STBL is *mixed layer theory* (Lilly 1968) which describes the vertical structure of the vertical turbulent fluxes that are required to maintain a well-mixed layer given the various forcings applied to it.

In order for a layer to remain well mixed the vertical energy and moisture fluxes must be linear functions of height. For nonprecipitating mixed layers the vertical turbulent flux of total water must be linear with height. Since entrainment fluxes of dry air are often comparable to the surface moisture flux, the turbulent moisture flux can either increase or decrease with height. However, precpitation and even cloud droplet sedimentation are frequently important contributors to moisture transport (Brost et al. 1982b; Nicholls 1984; Duynkerke et al. 1995; de Roode and Duynkerke 1997; Wood 2005a). In the cloud layer itself the vertical turbulent flux of cloud liquid water can be an important contributor to the total water flux (Nicholls 1984; Duynkerke et al. 1995). It is unknown, but unlikely that *turbulent* transport of precipitation can be an important contributor to the overall moisture flux, although there is observational and modeling evidence that such transport is important for the formation of large drizzle drops (Nicholls 1987; Vali et al. 1998). It should be stressed that reliable and accurate estimates of the total water flux are difficult to establish from aircraft, partly due to measurement problems and partly because of sampling limitations caused by large horizontal lengthscales in convective boundary layers (Lenschow and Stankov 1986), a problem that is particularly acute for the STBL (de Roode et al. 2004).

Under most circumstances, the buoyancy flux [3] is the primary source of TKE in the STBL (Moeng et al. 1992; Bretherton and Wyant 1997) and nearly always has a maximum in the cloud layer (Nicholls and Leighton 1986; Garratt 1992), with smaller values in the subcloud layer. For mixed layers, there is be a sharp increase in the buoyancy flux above the cloud base due to latent heat release, and this jump is primarily determined by the turbulent moisture flux at cloud base (Bretherton and Wyant 1997). A consequence is that during the daytime, and in cases of less well-mixed STBLs, the buoyancy flux can be close to zero, or even negative, just below the stratocumulus cloud base (Nicholls and Leighton 1986). Substantially subzero buoyancy fluxes are a sink of turbulence and lead to layer decoupling (Turton and Nicholls 1987; Bretherton and Wyant 1997; Stevens 2000).

Vertical momentum transport in the STBL is important for setting the surface fluxes of moisture and temperature (Stevens et al. 2002). There are some observations of the STBL (e.g. Brost et al. 1982b) which are consistent with those expected under near-neutral conditions.

2) Vertical and horizontal wind fluctuations

Figure 12 shows measurements of the vertical structure of the vertical wind variance $\overline{w'^2}$ during the daytime and during the night, in a shallow (450-600 m deep) marine STBL. The horizontal scale of the energy-containing eddies (often termed the *large eddies*) is of the order of the depth of the STBL (see below). Both during the day and at night the strongest updrafts and downdrafts are found away from the boundaries and particularly in the upper half of the STBL consistent with the primary driver of the turbulence being longwave cooling near cloud top. The eddies are more vigorous during the night; buoyancy produc-

[3] The buoyancy flux is defined as $\overline{w'b'} = (g/\theta_v)\overline{w'\theta'_v}$, where g is the gravitational acceleration, θ_v is the virtual potential temperature, and w' is the vertical velocity fluctuation.

tion is greatest at this time because the stabilizing effect of shortwave absorption is absent (Hignett 1991). Typically, downdrafts in the STBL are smaller and stronger than updrafts (Nicholls 1989).

For shallow, relatively well-mixed STBLs, and for mixed layers forming part of a more decoupled STBL, the magnitude and vertical profile of $\overline{w'^2}$ scales fairly well with a convective velocity scale w_* defined using the vertical integral over the mixed layer depth h of the buoyancy flux (see Deardorff 1980b):

$$w_*^3 = 2.5 \int_0^h (g/\theta_v)\overline{w'\theta_v'}dz. \quad (1)$$

Observations show that $\overline{w'^2}/w_*^2$ tends to maximize at values of 0.3-0.5 in the upper quarter of the mixed layer (Nicholls and Leighton 1986; Nicholls 1989; Garratt 1992; Nieuwstadt and Duynkerke 1996; de Roode and Duynkerke 1997), and decreases sharply toward the cloud top and more gradually toward the mixed layer base. The magnitude of w_* is controlled by the key buoyancy-influencing processes in the mixed layer, most importantly the radiative cooling/warming at cloud top, latent cooling/warming in convective downdrafts/updrafts, the mixing down of stable entrained air, and precipitation. Thus, mixing in most stratocumulus cloud systems is primarily driven by buoyancy. However, in some cases, particularly in regions with strong horizontal gradients in boundary layer depth, vertical shear in the horizontal winds can also influence $\overline{w'^2}$ (Brost et al. 1982a,b; Nicholls and Leighton 1986; Wang et al. 2008). Values of w_* in the range 0.25-1.25 m s^{-1} are typical in the STBL (see e.g. numerous case studies summarized in Nicholls and Leighton 1986; de Roode and Duynkerke 1997; Wood 2005a).

The radiatively-driven diurnal variation in buoyancy production is the primary reason why stratocumulus clouds exhibit such a strong diurnal cycle (see Section 5 below).

The structure of the horizontal wind fluctuations is more complex than the vertical wind fluctuations since the energy-containing horizontal scales of these components are not constrained to be comparable to the boundary layer depth (see de Roode et al. 2004, for references) and continuity requires that vertical wind damping below the inversion would lead to stronger horizontal wind fluctuations there (as observed in Nicholls 1989). This allows energy to build up in the horizontal components so that for deeper STBLs these components may become increasingly important in the TKE budget (e.g. de Roode and Duynkerke 1997). The horizontal wind variances do not appear to scale as well with the convective velocity scale as do the vertical wind variances (Nicholls 1989).

c. *Entrainment*

1) Entrainment interfacial layer

The STBL is capped by a shallow layer over which there are strong gradients in thermodynamic properties (temperature, humidity, cloud water), tracers, and radiative cooling rates. This layer has been termed the entrainment interfacial layer (EIL) by Caughey et al. (1982), but is often referred to as the *inversion* since the universal and often the defining feature of the EIL is a significant increase in temperature with height which may exceed 1 K m^{-1} in some cases. However, since the EIL represents the layer between the cloud top and the upper limit of mixing influence from the STBL, it is most appropriate to define the EIL using a conserved variable such as total water or ozone mixing ratio.

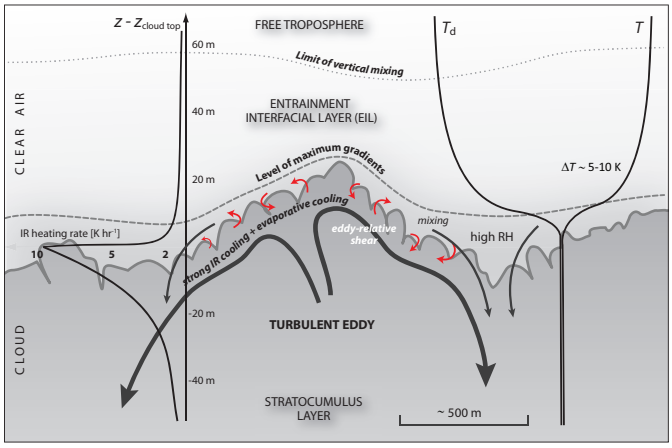

FIG. 13. Schematic of the entrainment interfacial layer (EIL) atop a layer of marine stratocumulus.

The structure of the EIL has been documented in a number of observational studies (Caughey et al. 1982; Lenschow et al. 2000; Van Zanten and Duynkerke 2002; Gerber et al. 2005; Haman et al. 2007), summarized in Fig. 13, which demonstrate that the EIL atop the STBL is typically less than a few tens of meters thick but with a highly variable thickness within the same cloud system (see also the model simulations of Moeng et al. 2005) leading to a horizontally averaged EIL that is substantially thicker than the local one (Garratt 1992). The top of the EIL is less well-defined than the base, with weaker vertical gradients relaxing to free-tropospheric values over several meters or tens of meters in some cases. This is in stark constrast with the sharp temperature gradient discontinuity at the base of the EIL (Caughey et al. 1982; Lenschow et al. 2000) which tends to coincide with, or lie above, the local stratocumulus cloud top (Roach et al. 1982; Caughey and Kitchen 1984; Lenschow et al. 2000; Moeng et al. 2005). The EIL consists of relatively moist and cool air compared with the free-troposphere (Brenguier et al. 2000a; Wang and Albrecht

1994), intermittent turbulence, and can also contain intermittent filaments of cloudy and clear air in different stages of mixing (Haman et al. 2007), particularly near the base of the EIL. From these features it may be concluded that the EIL represents a region that contains a mixture of STBL and free-tropospheric air and that the cloud top does not represent the upper limit of the STBL (Lenschow et al. 2000).

It has been argued that the EIL may play a fundamental role in setting the entrainment rate and in determining the degree of cloud top stability to entrainment (Wang and Albrecht 1994; Gerber et al. 2005; de Roode and Wang 2007), but high temporal resolution, *colocated* measurements of liquid water, temperature, inactive tracers, humidity and turbulence, preferably from a slow moving or stationary platform, will be required to fully characterize and understand the EIL and its role in entrainment.

2) Entrainment dynamics

One of the key unresolved questions in stratocumulus dynamics is how the entrainment rate at the top of the STBL relates to the structure of the turbulence in the STBL (see e.g. Driedonks and Duynkerke 1989; Stevens 2002), and specifically the extent to which entrainment is controlled by the large eddies (those dominating the TKE and mixing in the MBL) as opposed to small scale mixing processes and direct non-turbulent radiative and possibly evaporative cooling of the EIL. The non-turbulent processes would depend sensitively upon the details of very small scale cloud and thermodynamic structure near the inversion. So to what extent do physical models of entrainment need to account for the detailed small-scale structure of the entrainment interface?

There are two broad classes of entrainment rate formulations: (a) *flux-partitioning closures* assume that the entrainment rate adjusts to maintain a constant ratio of some measure of TKE-destroying (negative) buoyancy fluxes to the TKE-producing (positive) buoyancy fluxes (see e.g. vanZanten et al. 1999, for a review); (b) w_* *closures* assume that entrainment scales with the vertical integral of the buoyancy flux irrespective of how the TKE is produced (Deardorff 1976).

Flux-partitioning closures are very effective for the clear convective boundary layer but observations of the STBL violate this class of closure's basic assumptions. Specifically, we observe shallow STBLs for which the buoyancy flux is positive throughout the subcloud layer. Thus, most modern entrainment formulations are of the w_* closure form, and can be written (Stevens 2002) as

$$w_e = E\left(\frac{W}{\Delta b}\right) + w_{dir} \tag{2}$$

where the first term on the RHS represents *turbulent* entrainment, which increases with W, an appropriate measure of the rate of turbulent work in the STBL, decreases with Δb, the buoyancy jump atop the STBL, and can be modulated by a state-dependent efficiency E. The second term on the RHS w_{dir} is the direct, non-turbulent deepening of the STBL (Deardorff 1980a). Most bulk entrainment formulations can be couched in the form of (2). As discussed at length in Stevens (2002), the difficulty has been to determine the how W, E, and w_{dir} depend upon the mean state and turbulent properties of the STBL. The following are all factors that hinder progress:

i. It has been particularly challenging to make sufficiently accurate measurements of the entrainment rate in STBLs to cleanly distinguish between different entrainment formulations (e.g. Faloona et al. 2005; Gerber et al. 2005);

ii. The strong, sharp inversion atop the cloud makes it difficult to measure (and resolve in numerical models) the radiative cooling profile, thermodynamic structure, and dynamics of the entrainment interfacial layer sufficiently well to separate the turbulent from the non-turbulent entrainment (e.g. Kawa and Pearson Jr. 1989; Lewellen and Lewellen 1998);

iii. Key processes such as radiative and evaporative cooling which drive TKE generation and small-scale interfacial mixing in the MBL occur close to the interface itself, unlike the situation in the dry convective boundary layer;

The question of how to determine the appropriate rate of work W is still open. A number of entrainment formulations set the rate of working W (Eqn. 2) as proportional to the mean rate of TKE production by buoyancy, i.e. the mean buoyancy flux over the mixed layer (Eqn. 1), i.e. $W = w_*^3/h$. Doing this, and setting $w_{dir} = 0$, leads to an expression for the dimensionless entrainment rate w_e/w_* that is inversely proportional to a Richardson number representing the ratio of the stability to the turbulent kinetic energy in the STBL, i.e.

$$\frac{w_e}{w_*} = E\left(\frac{w_*^2}{h\Delta b}\right) = \frac{E}{Ri} \tag{3}$$

Formulating entrainment in this way works well for the dry surface-driven convective boundary layer (CBL) (Driedonks 1982), for which an efficiency $E \approx 0.2$ is appropriate.

Entrainment efficiencies for the STBL, defined using (3), are found to be much greater than 0.2, with values greater than unity implied from observations (Nicholls and Turton 1986; de Roode and Duynkerke 1997; Faloona et al. 2005; Caldwell et al. 2005). However, there is a large spread in implied efficiencies derived from different observational cases (e.g. Caldwell et al. 2005), which has been used to

argue that the efficiency is dependent on some other aspect of the STBL state.

Buoyancy fluctuations near the inversion driven by evaporative cooling can significantly enhance the entrainment efficiency (Lilly 1968; Deardorff 1980a; Randall 1980; Nicholls and Turton 1986). The process of mixing dry free-tropospheric air into the cloud can in some cases create some mixtures which are negatively buoyant with respect to the unmixed cloudy air (see e.g. Nicholls and Turton 1986; Stevens 2002, for illustrations). The term *buoyancy reversal* is used to describe the case where negatively buoyant mixtures are possible. Negatively buoyant mixtures can enhance the mixing process near cloud top and in some cases through the entire depth of the mixed layer. It was originally thought that buoyancy reversal would lead to rapid runaway entrainment (Deardorff 1980a; Randall 1980) in a process known as cloud top entrainment instability (CTEI), but conditions under which destructive CTEI occurs are now known to be less common than originally thought (see e.g. Siems et al. 1990). A more complete discussion of the role of CTEI in stratocumulus dissipation is presented in Section 4c below. Nevertheless, buoyancy reversal appears to be important for driving small-scale turbulent enhancement near cloud top which should enhance entrainment, and has been used to propose new or modified w_* entrainment closures (Eqn. 2). These include modifications to the buoyancy jump term Δb (e.g. Nicholls and Turton 1986) and the working term W (Lock 1998) rather than the entrainment efficiency term E per se.

Other factors affecting cloud top entrainment in stratocumulus are the specifics of whether the TKE in the STBL is primarily driven from the top or the surface (Lewellen and Lewellen 1998; Lilly 2002). The spread in E also partly reflects uncertainties in making reliable observational entrainment estimates (Faloona et al. 2005; Gerber et al. 2005). There is also evidence from high resolution eddy resolving models suggesting that it is unrealistic to assume $w_{dir} = 0$. In fact, direct radiative cooling of the inversion may constitute a signficant fraction (perhaps as much as 30-60%) of the total entrainment rate (Lewellen and Lewellen 1998; Lock 1998), although observationally constrained estimates of the importance of above-cloud radiative cooling differ Nicholls and Leighton (1986); Van Zanten and Duynkerke (2002) primarily due to uncertainty over what cooling-layer thickness is relevant. In reality, it is likely that a number of effects have some role to play in increasing the entrainment efficiency of the STBL compared with that for the dry CBL (Lewellen and Lewellen 1998). An important question is whether it is appropriate to include the nonturbulent entrainment rate in the efficiency term E.

Recent work suggests that it is more appropriate to define W by giving greater relative weighting to buoyancy flux in the upper boundary layer and less to that occurring lower down (Lewellen and Lewellen 1998; Lilly 2002; Lilly and Stevens 2008). Stronger weighting toward buoyancy flux near the top for the case is appropriate for a weak turbulent diffusion to dissipation ratio (Lilly and Stevens 2008). This is consistent with arguments made in earlier work (Stage and Businger 1981; Lewellen and Lewellen 1998) that it is the characteristics of the energy-containing (large) eddies when they impinge upon the inversion that ultimately determines their ability to entrain air from above.

4. Formation, maintenance and dissipation

Stratocumulus is fundamentally a convective cloud system, and as such, its maintenance is critically dependent upon the generation of convective instability at the top of the cloud. This instability and its release ultimately determines the structure and dynamics of stratocumulus cloud systems. This permits an alternative, more useful, and dynamically-focused definition of stratocumulus as a low level cloud system whose dynamics are primarily driven by convective instability associated with strong infrared cooling near the top of the cloud layer. This definition distinguishes stratocumulus from stratus (which by a definition of the same type are low level clouds without significant convectively-driven motions), and from cumulus (which are low clouds primarily driven by heating from below).

a. Formation

There are few studies that investigate the initial formation of stratocumulus, while many exist detailing its maintenance and evolution. In general, stratocumulus forms in response to large scale cooling or moistening of the boundary layer, driven by radiative processes, by buoyancy- or shear-driven mixing, or by a mixture of these processes.

Under clear skies the lower atmosphere can cool by several K day^{-1} by the emission of longwave radiation (e.g. Garratt and Brost 1981; Tjemkes and Duynkerke 1989), with a significantly weaker diurnal mean solar absorption by water vapor (e.g. Barker et al. 1998). Thus radiation alone tends to drive the atmosphere towards saturation. However, turbulent mixing also acts to change the moisture and temperature structure of the boundary layer and under many circumstances may be a more efficient means for generating large scale saturation. Under clear skies the primary source of this turbulence is either vertical shear of the horizontal wind (Garratt 1992) or buoyancy generated by exchange with the surface.

The effect of exchange with the surface upon vertical mixing is critically dependent upon the buoyancy of the air immediately adjacent to the surface that has been modified by the exchange (Paluch and Lenschow 1991). A parcel's virtual potential temperature T_v perturbation from the mean at a level is approximately expressed as

$$T_v' \approx T' + (\epsilon^{-1} - 1)\overline{T}q' \quad (4)$$

where ϵ (=0.622) is the ratio of the molar masses of water vapor and dry air, and $\overline{T}$ is the mean temperature of the layer. For a parcel modified by exchange with the surface the relative changes in T' and q' are critical to determining if the modified parcel will be positively buoyant. For an unsaturated near-surface layer, q' is always positive because evaporation will occur, and so the sign of the resulting parcel buoyancy is determined by T' which critically depends upon the surface-air temperature difference.

Consider the case of clear skies over the ocean. If the sea surface temperature is warmer than the air temperature then parcels of air moistened by surface evaporation are also warmed and will thus always be positively buoyant. This can even occur when the SST is cooler than the air temperature provided that $T_v' > 0$. These parcels rise and result in mixing and temperature profiles that are near-neutral. Such layers are the precursors of stratus and stratocumulus formation (Paluch and Lenschow 1991). In contrast, when $T_v' > 0$ the modified parcels remain close to the ocean surface which leads to moisture build up near the surface, and stratified boundary layers, which eventually favor the formation of shallow cumulus convection, or, if the temperature stratification is very strong, sea fog.

Over land the physical processes are essentially the same, but the moisture supply is sensitive to the nature of the underlying surface, and shear within the developing boundary layer can also play an important role (Zhu et al. 2001).

The formation of stratus occurs when the upper parts of the near-neutral layer reach saturation. At this point the inversion is not strongly defined because the turbulent eddies are fairly weak and reach varying altitudes. Once the saturated layer becomes thicker than a few tens of meters, it becomes strongly radiatively active and infrared emission from the upper parts of the cloud cools the cloud layer (see e.g. Paluch and Lenschow 1991). This sharpens the inversion and, if sufficiently strong generates convective instability which can dominate the dynamics of the layer, which is by then a layer capped by stratocumulus.

A number of studies have used numerical and analytical modeling to determine whether a given set of meteorological forcings will result in the formation of stratocumulus (e.g. Randall and Suarez 1984; Chlond 1992). Over the ocean, the key requirements are heating from below (as discussed above) coupled with relatively strong lower tropospheric stability to prevent deep cloud development, and subsidence rates that are not so strong as to prevent the PBL to deepen to the point where the surface based LCL is below the inversion (Randall and Suarez 1984).

b. Maintenance

Stratocumulus layers will persist as long as the layer they reside in remains saturated. The turbulent mixing within stratocumulus-topped boundary layers is frequently sufficient to maintain a well-mixed state (e.g. Nicholls and Leighton 1986; Stevens et al. 2003; Wood 2005a; Caldwell et al. 2005). For well-mixed layers the existence of a saturated sublayer at the top of the PBL requires that the inversion base height z_i is higher than the surface-based lifting condensation level (LCL). As the LCL is determined by the surface temperature and moisture (i.e. the conserved variables), it is straightforward to understand that processes that moisten and/or cool the mixed layer will lower the LCL, and, assuming that z_i does not change, this will thicken the cloud (Randall 1984). Processes such as large scale subsidence or entrainment will lead to z_i changes, and entrainment also leads to changes in the LCL (Randall 1984; Wood 2007). Thus, we can see how, for a mixed-layer, both thermodynamic and dynamic processes are responsible the maintenance of the saturated sublayer.

Approximately 1 K of PBL cooling, or 0.2-0.6 g kg^{-1} of moistening[4] is required to lower the LCL by 100 m (e.g Wood 2007, Appendix). From this perspective, given typical stratocumulus cloud thicknesses of a few hundred meters, it would appear that the maintenance of stratocumulus clouds is extremely sensitively dependent upon small changes in the surface or entrainment fluxes, or in the radiative cooling. And yet, in many regions the persistence of stratocumulus sheets is remarkable.

Stratocumuli can also persist in boundary layers in which the coupling of the cloud layer to the surface is intermittent and localised (Betts et al. 1995; Albrecht et al. 1995b) and which cannot be considered to be well-mixed. Such layers are often referred to as *decoupled* boundary layers, but the term *decoupled* presumes to imply the absence of a connection between the cloud layer and the surface moisture source. Instead, it is more appropriate to refer to these layers as *intermittently-coupled* or *locally-coupled* boundary layers, because some degree of coupling is necessary to provide a moisture source for the stratocumulus (Martin et al. 1995). For many *intermittently-coupled* boundary layers, especially those over the subtropical oceans, the coupling is achieved by cumulus clouds with roots in the subcloud layer which loft and then vent moisture into the stratocumulus deck above (Martin et al. 1995; Miller and Albrecht 1995; Wang and Lenschow 1995). Such layer are also known as *cumulus-coupled* PBLs (Krueger et al. 1995b).

[4]The partial derivative of LCL lifting with respect to water vapor mixing ratio strongly decreases with temperature via the Clausius-Clapeyron equation, (see e.g. Wood 2007, for explicit expressions). The range given here encompasses temperatures from 270-290 K.

c. Dissipation and breakup

Primary factors that reduce the thickness of the saturated layer in which stratocumuli reside include: strong subsidence which can lower the inversion (Randall and Suarez 1984) especially in coastal regions affected by land-sea interactions (Sundararajan and Tjernstrom 2000); an increase in the temperature of the PBL by increased heat fluxes or especially solar radiation (Turton and Nicholls 1987; Rogers and Koracin 1992); removal of moisture by drizzle (Ackerman et al. 1993) or precipitation falling through the layer from aloft (e.g Rutledge and Hobbs 1983); entrainment of warm, dry air from aloft (Deardorff 1980a; Randall 1980, 1984).

1) Transition to cumulus

In addition to consideration of the dissipation mechanisms for stratocumuli in boundary layers that remain relatively well-mixed, mechanisms by which stratocumulus clouds dissipate and/or break up involve the transition to a stratified and intermittently coupled boundary layer (Garratt 1992; Paluch et al. 1994). Often, but not always, the transition to vertical stratification is accompanied by increased horizontal heterogeneity (Wang and Lenschow 1995; Wood and Hartmann 2006). The transition from overcast stratocumulus to trade cumulus clouds is an example of this type of stratocumulus breakup (Albrecht et al. 1995a,b; Bretherton and Wyant 1997), and is critical for setting the distribution of cloud cover over the subtropical and tropical oceans. The transition typically occurs as airmasses move equatorward around the eastern side of subtropical oceanic high pressure systems. As they do so, the STBL, initially shallow due to the relatively strong subsidence associated with the high, deepens and warms due to increased surface fluxes (particularly latent heating) as the airmass moves over progressively warmer water (Krueger et al. 1995a; Wyant et al. 1997). This drives strong entrainment which results in increasingly negative subcloud buoyancy fluxes which decouple the layer (Bretherton and Wyant 1997), allowing cumulus clouds to form below the stratocumulus. This process of decoupling the STBL is termed the *deepening-warming* mechanism (Bretherton and Wyant 1997). The cumuli initially help to maintain extensive stratocumulus cloud cover by supplying moisture (Martin et al. 1995; Miller and Albrecht 1995; Wang and Lenschow 1995). As the cumuli become more vigorous they encourage stronger entrainment of dry air from aloft (Wyant et al. 1997), and the entrained air is spread over a thinner layer than for a well-mixed STBL (Xiao et al. 2010), both of which lead to stratocumulus breakup.

2) Cloud top entrainment instability

An additional mechanism for the breakup of stratocumulus clouds was proposed independently by Deardorff (1980a) and Randall (1980), following ideas discussed initially by Lilly (1968). Known as it cloud top entrainment instability[5] (CTEI), this mechanism is based on the idea that evaporation in mixtures of saturated (cloudy) and dry air from above the STBL can under certain circumstances generate negatively buoyant downdrafts which might increase the turbulence kinetic energy (TKE) in the STBL, leading to further entrainment and thus serving as a positive feedback that can rapidly dry the STBL and dissipate cloud. This is in contrast to dry entrainment in which the buoyancy force associated with mixing warm air into the STBL destroys TKE.

The Randall-Deardorff criterion for CTEI, which is derived assuming that the parcel containing a mixture of cloudy and free-tropospheric air remains just saturated, can be defined simply as a function of the jumps in equivalent potential temperature θ_e and total water mixing ratio q_t across the cloud top inversion (Δ indicates a difference between the free-tropospheric value and the value in the top of the STBL):

$$\Delta\theta_e < \kappa \frac{L_v}{c_p} \Delta q_t \tag{5}$$

where L_v is the latent heat of condensation of water, c_p is the heat capacity of air at constant pressure, and κ is a thermodynamic constant that depends on temperature and pressure ($\kappa = 0.16$ at a temperature of 280 K and a pressure of 900 hPa). Equivlently, the criterion can be expressed in terms of the inversion jump in liquid potential temperature $\theta_l \approx \theta - L_v q_l / c_p$, where q_l is the liquid water mixing ratio:

$$\Delta\theta_l < -\Delta q_t \frac{L_v}{c_p}(1-\kappa). \tag{6}$$

Since the jump $\Delta\theta_l$ is close to the inversion strength ΔT, this latter form of the Randall-Deardorff CTEI criterion is a little more intuitive, and essentially states that the combination of weak inversions and/or strong hydrolapses (stronger evaporative potential) would lead to CTEI.

Numerous field measurements show that persistent stratocumulus layers can exist even when the criterion for CTEI as defined by Eqns. (5)/(6) is met (e.g. Kuo and Schubert 1988; Weaver and Pearson 1990; de Roode and Duynkerke 1997), and controlled laboratory analogue experiments led to the same conclusions (Siems et al. 1990). This finding drove a search for extensions of the original theoretical arguments and modified criteria. The primary concern

[5]This title was proposed by Deardorff (1980a) and was termed "Conditional instability of the first kind upside-down" by Randall (1980).

with the Randall-Deardorff criterion is that it assumes the entrained parcel remains saturated, i.e. there is no limit to the amount of liquid water available for evaporation. Thus the Randall-Deardorff criterion therefore can be seen to represent the maximum cooling potential that could be gained if liquid is unlimited. This is often not the case, however, and parcels entering and mixing with STBL air can in many cases become subsaturated before their cooling potential is realized. Adjustments to the CTEI crierion that take this consideration into account were conceived by MacVean and Mason (1990), Siems et al. (1990) and Duynkerke (1993). For relatively small moisture jumps Δq_t, the criterion of Duynkerke (1993) relaxes to that of Randall-Deardorff for realistic liquid water contents found in stratocumulus clouds, and for zero cloud liquid water it relaxes to the dry adiabatic stability criterion ($\Delta\theta_v > 0$). For strong hydrolapses typical of most STBLs, the condition for instability in Duynkerke (1993) is more stringent than that from Randall-Deardorff. Although the exact formulations used by MacVean and Mason (1990) and Siems et al. (1990) differ somewhat from Duynkerke (1993), the stability criteria emanating from all three studies share the common element of requiring a weaker inversion than Randall-Deardorff, for a given moisture jump, to generate instability. Thus, the conditions under which the STBL will undergo CTEI are less likely to be found in nature than was originally supposed.

[GIVE ANALYTICAL EXPRESSION FOR DUYNKERE]

$$\Delta\theta_l < -\Delta q_t \frac{L_v}{c_p}(1-\kappa). \tag{7}$$

The modified CTEI criteria are much more consistent with the observations of unbroken stratocumulus cloud decks than is the Randall-Deardorff criterion (see e.g. Duynkerke 1993; de Roode and Duynkerke 1997), in that the stratocumulus cases tend to exist in stable CTEI conditions. This alone might hint that some form of CTEI may still be relevant for understanding the breakup of stratocumulus clouds in nature. More recent research, however, suggests that the cloud-dessicating effects of CTEI may to a significant extent be masked by other processes such as cloud top radiative cooling which serve to maintain clouds (Yamaguchi and Randall 2008). Other recent research using extremely high resolution numerical simulation (Stevens 2010; Mellado 2010) suggests that buoyancy reversal is not a sufficient condition for the rapid breakup of stratocumulus layers. Instead, while negatively-buoyant evaporatively-driven thermals do increase the transport of entrained mass away from the inversion, i.e. they enhance the entrainment rate (see Section 3c), they do not feed back onto the interfacial dynamics in such a way as to drive a positive feedback on the entrainment rate, i.e. CTEI. Therefore, despite three decades of research into CTEI, its relevance to the breakup of stratocumulus sheets remains somewhat uncertain.

3) Dissipation induced by precipitation

Although not a necessary condition for stratocumulus breakup, there is evidence and a theoretical basis for increased precipitation promoting decoupling and stratocumulus breakup (Nicholls 1984; Wang and Wang 1994; Miller and Albrecht 1995; Bretherton and Wyant 1997; Stevens et al. 1998; Mechem and Kogan 2003; Caldwell et al. 2005; Comstock et al. 2005). The relative importance of precipitation-induced decoupling compared with the deepening-warming mechanism for driving the stratocumulus to cumulus transition is currently not well understood and is a focus for current research activity (see discussion of the effects of precipitation in Section 6g below).

5. Climatology of stratocumulus

Stratocumulus clouds are the earth's most areally extensive cloud type, covering 23% of the ocean surface and 12% of the land surface (Warren et al. 1986, 1988; Hahn and Warren 2007).

a. Annual Mean

Figure 14 shows the annual mean coverage of stratocumulus clouds globally. The subtropical eastern oceans are marked by extensive regions, often referred to as the *semi-permanent subtropical marine stratocumulus sheets*, in which the stratocumulus cover exceeds 40%, and in places (e.g. the southeastern subtropical/tropical Pacific and Atlantic oceans) the annual mean stratocumulus cover can be as high as 60%. These sheets are approximately latitudinally symmetric about the Atlantic/Pacific ITCZ which is centered on approximately 10°N. The maxima in stratocumulus cover are not located immediately adjacent to the coast, but are displaced roughly 5-10°to the west, where the winds are typically stronger and the STBL is deeper (Neiburger et al. 1961; Wood and Bretherton 2004) than at the coast. The greater mean stratocumulus cover for the southern hemisphere marine stratocumulus sheets is thought to be related to the occurrence and configuration of significantly elevated terrain to their east (Xu et al. 2004; Richter and Mechoso 2004, 2006).

Stratocumulus also swathe large regions of the midlatitude oceans where their coverage is typically 25-40%. Over land, the regions with the highest stratocumulus cover are chiefly in the midlatitudes and in the coastal hinterlands adjacent to the subtropical semi-permanent marine stratocumulus sheets. However, the south and east of China is notable for being the only subtropical continental region with a high coverage of stratocumulus.

The western sides of the major ocean basins in the developed trade winds and the adjacent landmasses have the lowest coverage of stratocumulus, but Fig. 15 demonstrates

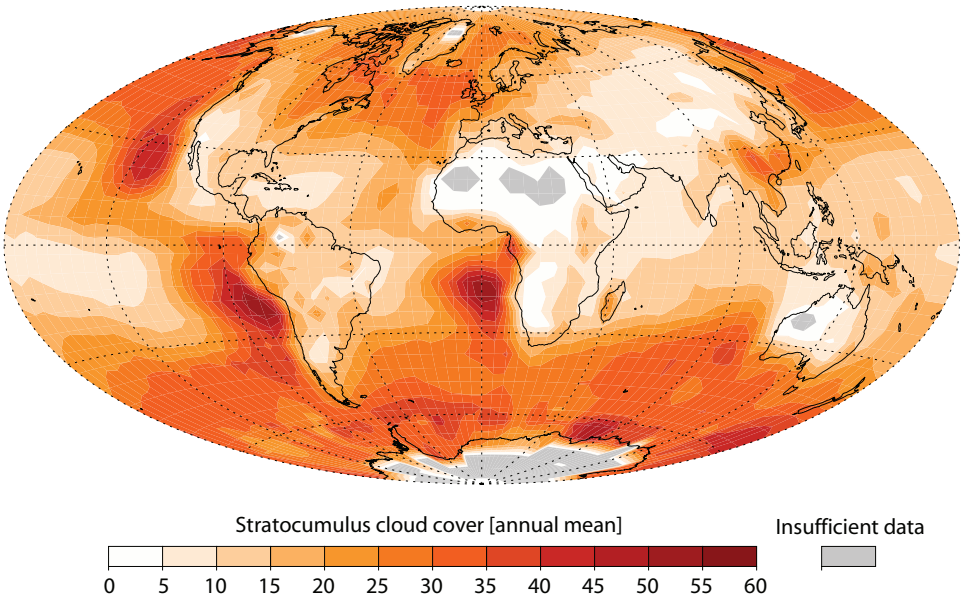

FIG. 14. Annual mean coverage of stratocumulus clouds. Locations with no reports of stratocumulus (either because of a lack of stratocumulus or a lack of observations) are shown as gray. Data are from the combined land/ocean cloud atlas database (Hahn and Warren 2007).

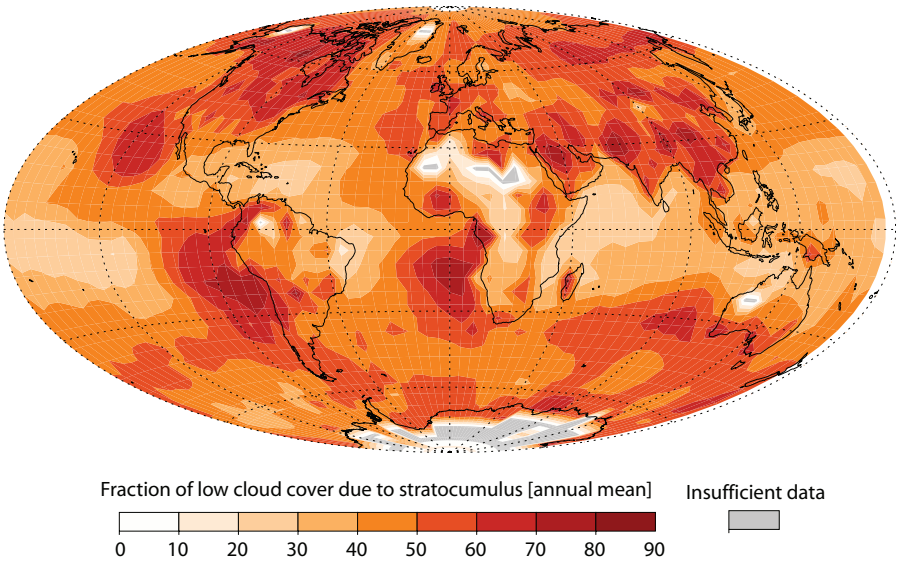

FIG. 15. Fraction of annual mean low cloud cover associated with stratocumulus clouds. Locations with no reports are shown as gray. Data are from the combined land/ocean cloud atlas database (Hahn and Warren 2007).

that even in these regions of minimal stratocumulus, stratocumulus clouds typically constitute over 20% of the overall low cloud cover. For 97% of Earth's surface stratocumulus clouds constitute 25% or more of the low cloud cover. Thus, there are few regions of the planet where stratocumulus clouds are not climatologically important.

Typical climatological mean liquid water paths for regions dominated by marine stratocumulus are 40-150 g m^{-2} (Weng and Grody 1994; Greenwald et al. 1995; Weng et al. 1997; Wood et al. 2002b; O'Dell et al. 2008), but since the cloud cover in these regions is not 100% the cloud-conditional liquid water paths are likely to be somewhat higher than this (Greenwald et al. 1995).

Stratocumulus climatological mean cloud thicknesses are difficult to estimate directly since a significant fraction of stratocumuli will fully attenuate a lidar beam. Thicknesses may be estimated indirectly from the LWP climatology and the assumption of an adiabatic cloud. An-

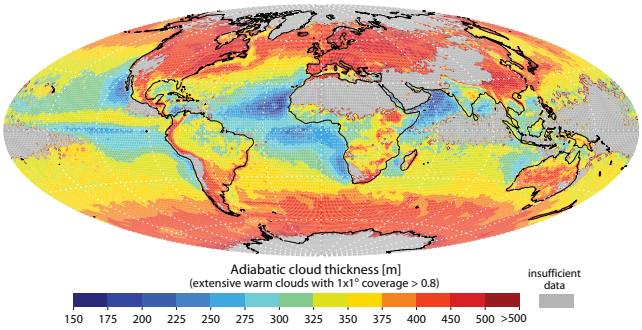

FIG. 16. Annual mean cloud thickness for horizontally-extensive (instantaneous coverage exceeding 80% at the 1×1 °scale) warm clouds. Adiabatic thickness is deduced from MODIS Terra liquid water path estimates at ∼ 10:30 local time (close to the time where the cloud thickness is close to the mean daily value), and is based on the assumption that the clouds are adiabatic (see Section 3a). The vertical liquid water gradient is estimated using the MODIS-derived cloud top temperature. See Wood and Bretherton (2004) for additional details.

nual mean values of this adiabatic cloud thickness for horizontally extensive liquid clouds are shown in Fig. 16. Mean cloud thickness h ranges from 200-300 m over most of the cold subtropical eastern oceans to 400 m or more over the midlatitude oceans and continents. In a sense, this represents an intriguing *lack* of geographical variability ($200< h < 400$ m almost everywhere) and hints at important feedbacks that limit the range of thicknesses that stratocumuli can assume.

b. *Climatological Variability*

Stratocumulus cloud systems exhibit variability on a wide range of timescales. Stratocumuli are modulated by variability in large scale dynamic and thermodynamic conditions and in the radiation field.

1) Seasonal Cycle

In many regions, stratocumulus cloud cover is strongly seasonal. Figure 17 shows the amplitude of the seasonal cycle and the month of maximum stratocumulus cover. For the subtropical marine stratocumulus sheets, especially those in the southern hemisphere, the seasonal amplitude of the cover is greatest a few hundred kilometers downwind of the annual mean stratocumulus cover (compare with Fig. 14). Spring or early summertime maxima are typical for these regions and over the northern hemisphere midlatitude oceans, and it is notable that the stratocumulus cover of the two major southern hemisphere subtropical marine sheets has a much stronger seasonal cycle and peaks earlier in the season than over the northern hemisphere subtropics. This hemispheric asymmetry is driven by greater orographic forcing from the elevated continent to the east for the southern sheets (Richter and Mechoso 2004, 2006). There are major differences in the seasonal phase between the western and the eastern sides of the midlatitude North Atlantic and Pacific Oceans, with a wintertime peak over the western sides and summertime peaks over the eastern sides (Weaver and Ramanathan 1997), which probably reflects the greater importance of surface forcing (e.g. during wintertime cold-air outbreaks) for stratocumulus on the western side. Over the tropical oceans, there does not appear to be a systematic favored month of maximum stratocumulus cover, apart from over the equatorial eastern oceans where annually varying cross-equatorial flow plays a major role (Mitchell and Wallace 1992). Over land, especially in the midlatitudes, winter maxima are typical (Fig. 17). The patterns of seasonal stratocumulus variability largely follow the seasonal cycle of lower tropospheric static stability (Klein and Hartmann 1993; Wood and Bretherton 2006; Richter and Mechoso 2004, 2006).

Stratocumulus cover over the Artic Ocean is strongly seasonal, peaking in late summer. Unlike most other regions, this seasonality is not explained by static stability which is actually greatest during winter (Klein and Hartmann 1993). The summertime maxima has been attributed to warmer temperatures and therefore greater moisture availability over the melting sea ice (Hermann and Goody 1976) but the dessication of clouds during wintertime through ice formation has also been hypothesized to be a driver of the seasonal cycle (Beesley and Moritz 1999).

2) Synoptic Variability

The thickness and coverage of stratocumulus clouds is strongly modulated by the changing synoptic setting in which they exist. While no single meteorological parameter can fully explain the synoptic variability in stratocumulus clouds (Klein 1997), in general, over oceans, stratocumuli are associated with ridging conditions, with a frequency that is maximal to the east of the ridge line under conditions of cold air advection and large scale subsidence (Norris and Klein 2000). Thus the semi-permanent subtropical highs nurture semi-permanent stratocumulus sheets on their eastern flanks (Fig. 14), but there is significant synoptic variability in low cloud cover and type associated with the strengthening and weakening of the subtropical high (Klein et al. 1995; Klein 1997; George and Wood 2010) and with changes in its position (Klein et al. 1995; Garreaud et al. 2001). At higher latitudes extensive stratocumulus sheets are common but are transient and echo the eastward drift of large scale baroclinic waves (Ciesielski et al. 1999; Norris and Klein 2000), and such waves (or more precisely wave *packets*), with typical timescales of 20 days or less (Wang et al. 1999; Hakim 2003) are also the primary synoptic modulators of the semi-permanent stratocumulus sheets (Garreaud and Rutllant 2003; George and Wood 2010). Stratocumuli associated with cold air outbreaks occur behind the trailing cold fronts of midlatitude cyclones.

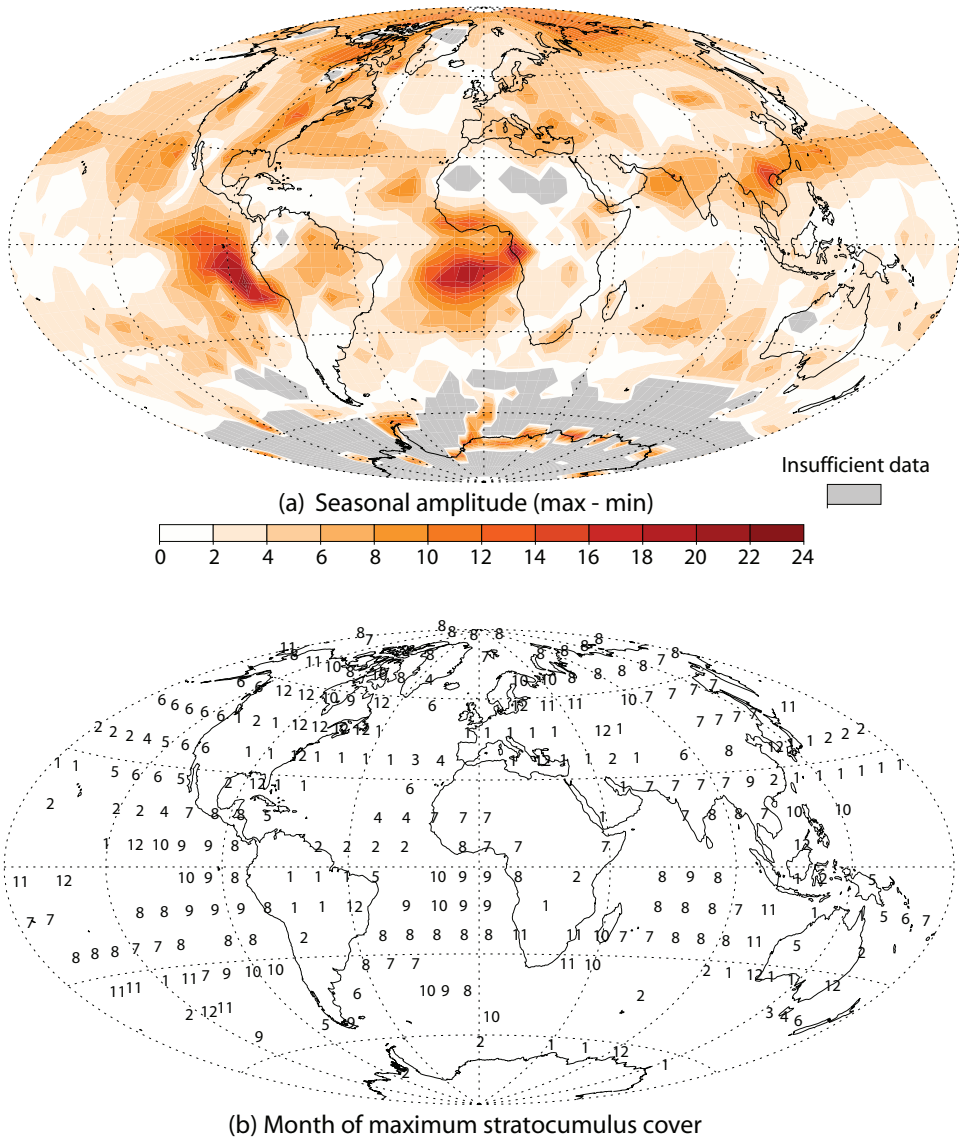

FIG. 17. (a) Seasonal amplitude (maximum-minimum coverage), and (b) month of maximum stratocumulus cover. Locations with no reports, or where the seasonal amplitude of stratocumulus cover is less than 2.5% are not shown. Data are from the combined land/ocean cloud atlas database (Hahn and Warren 2007).

Over continents, stratocumuli are typically associated with subsidence and equatorward flow (Kollias et al. 2007).

3) Interannual variability

The magnitude of the interannual variability of low clouds is comparable to that in synoptic and seasonal variability (Klein and Hartmann 1993; Stevens et al. 2007), but few studies have focused specfically upon stratocumulus. In subtropical marine stratocumulus regions, the interannual variability in low cloud cover and visible reflectance is well-correlated with lower tropospheric static stability (LTS) where gradients in LTS are aligned with those in mean low cloud amount (e.g. Klein and Hartmann 1993) but less so in regions where this is not so (Stevens et al. 2007). Because LTS is strongly connected to the sea surface temperature (SST), negative interannual correlations between SST and marine low cloud cover are observed over much of the ocean (e.g Hanson 1991; Klein et al. 1995), and are strongest in the regions of transition from stratocumulus to cumulus (Norris and Leovy 1994) during summer. Low cloud responses to ENSO are due in part to the response to SST anomalies but also due to mid-latitude storm-track teleconnection responses which affect temperature advection (Park et al. 2004).

Interannual variability in LTS is controlled by both sea surface temperature and free-tropospheric temperature, but

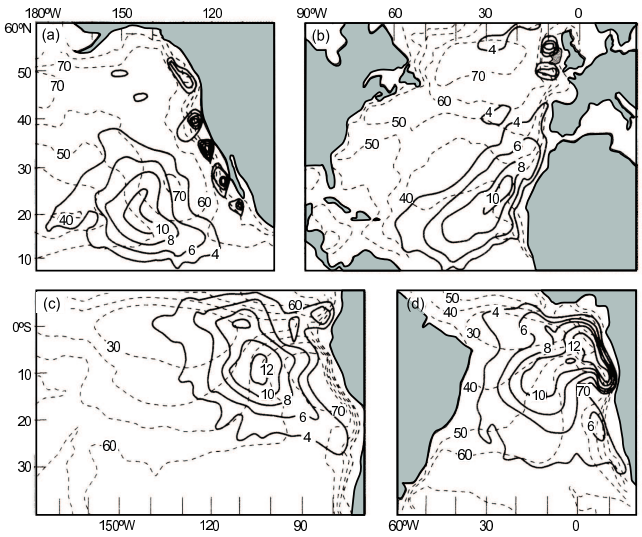

FIG. 18. Amplitude of the first harmonic of the diurnal cycle (solid) and mean low cloud cover (dashed) for four regions where stratocumulus is a prevalent cloud type. Data from the International Satellite Cloud Climatology Project (ISCCP, Rossow and Garder (1993)) for June-July-August 1984-1990. From Rozendaal et al. (1995). (c)American Meteorological Society. Reprinted with permission.

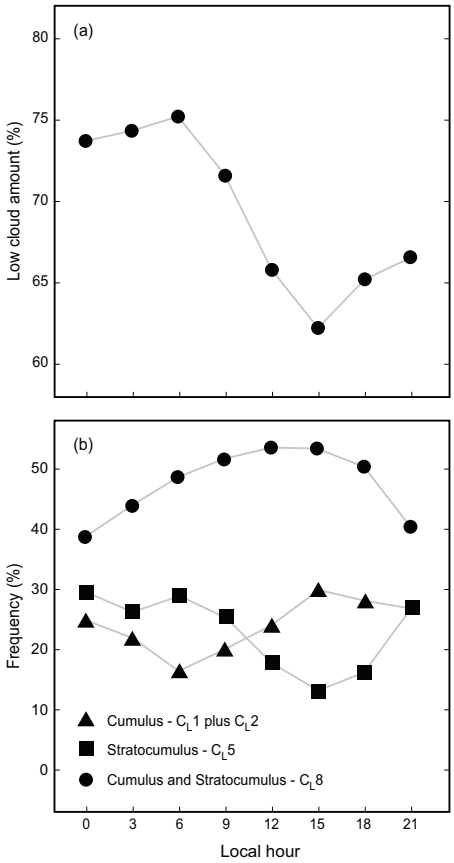

FIG. 19. Mean summertime (June-September) diurnal cycle of (a) low cloud amount; (b) frequency of occurrence of different WMO low cloud types for cases of cold advection at 30°N,140°W, a region of stratocumulus to cumulus transition. From Klein et al. (1995). (c)American Meteorological Society. Reprinted with permission.

there is evidence suggesting that the free-tropospheric interannual variability is dominant in some regions (Stevens et al. 2007), while in others such as the equatorial eastern Pacific the SST dominates (Klein and Hartmann 1993). Interannual correlations are highest for cloud cover correlated with SST perturbations approximately 24 hours upwind Klein et al. (1995), indicating the importance of the Lagrangian history of the airmass in controlling low clouds.

Relatively small secular trends in the coverage of low clouds would be sufficient to significantly affect Earth's climate sensitivity. For example, Randall et al. (1984) and Slingo (1990) point out that increases in the absolute area covered by low clouds of between 3.5 and 5% would be sufficient to offset the warming induced by a doubling of CO_2. Identification of long term secular trends in low cloud properties is critical but is currently limited because our observing system is ill-suited to this challenge (Dai et al. 2006; Evan et al. 2007; Norris and Slingo 2009). There are no reliable studies specifically focused upon stratocumulus clouds.

4) Diurnal Cycle

Stratocumulus clouds exhibit significant diurnal modulation largely due to the strong diurnal cycle of solar insolation and consequent radiative heating of the cloud layer (see Section 6b). In contrast to clouds driven by convective heating from below, such as cumulus clouds which tend to exhibit afternoon maxima, the maximum coverage of stratocumulus tends to be during the early morning hours before sunrise (Rozendaal et al. 1995; Bergman and Salby 1996). Diurnal maxima in cloud thickness and vertically integrated cloud liquid water content (liquid water path) also typically occur in the early morning hours (Zuidema and Hartmann 1995; Wood et al. 2002a; Bretherton et al. 2004; Zuidema et al. 2005). The amplitude of the diurnal variation in cloud cover and LWP can exceed 20% of the mean values (Rozendaal et al. 1995; Wood et al. 2002a) over the eastern subtropical oceans. Dedicated studies of the mean diurnal cycle of continental stratocumulus cloud properties are lacking, but data from Hahn and Warren (2007) show that the relative diurnal amplitude of stratocumulus cover (i.e. amplitude expressed as a fraction of the mean coverage) is roughly double that over the ocean.

The absorption of solar radiation during the daytime in the upper regions of the cloud acts to weaken the net cooling and thus suppresses the total radiative driving, resulting in weaker circulations (Hignett 1991; Duynkerke and Hignett 1993) and a less efficient coupling of the clouds with the surface moisture supply (Turton and Nicholls 1987;

Rogers and Koracin 1992, see also section 4.1). Because it is strongly related to turbulence in the STBL, the entrainment of warm, dry, free-tropospheric air into the STBL is strongly diurnally varying (Caldwell et al. 2005), which itself impacts the turbulent structure.

Strong diurnal variability in cloud cover is observed downwind of the subtropical maxima in cloud cover (Fig. 18) towards the regions of transition from stratocumulus to trade cumulus (Rozendaal et al. 1995; Klein et al. 1995; Miller et al. 1998), where the STBL is deeper than it is closer to the coast. In these regions, the STBL is often decoupled, and the diurnal march consists of an increasing frequency of cumulus clouds during the day from a noctural STBL that contains stratocumulus with cumulus below (see Fig 19, from Klein et al. (1995)). There is evidence that the strength of the diurnal cycle in these regions is not controlled by STBL decoupling and recoupling per se (since the STBL is never fully coupled), but by the increased daytime stability of the stable layer atop the surface mixed layer (Klein et al. 1995; Miller et al. 1998; Ciesielski et al. 2001) which results in a more intermittent (albeit locally stronger) cumulus-coupling of the STBL. The moisture supply into the overlying stratocumulus layer is thereby limited and diurnal breakup enhanced. Drizzle too has a strong diurnal cycle (Leon et al. 2008; Comstock et al. 2004), with peak precipitation rates occurring during the night when the STBL tends to be most strongly coupled. This makes it difficult to isolate the effects of drizzle from other processes in driving the diurnal cycle in cloud cover and LWP.

In some regions diurnal variability in the large scale dynamics (primarily subsidence rate) also plays an important role in the diurnal cycle of stratocumulus (Ciesielski et al. 2001; Duynkerke and Teixeira 2001; Garreaud and Muñoz 2004; Bretherton et al. 2004; Caldwell et al. 2005; Wood et al. 2009a). While this is especially true in near-coastal regions (e.g. Rozendaal et al. 1995), significant diurnal modulation of surface divergence is actually observed in remote oceanic regions (Wood et al. 2009a), which most likely stems from long-range propagation of diurnally forced gravity waves from continents or from regions of deep convection. There is some evidence that such waves can either enhance or decrease the existing cloud diurnal variability depending upon the local phase of the wave with respect to the solar cycle (Wood et al. 2009a).

6. Controlling physical processes

a. External meteorological forcings

The great variety of morphological forms that stratocumulus clouds can adopt ultimately results from the wide range of possible meteorological conditions under which these clouds can exist. This allows stratocumulus cloud systems to exist for several days over which time the clouds experience time-dependent meteorological conditions. Even without strong changes in conditions, the development of mesoscale structure in stratocumulus can take many hours (Shao and Randall 1996; de Roode et al. 2004).

The chief external meteorological forcings affecting stratocumulus cloud systems are elegantly summarized in Stevens and Brenguier (2008), here modified slightly, as the (time-dependent) meteorological forcing vector M:

$$M(t) = [F_+, D, V, T_{sfc}, q_{sfc}, T_+, q_+] \tag{8}$$

where F is the downward (longwave+shortwave) irradiance, D is the large scale divergence, V is the surface wind speed, T is temperature, and q is the water vapor mixing ratio. The "sfc" subscripts indicate values immediately adjacent to the surface. The plus-sign subscripts indicate values in the free troposphere immediately above the inversion top at a height clear of influence (radiative or turbulent) from the cloud itself. Thus, from (8) we understand that there are important external[6] radiative, dynamic, and thermodynamic controls on stratocumulus clouds. To understand how these forcings impact stratocumulus structure requires an understanding of the physical processes that control the cloud dynamics. This section focuses upon these processes.

b. Radiation

The downwelling flux F_+ at the top of the STBL provides the external radiative forcing on the STBL, but the overall effect of radiation on the cloud depends upon the vertical profile of radiative heating. Radiative heating/cooling rates in the STBL impact cloud dynamical driving by influencing buoyancy. Stratocumulus clouds also impact the

[6] It is important to note that both the surface and free-tropospheric variables in (8) are not *entirely* external to the system but can be modified (generally to a small degree) by the dynamics and structure of the clouds. Over the oceans, the efficiency with which moisture from the surface is transported to the atmosphere is also strongly tied to T_{sfc} and V (e.g. Hartmann 1994) and so q_{sfc} is not a distinct controlling variable for the oceanic case. Infrared irradiance from the surface is also strongly tied to T_{sfc} and so we do not consider that to be an independent variable in most cases. Surface albedo is small over the ocean where the majority of stratocumulus reside, and so radiation reflected from the surface is in many cases negligible. Stratocumuli modify the free-tropospheric structure immediately above them by mixing (see de Roode and Wang 2007, for a discussion) but observations suggest that the mixing is confined to a layer thinner than 100 m (Faloona et al. 2005). While the presence of a cloud layer can significantly affect the temperature structure of the free-troposphere remotely by influencing the longwave heating rate for several hundred meters above the layer (Nieuwstadt and Businger 1984; Siems et al. 1993; Caldwell et al. 2005; Caldwell and Bretherton 2008), unless the cloud layer is highly broken or of significantly diminished emissivity (generally not the case for most stratocumuli), the modification to the free-tropospheric structure should be relatively independent of the cloud structural properties and can be accounted for quite simply (e.g. Caldwell et al. 2005).

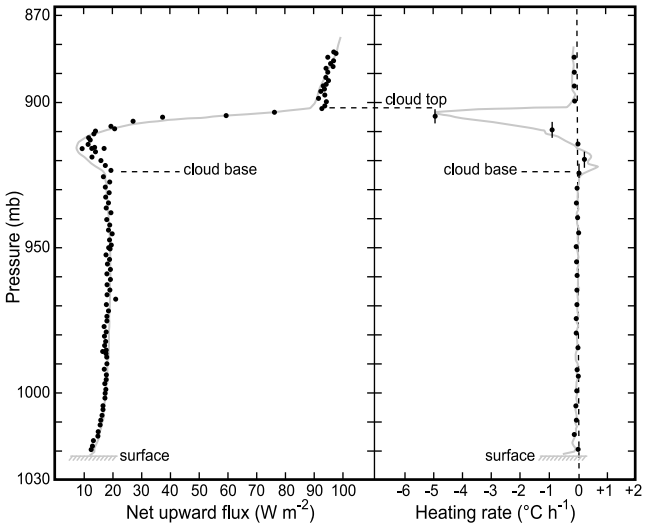

FIG. 20. Profiles of observed (dots) and theoretical (solid lines) net upward infrared flux (left) and associated heating rates (right) for a nocturnal stratocumulus layer. From Slingo et al. (1982a).

radiative budget at the top of the atmosphere and the surface, and the latter can impact other elements of the meteorological forcing vector (e.g. surface temperature). A detailed treatment of the interaction of radiation and clouds is found in Liou (1992).

Liquid water clouds scatter and absorb radiation to a degree that depends primarily upon the wavelength but also upon the cloud droplet size. They also emit substantially in the thermal infrared ($4 < \lambda < 50$ μm). Cloud droplets scatter radiation at all wavelengths across the visible and infrared. Absorption, which is critical for determining the radiative heating rates, becomes important for the interaction of droplets and radiation in some bands in the near-infrared ($0.8 < \lambda < 4$ μm), and dominates in the thermal infrared. For visible wavelengths ($\lambda < 0.8$ μm) there is very little absorption by liquid water.

1) Terrestrial radiation

Terrestrial radiation is the primary driver of convective instability in stratocumulus clouds, and longwave cooling is typically the leading term in the energy budget of the STBL. Most stratocumulus clouds contain liquid water in sufficient abundance that they are largely opaque to terrestrial thermal infrared radiation (Paltridge 1974; Platt 1976). The volume absorption coefficient in the terrestrial thermal infrared increases approximately linearly with the liquid water content (Platt 1976; Pinnick et al. 1979) and can be expressed as $\beta_\lambda = \kappa_\lambda \rho q_l$ where q_l is the liquid water mixing ratio, ρ is the air density, and κ_λ is a spectrally-dependent mass absorption coefficient.

The mass absorption coefficient in the thermal infrared is virtually independent of cloud droplet size for droplet effective radius[7] r_e smaller than the wavelength of light (Stephens 1978a; Chylek et al. 1992), but depends upon effective radius when a significant fraction of the mass is contained in droplets larger than the wavelength (see review by Stewart and Essenwanger 1982) and papers by Chylek et al. (1992) and Garrett et al. (2002). For stratocumulus and stratus clouds with low particle concentrations and low liquid water contents such as those commonly found in the Arctic or in very clean regions of the droplet size must therefore be taken into account when considering the infrared emissivity, which leads to the potential for such clouds to exhibit indirect aerosol effects in the infrared (Garrett et al. 2002).

Because of the spectral and microphysical dependence of κ_λ, appropriate values of κ representative of the entire thermal infrared spectrum vary depending upon the emission temperature of the radiation impingent upon the cloud and upon the droplet effective radius. Values in the range 100-160 m^2 kg^{-1} have been used (see e.g. Larson et al. 2007, for a discussion). In general, κ decreases with increasing droplet effective radius.

The thermal infrared optical thickness is $\tau = \beta h$ where h is the cloud thickness. Thus, from the values given above, we see that even a modest cloud with a mixing ratio of 0.25 g kg^{-1} and a thickness of 200 m will have an infrared optical thickness of in the range 5-8 and so will be practically opaque to thermal infrared radiation. The liquid water content at the tops of stratocumuli are often significantly greater than this (e.g. Stevens et al. 2003; Wood 2005a).

Stratocumuli typically occur under conditions of large scale subsidence. The free-troposphere above them tends to be dry so that the downwelling longwave radiative flux just above the cloud top is significantly less than the upwelling flux. A short distance below the cloud top (typically ten meters or so, e.g. Slingo et al. (1982a), reproduced in Fig 20) downwelling and upwelling fluxes are almost equal, and thus the upper few meters of the cloud experiences strong cooling rates. The flux divergence across this layer is usually tens of W m^{-2} and is typically 50-90 W m^{-2} (e.g. Nicholls and Leighton 1986; Wood 2005a; Caldwell et al. 2005) with the greatest values occurring under a dry free-troposphere (Siems et al. 1993). This cooling destabilizes the stratocumulus cloud layer and the instability is generally released in the form of convective eddies. Thus longwave cooling at cloud top is frequently the primary driver of stratocumulus dynamics (Lilly 1968; Nicholls 1984, 1989; Moeng et al. 1996).

While there is strong longwave cooling *within* the upper

[7]The droplet effective radius is the ratio of the third to the second moment of the droplet size distribution $n(r)$, so $r_e = \int_0^\infty r^3 n(r) dr / \int_0^\infty r^2 n(r) dr$ and thus relates the total surface area of the droplets to their combined mass (Hansen and Travis 1974). Calculations show that r_e is sufficient to encapsulate information about the droplet size distribution in radiative transfer calculations (Hu and Stamnes 1993).

reaches of the cloud, there can also be significant cooling in the layer above cloud top (Deardorff 1981; Nieuwstadt and Businger 1984; Siems et al. 1993). The presence of highly emissive cloud below increases the free-tropospheric cooling up to a height that is dependent upon the atmospheric emissivity but which can be several kilometers above the cloud top (Stevens et al. 2005b; Caldwell and Bretherton 2008). Peak above-cloud cooling rates are found immediately adjacent to the cloud top (Van Zanten and Duynkerke 2002), but because this cooling extends over a layer significantly deeper than the turbulent interface itself, it primarily acts to reduce the strength of the inversion atop the boundary layer and thereby facilitates entrainment (Nieuwstadt and Businger 1984). However, there is evidence that a fraction of the cooling serves to enhance the subsidence rate above cloud top rather than directly cool the layer, with the partitioning between the two outcomes dependent upon the ability of the atmosphere to sustain large-scale horizontal gradients in temperature (Caldwell and Bretherton 2008). Indeed, there is a lack of definitive research on the factors controlling the fraction of total longwave flux divergence that occurs above the cloud. Both the free-tropospheric moisture and the temperature jump at the inversion are likely to be important (Nieuwstadt and Businger 1984).

Close to but above the base of the cloud there is also a net infrared flux convergence which results in heating, which can enhance the circulation within the cloud layer. Because the liquid water contents here tend to be significantly less than at the cloud top (see the adiabatic model of stratocumulus in section 2.3), and because the subcloud layer is moist, the flux divergence is spread over a deeper layer (Roach and Slingo 1979) which is typically of order 100 meters thick. If the cloud base is significantly elevated above the surface the net flux divergence across the base can be several W m^{-2} to around 20 W m^{-2} (Slingo et al. 1982a, see also Fig. 20). Away from the cloud boundaries and below the cloud the infrared flux divergence is quite small and does not contribute significantly to the net heating/cooling of the STBL.

Recently, simple analytical parameterizations for the thermal infrared heating rate profiles in idealized (plane-parallel but vertically stratified) stratocumulus clouds have been investigated (Stevens et al. 2005b; Larson et al. 2007), and the profiles are parameterized as a function of the irradiances incident on the top and bottom of the cloud layer and the liquid water profile. Use of such formulations can greatly reduce the complexity required to represent the impacts of terrestrial radiation upon stratocumulus cloud dynamics in simple models.

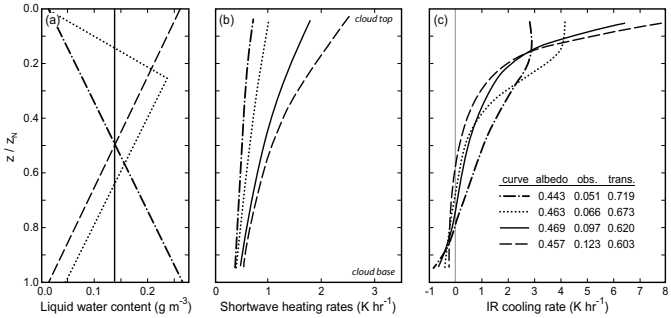

FIG. 21. Comparison of shortwave heating rates (center panel) and longwave cooling rates (right panel) in a stratocumulus-like idealized cloud layer (320 m thick, LWP=44 g m^{-2}) for different vertical profiles of liquid water content (left panel). From Stephens (1978a). (c)American Meteorological Society. Reprinted with permission. The meteorological conditions are described in Stephens et al. (1978), with a downwelling solar irradiance at the top of the cloud of 880 W m^{-2} typical for the subtropics around noon.

2) Solar radiation

All clouds scatter and absorb solar radiation (Stephens 1978a). Absorption of solar radiation is a major component of the energy budget of the STBL (e.g Caldwell et al. 2005), and is the primary driver of its diurnal cycle (Turton and Nicholls 1987; Rogers and Koracin 1992; Duynkerke and Hignett 1993, , and see also Section 5b). Scattering of solar radiation is important for the development of stratocumulus on generally longer timescales through its influence on the albedo of the cloud system and thereby its effects on the surface energy budget. It should be noted that absorption and scattering occur together and that the degree of scattering influences the radiation available for absorption.

Solar absorption

For cloud droplets containing nonabsorbing solute, practically all of the solar absorption occurs in the near-infrared, primarily for the absorption bands between 1.2-4 μm (Ramaswamy and Freidenreich 1991; O'Hirok and Gautier 1998). However, droplets formed on absorbing aerosols can absorb in the visible portion of the solar spectrum (Danielson et al. 1969; Chylek et al. 1996), and visible absorption by interstitial aerosols within the a cloud layer can also increase the total solar heating rates (Ackerman and Baker 1977; Haywood and Shine 1997; Ackerman et al. 2000). There is still some uncertainty regarding the contribution of absorbing aerosols in cloud droplets to the overall heating rate for the cloud layer (e.g Erlick and Schlesinger 2008), but for black carbon within cloud droplets the additional absorption estimated heating rates are unlikely to exceed about 10-15% of the total solar heating even in heavily polluted conditions (Chylek et al. 1996).

The fraction of incident solar radiation absorbed by a particular stratocumulus layer is of the order of a few

percent up to around 15% (Stephens 1978a; Slingo and Schrecker 1982; Slingo 1989; Taylor et al. 1996). The fractional absorption decreases with the solar zenith angle (Stephens 1978a) and increases with cloud optical depth τ up to a limit that depends upon droplet size and solar zenith angle and can reach 15% or more in clouds with $\tau > 100$ (Stephens 1978b; Twomey and Bohren 1980). For clouds of lower optical depth the fractional absorption is a function of the solar zenith angle (Stephens et al. 1984) and a logarithmic function of cloud liquid water path (Stephens 1978b; Stephens et al. 1984), with a weak dependence upon droplet effective radius (Stephens 1978a).

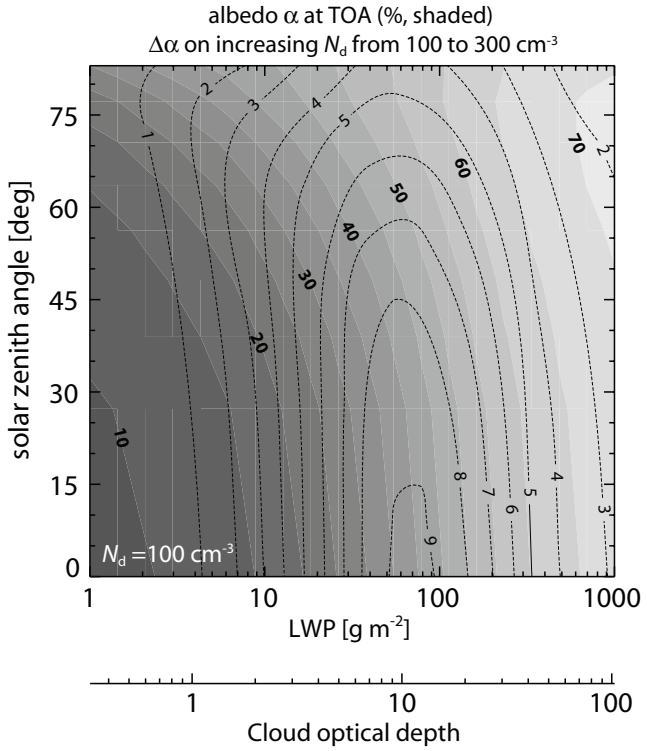

FIG. 22. Broadband solar albedo (at the top of the atmosphere) for an adiabatic plane-parallel liquid water cloud with a cloud droplet concentration of N_d=100 cm^{-3} as a function of the cloud liquid water path (LWP) and the solar zenith angle (shaded contours). Solid lines show the increase in albedo (upon increasing N_d from 100 to 300 cm^{-3}. Calculations use the Fu-Liou two-stream radiative transfer code. The tropical dry thermodynamic profile used is described in Caldwell et al. (2005).

A significant fraction of the absorption of solar radiation in the cloud layer is by water vapor (Stephens 1978a; Twomey and Bohren 1980), which increases with the temperature and thickness of the cloud layer. A doubling of the water vapor path in the cloud layer increases the fractional absorption by roughly 0.01 (Stephens 1978a).

For all solar zenith angles and cloud optical depths, the solar heating in a cloud layer is largest at the top of the cloud layer (Stephens 1978a) and decreases downwards (Fig. 21). This occurs even in clouds in which the liquid water content decreases with height (Stephens 1978a). This is chiefly because the strong scattering of solar radiation at the top of the cloud limits the absorption lower in the cloud. Vertical stratification of the cloud liquid water content (liquid water increasing upward) enhances the absorption differential between the cloud top and base (Stephens 1978a), and also increases the total absorption over that for a vertically homogeneous cloud (Li et al. 1994). For most realistic stratocumulus clouds, the shortwave absorption decreases much more slowly downwards through the cloud layer than the thermal IR cooling (with an effective e-folding distance of 100-300 m compared to only a few tens of meters for thermal IR, compare Fig. 21b,c) so that even with strong solar insolation the net effect of radiative heating is, in most cases, to destabilize the cloud layer.

Scattering

Most stratocumulus clouds reflect a significantly greater fraction of the incident solar radiation than they absorb (e.g. Stephens 1978a), hence their large albedo (Stephens et al. 1978). The albedo of liquid clouds is governed by the cloud optical thickness[8] τ, the single scattering albedo ω, the asymmetry parameter, and the solar zenith angle θ_0 (Liou 1992). In the visible and nonabsorbing parts of the near infrared $\omega = 1$ and $g = 0.82 - 0.86$ (Liou 1992), so that τ and θ_0 alone control the cloud albedo. Because much of the incoming solar irradiance is at wavelengths where absorption is negligible (Slingo and Schrecker 1982), conservative scattering approximations can be made to the radiative transfer equation (see King and Harshvardhan 1986, for a comparison of approaches), which yields useful analytical expressions that are quite accurate.

Figure 22 shows the albedo at the top of the atmosphere as a function of cloud optical depth (or liquid water path) and solar zenith angle for a plane-parallel adiabatic liquid cloud with a droplet concentration of N_d=100 cm^{-3}. Stratocumulus optical thicknesses vary tremendously even for completely overcast stratocumulus fields (e.g. Roach 1961), ranging from less than 1 to more than 20 (Hahn et al. 2001), and locally can be as high as 50 or more (Nakajima et al. 1991; Szczodrak et al. 2001). For a solar zenith angle of 30°, this represents a range of visible albedos from less than 10% to over 70% (Fig. 22).

Figure 1 demonstrates that within a region of arbitrary size containing stratocumulus, there is typically a large range of cloud albedo reflecting large spatial optical thickness variability. This emphasizes the importance of mesoscale organization (Wood and Hartmann 2006) and highlights the tremendous variability on all spatial scales

[8]Cloud optical thickness τ is the vertical integral of the volume extinction coefficient (see e.g. Petty 1994, page 190-191).

(see Section 2b). The concavity of the albedo-optical thickness relationship ($d\alpha/d\tau$ decreases with τ) means that the area-mean albedo of a spatially variable cloud field is lower than for the equivalent homogeneous field with the same mean τ (Cahalan et al. 1994), so that the effective optical thickness is lower than that for a homogeneous cloud. However, for regions of the oceans dominated by marine stratocumulus clouds the correction to τ is generally 10% or less (Rossow et al. 2002).

For stratocumulus, in which most droplets are significantly larger than the wavelength of solar radiation, the cloud optical thickness τ depends upon the vertical integral of the ratio of cloud liquid water content ρq_l to the droplet effective radius r_e:

$$\tau = \frac{3}{2\rho_w} \int_0^h \frac{\rho q_l}{r_e} dz \tag{9}$$

where ρ_w is the density of liquid water, ρ is the air density, q_l is the liquid water mixing ratio, and h is the cloud thickness ($z = 0$ is the base of the cloud). The simplest cloud model is one with no vertical stratification in q_l or r_e and gives

$$\tau = \frac{3L}{2\rho_w r_e} \tag{10}$$

where $L = \int_0^h \rho q_l dz$ is the liquid water path. However, q_l typically increases approximately linearly with height (see Section 3a above) with little vertical stratification in cloud droplet concentration (Wood 2005a), so that r_e increases as $z^{1/3}$ (Brenguier et al. 2000b; Szczodrak et al. 2001; Bennartz 2007). For this case,

$$\tau = \frac{9L}{5\rho_w r_e(h)} \tag{11}$$

Expressed in terms of the droplet number concentration N_d,

$$\tau = A_v \frac{(N_d k)^{\frac{1}{3}} L^{\frac{5}{6}}}{\rho_w^{\frac{2}{3}} \Gamma^{\frac{1}{6}}} \tag{12}$$

where $A_v = \frac{9}{5}(8\pi^2/9)^{\frac{1}{6}} = 2.585$, and k is the ratio of the cubes of the mean volume radius and the effective radius (Martin et al. 1994).

Since N_d is primarily determined by the availability of CCN, equation (12) neatly expresses the impacts of microphysical variability on the cloud optical thickness. Figure 22 also shows the increase in albedo upon tripling N_d from 100 to 300 cm^{-3} while keeping L constant, demonstrating Twomey's findings (Twomey 1974, 1977) that there is considerable sensitivity of the cloud albedo to changes in cloud droplet concentration. The microphysical susceptibility of the albedo α (defined as $d\alpha/dN_d$) is maximal for an albedo close to 50% (Platnick and Twomey 1994), corresponding to liquid water paths in the range 50-200 g m^{-2} (Fig 22). Most stratocumuli have liquid water paths in this range (e.g. Wood 2005a; Zuidema et al. 2005; O'Dell et al. 2008), making them particularly sensitive to increases in cloud droplet concentration caused by increased anthropogenic aerosol concentrations. Figure 22 also shows heightenend microphysical susceptibility for high sun. This is because α depends more strongly upon cloud optical thickness at low solar zenith angle (King and Harshvardhan 1986).

c. Large scale divergence and subsidence

By continuity, the large scale divergence profile $D(z)$ determines the subsidence rate profile $w_s(z)$, and hence the rate at which the boundary layer would become shallower in the absence of entrainment. Over the oceans it is generally assumed that $D(z)$ is independent of height in the lower troposphere where stratocumuli reside, so that the subsidence rate increases linearly with height[9]. Then, given an entrainment rate w_e, the equilibrium boundary layer depth is $z_i^{eq} = w_e/D$. Since the STBL depth strongly influences many of its key structural and dynamical properties, D has an important influence upon stratocumulus (Randall and Suarez 1984; Zhang et al. 2009). This response is nonlinear since low divergence rates permit the MBL to grow sufficiently deep so that is decouples and can no longer support stratocumulus, while strong divergence can lower the MBL top below the LCL resulting in no clouds (Randall and Suarez 1984; Weaver and Pearson 1990; Zhang et al. 2009).

For the regions of the semi-permanent subtropical marine stratocumulus, the mean low-level divergence ranges from roughly 2-4$\times$ 10^{-6} s^{-1} (Zhang et al. 2009), leading to mean subsidence rates at the STBL inversion of 2-4 mm s^{-1} (Wood and Bretherton 2004). The low-level divergence then provides a timescale $\tau_{top} = D^{-1}$ which is the relaxation timescale over which the inversion height (cloud top height) responds to instantaneous forcing changes (Schubert et al. 1979b). Thus, given conditions favorable for stratocumulus, τ_{top} is 3-6 days, which is quite slow compared with typically more rapid forcing changes along airmass trajectories. This implies that the STBL depth is rarely in equilibrium with its instantaneous forcings.

Reduction in surface divergence, in addition to the more well-studied impact of increasing SST (Krueger et al. 1995a; Wyant et al. 1997, e.g.), can also play a role in the transition from shallow to deep MBL over the subtropical oceans (Norris and Klein 2000; Wood and Bretherton 2004), although recent research suggests that the lagrangian transition from overcast stratocumulus to more broken clouds downstream occurs upstream of the significant decrease in

[9]This is broadly consistent with high resolution analyses (e.g. Wood et al. 2009a), but it is difficult to know how good this assumption is since different reanalyses do not show consistent behavior (Stevens et al. 2007).

divergence (Sandu et al. 2010).

d. Surface fluxes

In the forcing vector (Eqn. 8), V, T_{sfc}, and q_{sfc} determine the surface sensible and latent heat fluxes via bulk flux formulations (e.g. Hartmann 1994). This requires knowledge of the surface air temperature and humidity which are internal variables of the STBL system.

e. Free-tropospheric temperature, static stability, and moisture

Much research has focused upon the influence of lower tropospheric static stability in controlling the coverage of low clouds, particularly over the oceans (Slingo 1987; Klein and Hartmann 1993; Wood and Bretherton 2006, inter alia). To provide a measure of static stability that can be considered a parameter external to the boundary layer system, the difference in potential temperature between some level in the free-troposphere (free of cloud influence) and the temperature of the surface is typically chosen (this is often termed the *lower tropospheric stability*, or LTS). Over the oceans the difference between the surface temperature and the surface air temperature is typically small compared with the stability itself and so several studies have used the surface air temperature in place of the surface temperature itself. Thus, in Eqn (8), it is essentially the difference $T_+ - T_{sfc}$ that defines the LTS. There is a remarkably good correlation between seasonal mean LTS and low cloud amounts over the major regions of tropical/subtropical stratocumulus (Klein and Hartmann 1993), and such a correlation works equally well over the midlatitude oceans if one accounts for the temperature-dependent (and therefore latitude-dependent) stability of the free-troposphere above the STBL (Wood and Bretherton 2006). Strong static stability means that more work must be done to maintain a boundary layer of a given depth through entrainment. This favors shallower and therefore more well-mixed boundary layers (Wood and Bretherton 2004; Wood and Hartmann 2006), with stronger capping inversions. In such boundary layers the cloud layer is strongly coupled to the ocean moisture source and the strong capping inversion results in horizontally extensive, albeit thin, saturated layers.

Mixed layer theory and eddy resolving cloud models indicate that the free-tropospheric moisture q_+ should also play a significant role in determining cloud thickness and height. All else being equal, dry free-tropospheric air favors a more elevated cloud base since the entrainment of said air into the STBL causes a lifting of the LCL. One might imagine that this would give rise to thinner clouds. However, the evaporative enhancement of entrainment (Section 3c) is greater for a drier free-troposphere, and the longwave cooling stronger, and the stronger entrainment these produce causes higher cloud tops. Within a mixed layer construct, equilibrium cloud thickness is actually a *decreasing* function of q_+. However, stronger entrainment favors a greater likelihood of decoupling-induced cloud breakup (See Section 4c). Therefore, the role of free-tropospheric moisture in determining stratocumulus properties is actually rather complicated. Further, since there is a strong correlation between the free-tropospheric humidity, and radiatively-driven subsidence, and stability, it is very difficult to isolate q_+ impacts from other meteorological controls.

f. Condensation and evaporation

Although longwave cooling may be viewed as the primary driver of convection in most stratocumulus, both condensation and evaporation of liquid water typically play important roles in the buoyant generation of turbulence in the STBL (Lilly 1968; Schubert et al. 1979a; Moeng et al. 1992; Bretherton and Wyant 1997). The mean profile of temperature in the cloud layer reflects the latent warming associated with the net conversion of vapor to liquid water required to form the cloud. However, if updrafts are warmer and downdrafts cooler than the mean profile, then the updrafts are more positively buoyant (and the downdrafts more negatively buoyant) than they would have otherwise have been. This is a source of buoyant turbulence production, and acts to strengthen the existing circulation. This asymmetry in between updrafts and downdrafts is primarily driven by differences in total water content between upward and downward moving eddies such that at a given height in cloud, the upward moving parcel has a higher liquid water content. Thus, the buoyant production of turbulence in the cloud by latent heating is strongly related to the vertical flux of liquid water by the eddies (Bretherton and Wyant 1997).

Aircraft studies of the STBL frequently show large increases in buoyancy flux immediately above stratocumulus cloud base (Nicholls and Leighton 1986; Duynkerke et al. 1995). Since these jumps are usually associated with significant vertical liquid water fluxes, this confirms that condensation/evaporation typically has a significant impact upon buoyancy production in the STBL.

In the absence of significant supersaturations in the cloud layer, the liquid water flux in the cloud layer is primarily governed by the vertical flux of water vapor into the cloud layer (Bretherton and Wyant 1997). However, recent large eddy simulations suggest that the departures from saturation within cloudy updrafts and downdrafts may be sufficient to significantly reduce (in some cases by tens of percent) the vertical liquid water flux in stratocumulus, and therefore the rates of released latent heat in updrafts and evaporative cooling in downdrafts (Kogan and Martin 1994; Wang et al. 2003). This *microphysically-limited condensation* is more acute for low droplet concentration N_d since the equilibrium supersaturation is inversely proportional to N_d (Squires 1952; Kogan et al. 1995). For

example, Kogan and Martin (1994) find that condensation rates are only a few percent lower than those assuming saturation in a stratocumulus case with $N_d = 400$ cm^{-3} but are almost 50% lower when $N_d = 25$ cm^{-3}. Further, modeling studies demonstrate that microphysically-limited condensation has effects upon the mean fields, and most importantly the cloud liquid water path (Kogan and Martin 1994; Wang et al. 2003; Lee et al. 2009; Lee and Penner 2010). Thus, besides this effect being important for determining the mean fields, it may constitute a significant aerosol indirect effect that has yet to be quantified on the regional or global scales (Lee and Penner 2010).

g. Precipitation

Stratocumulus clouds, especially those in marine airmasses, frequently produce light precipitation, mostly in the form of drizzle (Ohtake 1963; Nicholls and Leighton 1986; Petty 1995; Austin et al. 1995; Pawlowska and Brenguier 2003; Wood 2005a; Van Zanten et al. 2005; Leon et al. 2008). Drizzle (defined here as radar reflectivities exceeding -17 dBZ) is found 20-40% of the time in the regions of persistent marine stratocumulus (Leon et al. 2008; Wood et al. 2009a).

Much has been learned in recent years about the importance of precipitation as a process integral to the dynamics, structure and evolution of stratocumulus cloud systems. Drizzle begins to exert a significant influence on the dynamics of stratocumulus when the precipitation rate reaches a few tenths of a mm day^{-1}. A surface precipitation rate of 1 mm day^{-1} equates to a warming of the drizzle-producing cloud layer of 29 W m^{-2} which is a significant fraction of the longwave cooling driving the stratocumulus convection. Precipitation rates in stratocumulus tend to peak close to the cloud base and decrease significantly toward the top of the cloud (Wood 2005a), and so drizzle is often characterized by its rate R_{cb} at cloud base. Based on the forcing induced by the drizzle, values of R_{cb} can be classified as light ($R_{cb} < 0.5$ mm day^{-1}), moderate ($0.5 < R_{cb} < 2$ mm day^{-1}), and heavy ($R_{cb} > 2$ mm day^{-1}).

The effects of drizzle upon cloud dynamics are complex and are only just beginning to be fully appreciated. Besides warming and drying the cloud layer and thereby inducing stratification of the STBL, drizzle also evaporates readily below cloud base owing to the small size of drizzle drops. Mean volume radii $r_{v,D}$ of drizzle drops are typically in the range 30-100 μm at cloud base (Wood 2005a; Wood et al. 2010). The evaporation scale height (distance below cloud base over which precipitation rate falls off due to evaporation) grows rapidly over this range, from only 100 m for $r_{v,D} = 30$ μm to 400 m for $r_{v,D} = 50$ μm, to over 2 km $r_{v,D} = 100$ μm. Thus, the degree to which drizzle evaporates in the subcloud layer, is dependent upon the microphysics of drizzle formation. This is importance since evaporating drizzle can destabilize the subcloud layer, which can drive stronger penetrating cumulus (Jiang et al. 2002), cause cold pool formation (Jensen et al. 2000; Xue et al. 2008a), and enhance mesoscale variability and dynamics (Comstock et al. 2005, 2007; Savic-Jovcic and Stevens 2008; Xue et al. 2008a). Whether the drizzle evaporates or not, modeling studies show that drizzle tends to promote STBL stratification (Nicholls 1984; Wang and Albrecht 1986; Stevens et al. 1998; Mechem and Kogan 2003; Ackerman et al. 2009) and reductions in vertical wind variance (Stevens et al. 1998; Ackerman et al. 2009). Increasing drizzle may also reduce cloud liquid water path (Ackerman et al. 2009) and cloud cover (Savic-Jovcic and Stevens 2008; Xue et al. 2008b), although this does not always appear to be the case (Ackerman et al. 2004). In some cases drizzle may actually *increase* cloud thickness if it reduces the entrainment of very warm and dry air into the STBL (Ackerman et al. 2004; Wood 2007).

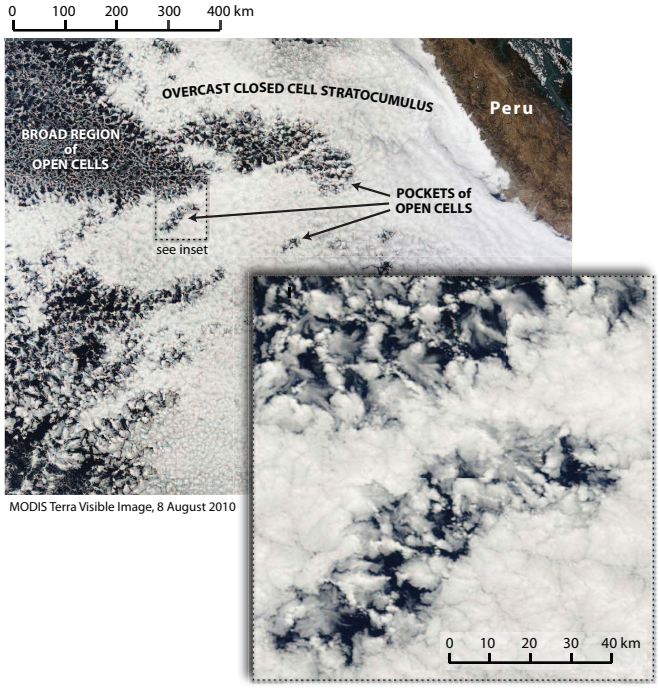

FIG. 23. Visible imagery from MODIS on the NASA Terra satellite showing Pockets of Open Cells (POCs) embedded in overcast closed cell marine stratocumulus over the tropical southeastern Pacific Ocean. The inset shows an enlarged region detailing the cellular structure within a POC.

The effects of heavy drizzle with rates of several mm day^{-1} are likely responsible for the sharp transitions from closed to open mesoscale cellular convection observed in regions of extensive marine stratocumulus (Savic-Jovcic and Stevens 2008; Wang and Feingold 2009). Often the open cells can be entirely surrounded by closed cells, in which case they have become known as *pockets of open cells* (POCs), as discussed in Bretherton et al. (2004) and Stevens et al. (2005a). Figure 23 shows an example of POCs, together

with broader regions of open cells, over the southeastern Pacific Ocean. The few in-situ case studies of POCs indicate that sharp cloud microphysical and aerosol transitions accompany the macroscale cloud transitions (Van Zanten and Stevens 2005; Sharon et al. 2006; Wood et al. 2008, 2010), and that the POCs contain stronger and larger drizzling cells (Comstock et al. 2007). The transition between the open and closed cell regions has also been observed to drizzle strongly (Comstock et al. 2007; Wood et al. 2010).

1) Phase of stratocumulus precipitation

There is significant evidence that much of the precipitation falling from clouds with tops colder than a few K lower than freezing is in the form of snow (Henrion et al. 1978; McFarquhar et al. 2007), but liquid precipitation has been observed to fall from supercooled stratocumulus even with tops as cold as -10 C (Huffman and Norman 1988), or even colder (Kajikawa et al. 2000). Drizzle drops are frequently present in Arctic stratocumulus clouds (Hobbs and Rangno 1998; Lawson et al. 2001). There is evidence that glaciation in supercooled liquid clouds tends to occur simultaneously with the production of drizzle drops (Rangno and Hobbs 1991). Artificial seeding of supercooled stratocumulus can create significant precipitation (Locatelli et al. 1983). Modeling studies show that depletion of ice nuclei is necessary for supercooled drizzle to form (Rasmussen et al. 2002). However, the process of ice formation in supercooled stratocumulus is still poorly understood (Cantrell and Heymsfield 2005) and is not considered further in this review.

Diurnal cycle

There are few studies describing the diurnal cycle of precipitation falling specifically from stratocumulus clouds, but a number of studies indicate that over both land and ocean the frequency of occurrence of drizzle precipitation tends to maximize during the night and early morning hours (Dai 2001; Bretherton et al. 2004; Stevens et al. 2005a; Sears-Collins et al. 2006; Leon et al. 2008; Serpetzoglou et al. 2008) when cloud thickness and liquid water path tend to be at their greatest (see Section 5b above). In more decoupled STBLs, the cumulus rising into stratocumulus appear to produce heavier drizzle during the late afternoon (Miller et al. 1998). This may help to explain why there are *daytime* maxima in the precipitation observed by the Tropical Rainfall Measuring Mission (TRMM) in regions of persistent tropical and subtropical marine stratocumulus, particularly downwind of the maxima in cloud cover (Yang and Smith 2006), since TRMM can detect only the heaviest drizzle events (radar reflectivity >17 dBZ).

7. Microphysics of stratocumulus

Details of the microphysical properties of stratocumulus clouds are important for setting their albedo (see Section 6b above) and for their ability to form precipitation (see e.g. Wood 2005a, for a discussion). Microphysical processes in stratocumulus are therefore critical for understanding the aerosol indirect effects on climate, and so we devote the remainder of this review to a discussion of key elements of these processes in stratocumulus clouds. Of all microphysical parameters it is the mean cloud droplet size that is the single most influential. Through (11), we see that the droplet radius influences the cloud optical thickness. From our understanding of the dependence of the collection efficiency upon the droplet size (e.g. Long 1974; Liu and Daum 2004; Wood 2006), we can appreciate its potential impacts upon precipitation formation. Finally, latent heating/cooling rates depend upon the rate at which the population of cloud droplets grows/evaporates in a supersaturated/subsaturated environment which is itself dependent upon the mean droplet size (e.g. Pruppacher and Klett 1997). This hints at possible links between cloud droplet size and cloud dynamics (Arnason and Greenfield 1972), even without consideration of precipitation.

For a given cloud liquid water content, the droplet radius is determined primarily by the cloud droplet concentration N_d. In this section we focus primarily upon the factors controlling N_d and then assess its impacts upon cloud dynamics and precipitation formation.

a. Cloud droplet concentration and controlling factors

1) Geographical distribution

Cloud droplet concentrations N_d in stratocumulus clouds range from fewer than 10 cm^{-3} in extremely aerosol-rare conditions (typically only observed over the oceans) to over 1000 cm^{-3} in airmasses with high aerosol concentrations. Figure 24 shows a global estimate of the annual mean value of N_d from warm, extensive stratiform clouds obtained using data from the Moderate Resolution Imaging Spectroradiometer (MODIS). There is a remarkably rich spatial variability in N_d (note the quasi-logarithmic color scale), with the most striking being one of great ocean-continent contrasts. This picture is corroborated by in-situ studies, collations of which are provided in Martin et al. (1994), Miles et al. (2000), Yum and Hudson (2002), and Fountoukis et al. (2007) *inter alia*.

Over the oceans the geographic variability in N_d is consistent with previous findings from Bennartz (2007) and Hu et al. (2007), with high concentrations ($N_d > 200$ cm^{-3}) typically found downwind of continental regions (e.g. off the Southern Californian coast, off the coast of Chile, off the eastern seaboard of the United States, the East China Sea and the Sea of Japan, and in the North Sea), and lower values over the remote oceans, especially those in the subtropics and tropics, where concentrations of 50 cm^{-3} or less are common. There is some in-situ observational support for modest increases in N_d towards the Southern Ocean

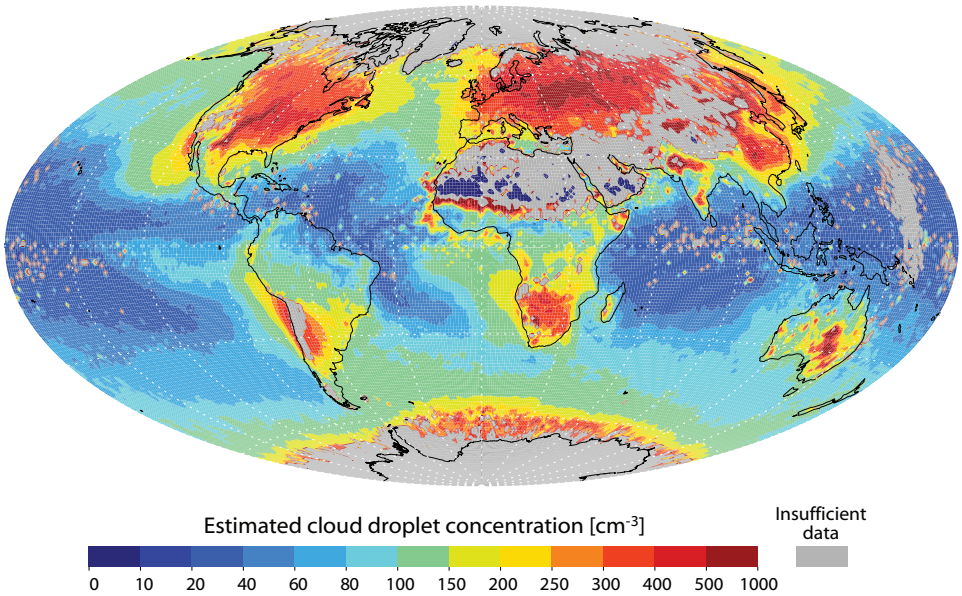

FIG. 24. Global mean cloud droplet concentration N_d for horizontally extensive liquid clouds estimated using visible/near-infrared retrievals of cloud top effective radius and optical thickness (King et al. 1997) from the Moderate Resolution Imaging Spectrometer (MODIS). Four years (2001-2004) of Level-3 daily aggregated MODIS data at 1°×1°resolution are used to create the plot. Data are screened to include only liquid clouds (cloud top temperature warmer than 270 K) and only those days for which at least 80% of the 1°×1°available pixels in each box are cloudy. Those regions for which fewer than 10 days from the possible 1461 days satisfy the selection criteria are colored gray. Droplet concentration is estimated from the MODIS retrievals using the method described in Bennartz (2007) assuming an adiabatic cloud layer.

and Antarctica (Yum and Hudson 2004) which has been attributed to the highly productive oceans there (e.g. Boers et al. 1994). However the values of 300 cm^{-3} or more close to the Antarctic peninsula seen in the MODIS data might reflect problems with the MODIS retrievals at high solar zenith angle or over ice surfaces, and the few in-situ measurements of aerosols and CCN do not support such high values of N_d (Odowd et al. 1997; Koponen et al. 2003).

Continental regions of the northern hemisphere show the greatest concentrations (Fig. 24), with mean values of N_d exceeding 200 cm^{-3} over and downwind of heavily industrialized areas, in accordance with in-situ measurements in these regions. But there are also continental regions (e.g. northern Amazonia and central Africa) with low concentrations.

2) Factors controlling cloud droplet concentration

The cloud droplet concentration in stratocumuli is limited by the availability of cloud condensation nuclei (Martin et al. 1994), but is also sensitive to the updraft strength. Based upon a well-developed understanding of the condensational growth process (see e.g. Pruppacher and Klett 1997, for a detailed treatment), Twomey (1959) derived an approximate analytical formulation for the number of droplets activated in an adiabatic parcel as a function of the CCN spectrum and the updraft speed[10]. Extensions to Twomey's formulation have been derived that account for more realistic variability in aerosol size distributions, kinetic effects, and more accurate treatments of the condensation rate integral (Cohard et al. 1998; Abdul-Razzak et al. 1998; Abdul-Razzak and Ghan 2000; Nenes and Seinfeld 2003), and this general approach forms the basis for aerosol activation parameterizations used in large scale models (Khain et al. 2000; Cohard and Pinty 2000). A recent summary of progress and outstanding questions in this area can be found in McFiggans et al. (2006).

In general, both the aforementioned theoretical treatments and observational attempts to constrain the droplet activation process (Snider et al. 2003; Fountoukis et al. 2007) demonstrate the importance of vertical velocity and the characteristic radius of the aerosol size distribution as primary variables determining the fraction f_{act} of aerosols that will activate. Aerosols composed of soluble salts activate at a critical supersaturation $S_* \propto r_{dry}^{-3/2}$ (Junge and McLaren 1971; Pruppacher and Klett 1997), where r_{dry} is the dry radius of the salt. Observations of atmospheric aerosols generally support such a relationship (McFiggans et al. 2006; Dusek et al. 2006), although some deviations are found, mostly because of incomplete aerosol solubility (Hudson 2007; Conant et al. 2004).

[10] Twomey's derivation is reproduced Pruppacher and Klett (1997).

(i) Dependence of N_d upon vertical velocity

For a given aerosol size distribution, stronger ascent raises the peak supersaturation and therefore reduces the minimum size of CCN activated, resulting in a higher f_{act} (Twomey 1959). The sensitivity to vertical velocity weakens for high values of f_{act} (Abdul-Razzak et al. 1998; McFiggans et al. 2006), which most typically occurs in clean conditions (Glantz et al. 2003; Snider et al. 2003).

(ii) Dependence of N_d upon aerosol properties

With a monomodal aerosol distribution, for a given aerosol concentration and updraft speed f_{act} is theoretically predicted to increase with the mean radius of the aerosols (Abdul-Razzak et al. 1998; McFiggans et al. 2006). This is expected despite lower peak supersaturations in the ascending parcel for the larger, and therefore more rapidly supersaturation-depleting particles. The sensitivity to mean radius is expected to be greatest at low updraft speeds (e.g. Snider et al. 2003) characteristic of stratocumulus, but observations to support this appear to be lacking, presumably for want of sufficient data to control for aerosol concentration and updraft speed.

For updrafts of less than 1 m s^{-1} that prevail in most stratocumulus clouds (e.g. Nicholls 1989), f_{act} is not strongly dependent upon the aerosol concentration except at very high concentrations ($\sim$300 cm^{-3} or higher) or when the mean radius is very small. Thus, in clean conditions the number of activated droplets in stratocumuli approaches the accumulation mode aerosol concentration N_a, and observations generally support this (Martin et al. 1994; Leaitch et al. 1996; Gultepe and Isaac 2004; Twohy et al. 2005; Lu et al. 2007). As N_a increases beyond $\sim$ 200 cm^{-3}, the droplet concentration increases more gradually, but observations still show a good case-to-case correlation between N_a and N_d (Martin et al. 1994), leading to the conclusion that accumulation mode aerosol concentration is the primary determinant of the cloud droplet concentration in stratocumulus clouds. Within a particular stratocumulus cloud system, where N_a does not strongly vary, there is evidence that variability in N_d is primarily controlled by variability in updraft speed (Lu et al. 2007, e.g.).

Increasing the breadth of the aerosol size distribution, either through broadening of a single mode (Abdul-Razzak et al. 1998), or the introduction of a coarse aerosol modes (Ghan et al. 1998; O'Dowd et al. 1999b), also leads to a reduced f_{act} due to increased competition for vapor from larger particles. When broadening is related to sea-salt particles as is the case at wind speeds over the ocean in excess of $\sim$ 7 m s^{-1} (O'Dowd et al. 1999a), the reduction tends to be greatest at high windspeed and high N_a and is estimated to reduce the total N_d by $\sim$ 20% for wind speeds of 15 m s^{-1} (Ghan et al. 1998).

Under most circumstances in which stratocumulus clouds form, chemical effects have a more limited impact upon N_d than do N_a, the aerosol size, and the updraft speed (Dusek et al. 2006; Feingold 2003) but there can be situations in which reduced solubility (Fountoukis et al. 2007; Hudson 2007), surface-tension changes (Facchini et al. 1999; Nenes et al. 2002), reductions in the mass accommodation coefficient due to film-forming compounds (Feingold and Chuang 2002), and the presence of additional condensible vapors (Kulmala et al. 1993) may have important impacts upon N_d, especially in highly polluted conditions (Nenes et al. 2002). An excellent review of these effects is provided in (McFiggans et al. 2006).

b. Microphysical impacts upon precipitation

The initial formation of drizzle in stratocumulus clouds requires coalescence of cloud droplets because growth by condensation to sizes significantly larger than 20 μm takes too long (Jonas 1996). During the initial stages of precipitation formation, where small embryonic drizzle drops are produced by the coalescence of condensationally grown droplets, coalescence growth is hindered for two reasons: (a) collisions between small droplets have a low efficiency (e.g. Hall 1980; Pruppacher and Klett 1997); (b) droplet size distributions (DSDs) become narrower with time under most condensational growth conditions because the deposition process is surface area limited (Howell 1949; Mordy 1959).

Collision efficiencies $E(R, r)$ between small ($R, r < 30\mu$m) water drops of radii R and r falling in still air are well known[11]. Recent measurements (Vohl et al. 2007) have filled in important gaps missed in earlier laboratory studies and generally confirm earlier theoretical treatments (see e.g. Pinsky et al. 2001, for a discussion and for tabulated efficiencies).

1) Autoconversion

The gravitational collection kernel $K(R, r)$ is the probability that a drop of radius R will collect another with

[11] Current uncertainties in collision efficiencies are those stemming from the effects of small-scale turbulence on the collision-coalescence process (Jonas 1996; Vaillancourt and Yau 2000; Pinsky and Khain 1997; Xue et al. 2008b). Recent attempts to use theory and direct numerical simulation to quantify the effects of small-scale turbulence suggest that turbulent dissipation rates ϵ required for droplet inertial effects to cause significant increases in the rapidity of precipitation initiation (10-20%) are of the order 10-100 cm^2 s^{-1} (Xue et al. 2008b). While there are certainly local regions within some stratocumulus clouds in which ϵ can reach these values (Siebert et al. 2006), we should note that 10-20% increases in the rapidity of precipitation formation can also be achieved with relatively modest increases in the liquid water content in typical stratocumuli (Table 5 in Xue et al. 2008b), or by small increases in the mean radius of the droplets (e.g. Gerber 1996). Thus, while small-scale turbulence may play a role in the initiation of precipitation in stratocumulus, its effects are likely to be quite modest and difficult to isolate from those related to cloud spatiotemporal variability.

radius r in a unit time if both drop sizes exist in unit concentration. This forms the heart of the stochastic collection equation (SCE) from which we can express the rate (termed the *autoconversion rate* A_c) at which mass crosses a particular radius threshold through coalescence (Beheng and Doms 1986; Wood and Blossey 2005, e.g.):

$$A_c = \frac{4}{3}\pi\rho_w \int_0^{r_0} \left[\int_{(r_0^3 - R^3)^{\frac{1}{3}}}^{r_0} K(R,r) r^3 n(r) dr \right] n(R) dR \tag{13}$$

As demonstrated by Long (1974), $K(R,r)$ is well represented by the square of the collector drop mass for $R <$ 50 μm (i.e. $K(R,r) \approx \kappa R^6$), and this can be used to provide an analytical approximation to (13). Following (e.g Liu and Daum 2004), if one sets the lower limit of the inner integral in (13) to zero, essentially allowing all coalescence events between cloud droplets to contribute to A_c, then

$$A_c \approx \kappa L \int_0^{r_0} R^6 n(R) dR \tag{14}$$

In this form, the autoconversion rate is presented as the product of the cloud water content L and the sixth moment of the cloud DSD. Thus, the dependence of the autoconversion rate upon the droplet size is clearly evident. Defining $R_i = \left[\int r^i n(r)dr / \int n(r)dr\right]^{1/i}$, as a the modal radius for the ith moment, we can write (14) as $A_c \approx \kappa N L R_6^6$.

For cloud DSDs in stratocumulus, the modal radii R_i are generally well correlated with one another[12]. Thus, we can write $r_6 = \beta_6 r_3$ and then $A_c \approx \kappa N_d L R_3^6$ and thus, since $L = \frac{4\pi\rho_w}{3} N_d R_3^3$, we reproduce Liu and Daum's result:

$$A_c \approx \left(\frac{3}{4\pi\rho_w}\right)^2 \kappa \beta_6^6 \frac{L^3}{N_d} \tag{15}$$

Despite overestimating the true A_c by as much as an order of magnitude (see e.g. Wood 2005b; Wood and Blossey 2005), Eqn (15) does reproduce dependencies of A_c upon L and N_d that are consistent with observational data (Wood 2005b), and thus clearly demonstrates the importance of the cloud droplet concentration N_d in modulating the rate at which coalescence between cloud droplets initiates the precipitation process. Interestingly, the dependencies of A_c on L and N_d are similar to those obtained using large eddy simulations with explicit microphysics (Khairoutdinov and Kogan 2000) but differ strongly from some widely used parameterizations. Most notably, the first bulk scheme ever used (Kessler 1969) does not have any dependency upon N_d. A summary of existing parameterizations for A_c is provided in (Liu and Daum 2004), and a comparison with observationally-derived rates can be found in (Wood 2005b).

[12]For example, using the various cloud DSD measurements from twelve drizzling and nondrizzling stratocumulus cases described in Wood (2005b) reveals that the correlation coefficient between r_6 and r_3 is 0.98. This behavior is also demonstrated in Martin et al. (1994) which considers the relationship between r_2 and r_3. For a discussion of these relationships see the Appendix in Liu and Daum (2004).

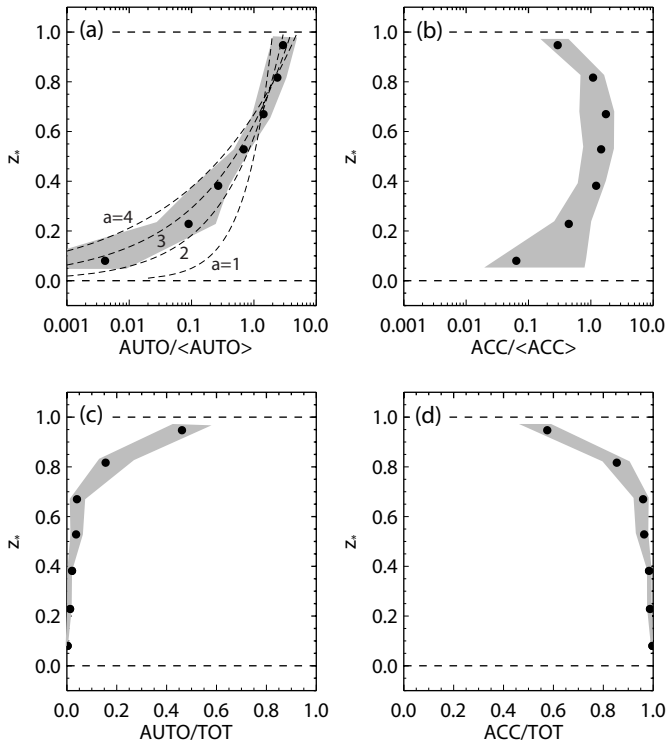

FIG. 25. Composite profiles from 12 cases of weakly to moderately drizzling stratocumulus of (a) autoconversion and (b) accretion rate normalized with the case mean in each case. The normalized height z_* is 0 at cloud base and 1 at cloud top. The process rates were derived by applying the SCE to observed drop size distributions. The lower panels show the fraction of total drizzle liquid water content production rate (autoconversion+accretion) contributed by (c) autoconversion and (d) accretion. In all plots solid circles are median values for each height bin; gray area encompass 25th and 75th percentiles. The dashed curves in (a) show the autoconversion rate expected for a cloud with a linear increase in cloud liquid water content with height and where autoconversion depends upon liquid water content to the power b, with $b = 1, 2, 3, 4$. From Wood (2005b). (c)American Meteorological Society. Reprinted with permission.

Given that the greatest values of L usually occur towards the top of stratocumulus layers (see Section 3a), from Eqn(15) it is clear that autoconversion is most important near cloud top (see also Fig. 25).

2) ACCRETION

Much of the precipitation liquid water content L_D in drizzling stratocumulus is ultimately produced by the accretion (collection) of cloud droplets by falling drizzle drops rather than by autoconversion (see Fig. 25). Even near cloud top, where autoconversion is maximal, accretion tends to contribute around 50% to the mass transfer from cloud

to precipitation. Maximum production of L_D by accretion occurs in the mid to upper levels of the cloud (Wood 2005b).

Differences between the various bulk formulations in the literature for the mass accretion rate K_c are much less than those for the autoconversion rate (Wood 2005b), primarily because the collision efficiency does not vary strongly for collector drops with radii greater than 50-100 μm and cloud droplets larger than 5 μm. Because of this, and because the terminal velocity of drops with $r > 40$ μm depends linearly upon r (Pruppacher and Klett 1997), for most bulk formulations K_c approximately scales with the product of the cloud and rain water mass (Kessler 1969; Tripoli and Cotton 1980; Beheng 1994; Khairoutdinov and Kogan 2000).

3) Precipitation rate

Recent field studies have shone important new light on the importance of cloud droplet concentration in driving variability in precipitation in stratocumulus. Bretherton et al. (2004) shows observations from the southeast Pacific stratocumulus region suggesting that drizzle rates in stratocumulus can be reduced in periods when N_d increases. A survey of in-situ observations in the literature (Wood 2005a) indicates that precipitation rates at cloud base decrease as N_d increases, and other recent studies in marine stratocumulus are consistent with this (Lu et al. 2007), as are observations from ship-tracks embedded in these clouds (Ferek et al. 2000; Lu et al. 2007). Recent spaceborne radar measurements are also consistent with drizzle suppression with increasing cloud droplet concentration (for fixed liquid water path) in marine stratocumulus regions (Leon et al. 2008). Large eddy simulations of stratocumulus with explicit representation of microphysics show similar suppression of precipitation as N_d is increased (Ackerman et al. 1995; Jiang et al. 2002; Savic-Jovcic and Stevens 2008).

Several recent observational studies of marine stratocumulus have found that precipitation rate at cloud base R_{cb} decreases with N_d but increases strongly with the cloud thickness h (Pawlowska and Brenguier 2003; Van Zanten et al. 2005), or liquid water path (Comstock et al. 2004; Kubar et al. 2009; Wood et al. 2009b). Some of these results are summarized in Fig. 26 taken from (Brenguier and Wood 2009). There remain significant discrepancies between the observationally-derived scalings, which are likely attributable in part to differences in the observational strategies used to determine the precipitation rates, cloud thickness, and N_d (see e.g. Geoffroy et al. 2008). However, it is also possible that factors (e.g. turbulence Nicholls 1987; Baker 1993; Austin et al. 1995) other than simply cloud thickness and droplet concentration play important roles in determining the precipitation rate. Further, recent observational and modeling results suggest that the sensitivity of precipitation rate to cloud droplet concentration (termed the *precipitation susceptibility* in recent papers by Feingold and Siebert (2009), Sorooshian et al. (2009)) varies with LWP, so that it is unlikely that a simple scaling of R_{cb} with droplet concentration (and cloud thickness or LWP) will be sufficient. There is still considerable discrepancy between different modeling and observational approaches to estimating the precipitation susceptibility, with large eddy simulation, parcel model results, and some observational studies (Feingold and Siebert 2009; Sorooshian et al. 2009; Jiang and Feingold 2010) suggesting that susceptibility increases with LWP up to some threshold LWP value ($\sim$1000 g m^{-2}) but with other observational studies (Lebsock et al. 2010) and simple steady-state bulk modeling (Wood et al. 2009b), suggesting that the susceptibility decreases monotonically with LWP. Further work is required to untangle these differences, which are likely to be particularly important given that climate models indicate such strong second indirect effects (Lohmann and Feichter 2005; Isaksen et al. 2009).

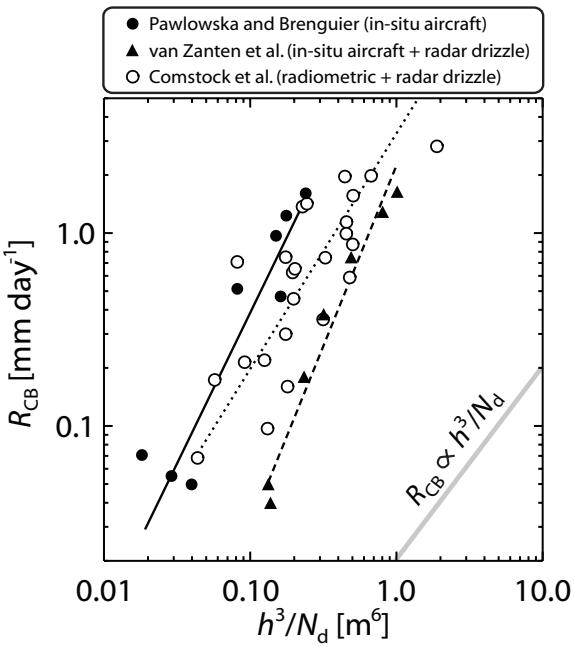

FIG. 26. Cloud base precipitation rates R_{CB} from observational case studies in subtropical marine stratocumulus, plotted against the ratio of the cube of the cloud thickness h to the cloud droplet concentration N_d. The lines represent linear least-distance regressions to the case studies for each field campaign. From Brenguier and Wood (2009).

c. Microphysical impacts upon turbulence and entrainment

As we have seen there is a large body of evidence suggesting that there are important microphysical controls on the precipitation rate in stratocumulus clouds. Since precipitation can play a major role in the dynamics of the STBL chiefly by promoting stratification its suppression by increasing aerosols would likely invigorate buoyant TKE

production and drive increases in cloud top entrainment (Ackerman et al. 2004; Wood 2007). Section 6g provides more information on the response of the STBL to precipitation.

In addition to precipitation-mediated turbulence changes associated with increasing aerosols, increase in N_d can also decrease the condensation timescale (by increasing the overall droplet surface area) which regulate the turbulent fields as discussed in Section 6g. Reduction in the condensation timescale will invigorate the buoyant TKE production and would therefore likely increase the cloud top entrainment rate. However, since this would occur without simultaneous changes to the surface moisture budget, the resulting cloud thickness and cover responses will be different from those associated with aerosol-driven precipitation suppression.

Increasing N_d also decreases the sedimentation rate of cloud droplets. While this does not have a major impact throughout the body of the cloud because the sedimentation rates of $\sim 10\mu$m droplets are so low (few cm s^{-1}), there may be a more significant impact near the sharp liquid water gradient at cloud top. Here, large eddy simulation indicates that the reduced removal of liquid water from the entrainment interface associated with increased N_d may result in a marked increase in the entrainment rate (Bretherton et al. 2007) without any significant impact on the TKE in the STBL. Whether this effect constitutes a significant aerosol indirect effect is currently unknown, although initial climate model tests indicate that globally it represents only a modest contribution compared with the Twomey effect (Chris Bretherton, personal communication).

Since all microphysically-driven impacts on stratocumulus cloud macrophysical properties such as thickness and coverage involve changes in the nature of the small scale turbulence (either in the bulk of the STBL or at the entrainment interface), representing these effects in climate models represents a formidable challenge. Currently, climate models that account for aerosol indirect effects other than the Twomey effect tend not to represent the STBL, and particularly its turbulent structure, explicitly. Instead, they often represent turbulent mixing within the STBL and between the STBL and the free-troposphere using rather crude dry diffusive models that tend to produce clouds that sit too close to the surface, produce too much surface drizzle and too little entrainment flux. Such models therefore balance their STBL energy and moisture budgets in a way that frequently differs from reality, and are likely to produce cloud macrophysical responses to aerosols that are unreliable.

8. Conclusions

Stratocumulus clouds are the Earth's most common cloud type and cover vast tracts of the globe and thus have a profound impact on Earth's radiation budget. Approximately four fifths of all stratocumuli are located over ocean regions which explains the persistent interest in marine stratocumuli in field and modeling studies over the last three decades. Marine stratocumuli are preferentially located in regions with strong static stability in the lower troposphere, but actually constitute 25% or more of the low cloud cover almost everywhere on Earth. Stratocumuli are susceptible to perturbations in atmospheric aerosol, through both microphysical and macrophysical mechanisms. Thus a better understanding of their behavior is as pertinent for quantifying aerosol indirect effects on climate as well as for quantifying how clouds respond to increasing greenhouse gases. Despite a substantial research focus on stratocumuli, there are many aspects of their behavior and structure that remain poorly understood. On a basic level, this is because a stratocumulus cloud system is the product of a tight coupling between radiation, turbulence and cloud microphysical processes occurring over a wide range of scales from millimeters to tens of kilometers.

Stratocumulus are convective clouds, a fact sometimes overlooked since they are morphologically stratiform, being vertically limited by the top of the boundary layer that they cap. Most of the energy in the vertical motion field in stratocumulus cloud systems occurs on horizontal scales close to the depth of the boundary layer, and yet these clouds frequently organize into mesoscale cellular convection with characeristic horizontal scales of several kilometers to several tens of kilometers (the scale increases as the STBL depth increases). This organization, which is particularly prevalent in marine stratocumulus, is associated with an intermittency imposed on the vertical coupling, suppressing it in places and concentrating it locally. Precipitation, which new observations are revealing to be a significant driver of stratocumulus behavior, further adds to the complexity of the organization through its combined effects of cloud layer latent heat release and subcloud layer evaporation. Indeed, the marine stratocumulus cloud system in general can be thought of as an organized and interconnected ensemble of marine boundary layer clouds in which both radiation and precipitation provide the key energetic forcings.

The turbulence generated in stratocumulus clouds modulates the cloud top entrainment rate, which in turn modulates the moisture and temperature in the STBL, thereby influencing the cloud thickness and ipso facto other processes (e.g. precipitation) which influence turbulence production. Through this feedback loop, stratocumulus cloud systems are strongly impacted by the nature of the free-tropospheric (FT) air above the STBL. Determining under which conditions the feedback is positive and negative is a key challenge for future work requiring improved measurement and modeling of the small scale interfacial mixing at the top of the STBL. One one hand increased entrain-

ment suppresses turbulence through its introduction of positively buoyant air into the STBL. However, by influencing moist processes in the STBL, under some circumstances increased entrainment might lead to stronger buoyant turbulent production. Entrainment instability associated with buoyancy reversal is now thought not to provide a means for a strong positive feedback. However, there are conditions (most notably a relatively moist FT, and/or a deep STBL) under which instantaneous entrainment increases can lead to cloud thickening. Since thicker clouds generate more buoyant TKE, this might serve as a positive feedback on entrainment. However, since thicker clouds tend to generate more precipitation, the ultimate response of the STBL to increased entrainment requires an understanding of interactions between the key driving processes.

Major technological improvements in the sensitivity of radars are revealing the rich structure and dynamics in stratocumulus cloud systems, and allowing us to quantify the effects of precipitation, particularly on the mesoscale. We can see, for example, that horizontal wind fluctuations in the STBL, unlike those in the vertical, are often dominated by motions with horizontal scales comparable with the mesoscale cells. Precipitating cells clearly show coherent inflows near cloud base and outflow near the top of the cloud layer which appear to supply moisture to the cell. Cold pools in the subcloud layer generated by the precipitation ultimately suppresses buoyant production in the cell, but can drive new cell formation at the confluence of the gravity currents the cold air produces. Light precipitation of this type has recently become observable from space, which opens up a new avenue for global mapping of the interactions between stratocumulus and the precipitation it produces.

Aerosol impacts on stratocumulus clouds include the purely microphysical (Twomey) impact of increase albedo due to increased droplet concentration and reduced droplet surface area, but also include impacts on macrophysical processes such as precipitation suppression, changes to evaporation/condensation rates due to decreased droplet integral radius, and the enhancement of cloud top entrainment through cloud droplet sedimentation suppression. Many of these effects of these processes on stratocumulus dynamics and structure remain poorly understood and in urgent need of future exploration.

Acknowledgments.

The author appreciates the encouragement of David Schultz and Robert Houze who both encouraged me and stimulated the this review article. Discussions with Tom Ackerman, Paul Field, Dave Leon, Sally McFarlane, Dave Turner, Rhea George, Chris Bretherton, Bruce Albrecht, Roberto Mechoso, Peter Blossey and numerous others provided important insight and guidance. Beth Tully helped with several of the figures. The author's work is supported by NSF grant ATM-0745702, NASA grant NNX10AN78G, NOAA grant NA07OAR4310282, DoE grant DE-SC0002081, and startup funds from the University of Washington.

REFERENCES

Abdul-Razzak, H. and S. J. Ghan, 2000: A parameterization of aerosol activation 2. multiple aerosol types. *Journal of Geophysical Research-Atmospheres*, **105 (D5)**, 6837–6844.

Abdul-Razzak, H., S. J. Ghan, and C. Rivera-Carpio, 1998: A parameterization of aerosol activation - 1. single aerosol type. *Journal of Geophysical Research-Atmospheres*, **103 (D6)**, 6123–6131, 32.

Ackerman, A. S., M. P. Kirkpatrick, D. E. Stevens, and O. B. Toon, 2004: The impact of humidity above stratiform clouds on indirect aerosol climate forcing. *Nature*, **432**, 1014–1017.

Ackerman, A. S., O. B. Toon, and P. V. Hobbs, 1993: Dissipation of marine stratiform clouds and collapse of the marine boundary-layer due to the depletion of cloud condensation nuclei by clouds. *Science*, **262 (5131)**, 226–229.

Ackerman, A. S., O. B. Toon, and P. V. Hobbs, 1995: Numerical modeling of ship tracks produced by injections of cloud condensation nuclei into marine stratiform clouds. *Journal of Geophysical Research-Atmospheres*, **100 (D4)**, 7121–7133.

Ackerman, A. S., O. B. Toon, D. E. Stevens, A. J. Heymsfield, V. Ramanathan, and E. J. Welton, 2000: Reduction of tropical cloudiness by soot. *Science*, **288 (5468)**, 1042–1047.

Ackerman, A. S., et al., 2009: Large-Eddy Simulations of a Drizzling, Stratocumulus-Topped Marine Boundary Layer. *Monthly Weather Review*, **137 (3)**, 1083–1110.

Ackerman, T. and M. B. Baker, 1977: Shortwave radiative effects of unactivated aerosol-particles in clouds. *Journal of Applied Meteorology*, **16 (1)**, 63–69.

Agee, E. M., 1987: Meso-scale cellular convection over the oceans. *Dyn. Atmos. Ocean.*, **10**, 317–341.

Agee, E. M., T. S. Chen, and K. E. Dowell, 1973: A review of mesoscale cellular convection. *Bull. Am. Meteor. Soc.*, **54**, 1004–1012.

Albrecht, B. A., C. S. Bretherton, D. Johnson, W. H. Schubert, and A. S. Frisch, 1995a: The atlantic stratocumulus transition experiment - ASTEX. *Bull. Am. Meteorol. Soc.*, **76**, 889–904.

Albrecht, B. A., C. W. Fairall, D. W. Thomson, A. B. White, J. B. Snider, and W. H. Schubert, 1990: Surface-based remote-sensing of the observed and the adiabatic liquid water content of stratocumulus clouds. *Geophys. Res. Lett.*, **17**, 89–92.

Albrecht, B. A., M. P. Jensen, and W. J. Syrett, 1995b: Marine boundary layer structure and fractional cloudiness. *J. Geophys. Res.*, **100 (D7)**, 14 209–14 222.

Arnason, G. and R. S. Greenfield, 1972: Micro- and macrostructures of numerically simulated convective clouds. *J. Atmos. Sci.*, **29**, 342–367.

Atkinson, B. W. and J. W. Zhang, 1996: Mesoscale shallow convection in the atmosphere. *Rev. Geophys.*, **34**, 403–431.

Austin, P., Y. Wang, R. Pincus, and V. Kujala, 1995: Precipitation in stratocumulus clouds: Observations and modelling results. *J. Atmos. Sci.*, **52**, 2329–2352.

Baker, M. B., 1993: Variability in concentrations of cloud condensation nuclei in the marine cloud-topped boundary layer. *Tellus*, **45B**, 458–472.

Barker, H. W., J. J. Morcrette, and G. D. Alexander, 1998: Broadband solar fluxes and heating rates for atmospheres with 3d broken clouds. *Quarterly Journal of the Royal Meteorological Society*, **124 (548)**, 1245–1271.

Beesley, J. A. and R. E. Moritz, 1999: Toward an explanation of the annual cycle of cloudiness over the arctic ocean. *Journal of Climate*, **12 (2)**, 395–415.

Beheng, K. D., 1994: A parameterization of warm cloud microphysical conversion processes. *Atmos. Res.*, **33**, 193–206.

Beheng, K. D. and G. Doms, 1986: A general formulation of collection rates of cloud and raindrops using the kinetic equation and comparison with parameterizations. *Beitr. Phys. Atmosph.*, **59**, 66–84.

Bennartz, R., 2007: Global assessment of marine boundary layer cloud droplet number concentration from satellite. *J. Geophys. Res.*, **112**, D02 201, doi:10.1029/2006JD007 547.

Bergman, J. W. and M. L. Salby, 1996: Diurnal variations of cloud cover and their relationship to climatological conditions. *Journal of Climate*, **9 (11)**, 2802–2820.

Betts, A. K., C. S. Bretherton, and E. Klinker, 1995: Relation between mean boundary-layer structure and cloudiness at the R/V Valdivia during ASTEX. *J. Atmos. Sci.*, **52**, 2752–2762.

Boers, R., G. P. Ayers, and J. L. Gras, 1994: Coherence between seasonal-variation in satellite-derived cloud optical depth and boundary-layer ccn concentrations at a midlatitude southern-hemisphere station. *Tellus Series B-Chemical and Physical Meteorology*, **46 (2)**, 123–131.

Bony, S. and J.-L. Dufresne, 2005: Marine boundary layer clouds at the heart of cloud feedback uncertainties in climate models. *Geophys. Res. Lett.*, in press.

Bony, S., et al., 2006: How well do we understand and evaluate climate change feedback processes? *J. Climate*, **19 (15)**, 3445–3482.

Brenguier, J. L., H. Pawlowska, L. Schuller, R. Preusker, J. Fischer, and Y. Fouquart, 2000a: Radiative properties of boundary layer clouds: Droplet effective radius versus number concentration. *Journal of the Atmospheric Sciences*, **57 (6)**, 803–821.

Brenguier, J.-L. and R. Wood, 2009: Observational strategies from the micro to meso scale. *Perturbed clouds in the climate system*, MIT Press.

Brenguier, J. L., et al., 2000b: An overview of the ACE-2 CLOUDYCOLUMN closure experiment. *Tellus*, **52B**, 815–827.

Bretherton, C. S., P. Austin, and S. T. Siems, 1995: Cloudiness and marine boundary layer dynamics in the ASTEX lagrangian experiments. Part II: Cloudiness, drizzle, surface fluxes and entrainment. *J. Atmos. Sci.*, **52**, 2724–2735.

Bretherton, C. S., P. Blossey, and J. Uchida, 2007: Cloud droplet sedimentation, entrainment efficiency, and subtropical stratocumulus albedo. *grl*, **34**, L03 813, doi:10.1029/2006GL027 648.

Bretherton, C. S., R. George, R. Wood, G. Allen, D. Leon, and B. Albrecht, 2010: Southeast pacific stratocumulus clouds, precipitation and boundary layer structure sampled along 20s during vocals-rex. *acpd*, **10**, 15 921–15 962.

Bretherton, C. S. and D. L. Hartmann, 2008: Large-scale controls on cloudiness. In Perturbed clouds in the climate system, j. heintzenberg and r. j. charlson (eds.). Ernst strungmann forum, Frankfurt Institute for Advanced Study.

Bretherton, C. S. and R. Pincus, 1995: Cloudiness and marine boundary layer dynamics in the ASTEX lagrangian experiments. Part I: Synoptic setting and vertical structure. *J. Atmos. Sci.*, **52**, 2707–2723.

Bretherton, C. S., T. Uttal, C. W. Fairall, S. E. Yuter, R. A. Weller, D. Baumgardner, K. Comstock, and R. Wood, 2004: The EPIC 2001 stratocumulus study. *Bull. Am. Meteor. Soc.*, **85**, 967–977.

Bretherton, C. S. and M. C. Wyant, 1997: Moisture transport, lower-tropospheric stability, and decoupling of cloud-topped boundary layers. *J. Atmos. Sci.*, **54**, 148–167.

Brost, R. A., D. H. Lenschow, and J. C. Wyngaard, 1982a: Marine stratocumulus layers. part i: Mean conditions. *J. Atmos. Sci.*, **39**, 800–817.

Brost, R. A., J. C. Wyngaard, and D. H. Lenschow, 1982b: Marine stratocumulus layers. part ii: Turbulence budgets. *J. Atmos. Sci.*, **39**, 818–836.

Cahalan, R. F., W. Ridgway, W. J. Wiscombe, T. L. Bell, and J. B. Snider, 1994: The albedo of fractal stratocumulus clouds. *J. Atmos. Sci.*, **51**, 2434–2455.

Cahalan, R. F. and J. B. Snider, 1989: Marine stratocumulus structure. *Rem. Sens. Environ.*, **28**, 95–107.

Caldwell, P. and C. S. Bretherton, 2008: Response of a subtropical stratocumulus-capped mixed layer to climate and aerosol changes. *J. Climate*, submitted.

Caldwell, P., R. Wood, and C. S. Bretherton, 2005: Mixed-layer budget analysis of the diurnal cycle of entrainment in SE Pacific stratocumulus. *J. Atmos. Sci.*, **62**, 3775–3791.

Cantrell, W. and A. Heymsfield, 2005: Production of ice in tropospheric clouds - a review. *Bulletin of the American Meteorological Society*, **86 (6)**, 795–807.

Caughey, S. J., B. A. Crease, and W. T. Roach, 1982: A field-study of nocturnal stratocumulus .2. turbulence structure and entrainment. *Quarterly Journal of the Royal Meteorological Society*, **108 (455)**, 125–144.

Caughey, S. J. and M. Kitchen, 1984: Simultaneous measurements of the turbulent and microphysical structure of nocturnal stratocumulus cloud. *Quarterly Journal of the Royal Meteorological Society*, **110 (463)**, 13–34.

Chen, T., W. B. Rossow, and Y. C. Zhang, 2000: Radiative effects of cloud-type variations. *J. Climate*, **13**, 264–286.

Chlond, A., 1992: Three-dimensional simulation of cloud street development during a cold air outbreak. *Bound. Layer Meteorol.*, **58**, 161–200.

Chylek, P., P. Damiano, and E. P. Shettle, 1992: Infrared emittance of water clouds. *J. Atmos. Sci.*, **49 (16)**, 1459–1472.

Chylek, P., G. B. Lesins, G. Videen, J. G. D. Wong, R. G. Pinnick, D. Ngo, and J. D. Klett, 1996: Black carbon and absorption of solar radiation by clouds. *Journal of Geophysical Research-Atmospheres*, **101 (D18)**, 23 365–23 371.

Ciesielski, P. E., W. H. Schubert, and R. H. Johnson, 1999: Large-scale heat and moisture budgets over the astex region. *Journal of the Atmospheric Sciences*, **56 (18)**, 3241–3261.

Ciesielski, P. E., W. H. Schubert, and R. H. Johnson, 2001: Diurnal variability of the marine boundary layer during astex. *Journal of the Atmospheric Sciences*, **58 (16)**, 2355–2376.

Cohard, J. M. and J. P. Pinty, 2000: A comprehensive two-moment warm microphysical bulk scheme. i: Description and tests. *Quarterly Journal of the Royal Meteorological Society*, **126 (566)**, 1815–1842, part A.

Cohard, J. M., J. P. Pinty, and C. Bedos, 1998: Extending twomey's analytical estimate of nucleated cloud droplet concentrations from ccn spectra. *Journal of the Atmospheric Sciences*, **55 (22)**, 3348–3357.

Comstock, K., C. S. Bretherton, and S. Yuter, 2005: Mesoscale variability and drizzle in Southeast Pacific stratocumulus. *J. Atmos. Sci.*, **62**, 3792–3807.

Comstock, K., R. Wood, S. Yuter, and C. S. Bretherton, 2004: Radar observations of precipitation in and below stratocumulus clouds. *Quart. J. Roy. Meteorol. Soc.*, **130**, 2891–2918.

Comstock, K., S. E. Yuter, R. Wood, and C. S. Bretherton, 2007: The three dimensional structure and kinematics of drizzling stratocumulus. *Mon. Wea. Rev.*, **135**, 3767–3784.

Conant, W. C., et al., 2004: Aerosol-cloud drop concentration closure in warm cumulus. *Journal of Geophysical Research-Atmospheres*, **109 (D13)**.

Curry, J. A., W. B. Rossow, D. Randall, and J. L. Schramm, 1996: Overview of arctic cloud and radiation characteristics. *Journal of Climate*, **9 (8)**, 1731–1764.

Dai, A., 2001: Global precipitation and thunderstorm frequencies. Part II: Diurnal variations. *Journal of Climate*, **14 (6)**, 1112–1128.

Dai, A. G., T. R. Karl, B. M. Sun, and K. E. Trenberth, 2006: Recent trends in cloudiness over the united states - a tale of monitoring inadequacies. *Bulletin of the American Meteorological Society*, **87 (5)**, 597–+.

Danielson, R. E., D. R. Moore, and Vandehul.Hc, 1969: Transfer of visible radiation through clouds. *Journal of the Atmospheric Sciences*, **26 (5P2)**, 1078–1087.

Davis, A., A. Marshak, H. Gerber, and W. J. Wiscombe, 1999: Horizontal structure of marine boundary layer clouds from cm to km scales. *J. Geophys. Res.*, **104**, 6123–6144.

Davis, A., A. Marshak, W. Wiscombe, and R. Cahahlan, 1996: Scale invariance of liquid water distributions in marine stratocumulus. Part 1: Spectral properties and stratinarity issues. *J. Atmos. Sci.*, **53**, 1538–1558.

de Roode, S. R. and P. G. Duynkerke, 1997: Observed lagrangian transition of stratocumulus into cumulus during ASTEX: mean state and turbulence structure. *J. Atmos. Sci.*, **54**, 2157–2173.

de Roode, S. R., P. G. Duynkerke, and H. J. Jonker, 2004: Large eddy simulation: how large is large enough? *J. Atmos. Sci.*, **61**, 403–421.

de Roode, S. R. and Q. Wang, 2007: Do stratocumulus clouds detrain? fire i data revisited. *Bound. Layer Meteorol.*, **122 (2)**, 479–491.

Deardorff, J. W., 1976: Entrainment rate of stratocumulus topped mixed layer. *Quart. J. Roy. Meteorol. Soc.*, **102**, 563–582.

Deardorff, J. W., 1980a: Cloud top entrainment instability. *J. Atmos. Sci.*, **37**, 561–563.

Deardorff, J. W., 1980b: Stratocumulus-capped mixed layers derived from a 3-dimensional model. *Boundary-Layer Meteorology*, **18 (4)**, 495–527.

Deardorff, J. W., 1981: On the distribution of mean radiative cooling at the top of a stratocumulus-capped mixed layer. *Quarterly Journal of the Royal Meteorological Society*, **107 (451)**, 191–202.

Driedonks, A. G. M., 1982: Models and observations of the growth of the atmospheric boundary-layer. *Boundary-Layer Meteorology*, **23 (3)**, 283–306.

Driedonks, A. G. M. and P. G. Duynkerke, 1989: Current problems in the stratocumulus-topped atmospheric boundary-layer - (survey paper). *Boundary-Layer Meteorology*, **46 (3)**, 275–303.

Dusek, U., et al., 2006: Size matters more than chemistry for cloud-nucleating ability of aerosol particles. *Science*, **312 (5778)**, 1375–1378.

Duynkerke, P. G., 1993: The stability of cloud top with regard to entrainment - amendment of the theory of cloud-top entrainment instability. *Journal of the Atmospheric Sciences*, **50 (3)**, 495–502.

Duynkerke, P. G. and P. Hignett, 1993: Simulation of a diurnal variation in a stratocumulus-capped marine boundary layer during FIRE. *Mon. Wea. Rev.*, **121**, 3291–3300.

Duynkerke, P. G. and J. Teixeira, 2001: Comparison of the ecmwf reanalysis with fire i observations: Diurnal variation of marine stratocumulus. *Journal of Climate*, **14 (7)**, 1466–1478.

Duynkerke, P. G., H. Q. Zhang, and P. J. Jonker, 1995: Microphysical and turbulent structure of nocturnal stratocumulus as observed during astex. *Journal of the Atmospheric Sciences*, **52 (16)**, 2763–2777.

Erlick, C. and D. Schlesinger, 2008: Another look at the influence of absorbing aerosols in drops on cloud absorption: Large aerosols. *Journal of the Atmospheric Sciences*, **65 (2)**, 661–669, erlick, Carynelisa Schlesinger, Dana.

Evan, A. T., A. K. Heidinger, and D. J. Vimont, 2007: Arguments against a physical long-term trend in global isccp cloud amounts. *Geophysical Research Letters*, **34 (4)**, evan, Amato T. Heidinger, Andrew K. Vimont, Daniel J.

Facchini, M. C., M. Mircea, S. Fuzzi, and R. J. Charlson, 1999: Cloud albedo enhancement by surface-active organic solutes in growing droplets. *Nature*, **401 (6750)**, 257–259.

Faloona, I., et al., 2005: Observations of entrainment in eastern pacific marine stratocumulus using three conserved scalars. *J. Atmos. Sci.*, **62**, 3268–3285.

Feingold, G., 2003: Modeling of the first indirect effect: Analysis of measurement requirements. *Geophysical Research Letters*, **30 (19)**.

Feingold, G. and P. Y. Chuang, 2002: Analysis of the influence of film-forming compounds on droplet growth: Implications for cloud microphysical processes and climate. *Journal of the Atmospheric Sciences*, **59 (12)**, 2006–2018.

Feingold, G. and H. Siebert, 2009: Cloud-aerosol interactions from the micro to the cloud scale. In Perturbed clouds in the climate system, j. heintzenberg and r. j. charlson (eds.). Ernst Strungmann Forum MIT Press, Cambridge, MA, p319-338, Frankfurt Institute for Advanced Study.

Ferek, R. J., et al., 2000: Drizzle suppression in ship tracks. *Journal of the Atmospheric Sciences*, **57 (16)**, 2707–2728.

Field, P. R. and R. Wood, 2007: Precipitation and cloud structure in midlatitude cyclones. *J. Climate*, **20**, 233–254.

Fountoukis, C., et al., 2007: Aerosol-cloud drop concentration closure for clouds sampled during the international

consortium for atmospheric research on transport and transformation 2004 campaign. *Journal of Geophysical Research-Atmospheres*, **112 (D10)**, fountoukis, Christos Nenes, Athanasios Meskhidze, Nicholas Bahreini, Roya Conant, William C. Jonsson, Haflidi Murphy, Shane Sorooshian, Armin Varutbangkul, Varuntida Brechtel, Fred Flagan, Richard C. Seinfeld, John H.

Garay, M., R. Davies, C. Averill, and J. Westphal, 2004: Actinoform clouds. *Bull. Amer. Meteorol. Soc.*, **85**, 1585–1594.

Garratt, J. R., 1992: *The atmospheric boundary layer*. Cambridge University Press.

Garratt, J. R. and R. A. Brost, 1981: Radiative cooling effects within and above the nocturnal boundary-layer. *J. Atmos. Sci.*, **38 (12)**, 2730–2746.

Garreaud, R. D. and R. Muñoz, 2004: The diurnal cycle in circulation and cloudiness over the subtropical southeast Pacific: A modeling study. *J. Climate*, **17**, 1699–1710.

Garreaud, R. D. and J. Rutllant, 2003: Coastal lows along the subtropical west coast of South America: Numerical simulation of a typical case. *Monthly Weather Review*, **131 (5)**, 891–908.

Garreaud, R. D., J. Rutllant, J. Quintana, J. Carrasco, and P. Minnis, 2001: Cimar-5: A snapshot of the lower troposphere over the subtropical southeast pacific. *Bull. Amer. Meteorol. Soc.*, **82**, 2193–2207.

Garrett, T. J., L. F. Radke, and P. V. Hobbs, 2002: Aerosol effects on cloud emissivity and surface longwave heating in the Arctic. *J. Atmos. Sci.*, **59 (3)**, 769–778.

Geoffroy, O., J. L. Brenguier, and I. Sandu, 2008: Relationship between drizzle rate, liquid water path and droplet concentration at the scale of a stratocumulus cloud system. *Atmospheric Chemistry and Physics*, **8 (16)**, 4641–4654.

George, R. C. and R. Wood, 2010: Subseasonal variability of low cloud properties over the southeast pacific ocean. *acp*, **10**, 4047–4063.

Gerber, H., 1996: Microphysics of marine stratocumulus with two drizzle modes. *J. Atmos. Sci.*, **53**, 1649–1662.

Gerber, H., G. Frick, S. P. Malinowski, J. L. Brenguier, and F. Burnet, 2005: Holes and entrainment in stratocumulus. *Journal of the Atmospheric Sciences*, **62 (2)**, 443–459.

Ghan, S. J., G. Guzman, and H. Abdul-Razzak, 1998: Competition between sea salt and sulfate particles as cloud condensation nuclei. *J. Atmos. Sci.*, **55**, 3340–3347.

Glantz, P., K. J. Noone, and S. R. Osborne, 2003: Scavenging efficiencies of aerosol particles in marine stratocumulus and cumulus clouds. *Quarterly Journal of the Royal Meteorological Society*, **129 (590)**, 1329–1350, part A.

Greenwald, T. J., G. L. Stephens, S. A. Christopher, and T. H. VonderHaar, 1995: Observations of the global characteristics and regional radiative effects of marine cloud liquid water. *Journal of Climate*, **8 (12)**, 2928–2946.

Gultepe, I. and G. A. Isaac, 2004: Aircraft observations of cloud droplet number concentration: Implications for climate studies. *Quarterly Journal of the Royal Meteorological Society*, **130 (602)**, 2377–2390, part A.

Hahn, C. J., W. B. Rossow, and S. G. Warren, 2001: ISCCP cloud properties associated with standard cloud types identified in individual surface observations. *J. Climate*, **14**, 11–28.

Hahn, C. J. and S. G. Warren, 2007: A gridded climatology of clouds over land (1971-96) and ocean (1954-97) from surface observations worldwide. Numeric Data Package NDP-026E ORNL/CDIAC-153, CDIAC, Department of Energy, Oak Ridge, Tennessee.

Hakim, G. J., 2003: Developing wave packets in the north pacific storm track. *Mon. Wea. Rev.*, **131**, 342–355.

Hall, W. D., 1980: A detailed microphysical model within a two-dimensional dynamic framework: Model description and preliminary results. *J. Atmos. Sci.*, **37**, 2486–2507.

Haman, K. E., S. P. Malinowski, M. J. Kurowski, H. Gerber, and J. L. Brenguier, 2007: Small scale mixing processes at the top of a marine stratocumulus - a case study. *Quarterly Journal of the Royal Meteorological Society*, **133 (622)**, 213–226.

Hansen, J. E. and L. D. Travis, 1974: Light scattering in planetary atmospheres. *Space Sci. Rev.*, **16**, 527–610.

Hanson, H. P., 1991: Marine stratocumulus climatologies. *International Journal of Climatology*, **11 (2)**, 147–164.

Hartmann, D. L., 1994: *Global Physical Climatology*. Academic Press.

Hartmann, D. L., M. E. Ockert-Bell, and M. L. Michelsen, 1992: The effect of cloud type on earth's energy balance - Global analysis. *J. Climate*, **5**, 1281–1304.

Haywood, J. M. and K. P. Shine, 1997: Multi-spectral calculations of the direct radiative forcing of tropospheric sulphate and soot aerosols using a column model. *Quarterly Journal of the Royal Meteorological Society*, **123 (543)**, 1907–1930, part A.

Henrion, X., H. Sauvageot, and D. Ramond, 1978: Finestructure of precipitation and temperature in a stratocumulus cloud. *J. Atmos. Sci.*, **35**, 2315–2324.

Hermann, G. and R. Goody, 1976: Formation and persistence of summertime arctic stratus clouds. *J. Atmos. Sci.*, **33**, 1537–1553.

Hignett, P., 1991: Observations of diurnal variation in a cloud-capped marine boundary layer. *J. Atmos. Sci.*, **48**, 1474–1482.

Hobbs, P. V. and A. L. Rangno, 1998: Microstructures of low and middle-level clouds over the beaufort sea. *Quarterly Journal of the Royal Meteorological Society*, **124 (550)**, 2035–2071.

Howell, W. E., 1949: The growth of cloud drops in uniformly cooled air. *Journal of Meteorology*, **6 (2)**, 134–149.

Hu, Y., et al., 2007: Global statistics of liquid water content and effective number concentration of water clouds over ocean derived from combined calipso and modis measurements. *Atmospheric Chemistry and Physics*, **7 (12)**, 3353–3359, hu, Y. Vaughan, M. McClain, C. Behrenfeld, M. Maring, H. Anderson, D. SunMack, S. Flittner, D. Huang, J. Wielicki, B. Minnis, P. Weimer, C. Trepte, C. Kuehn, R.

Hu, Y. X. and K. Stamnes, 1993: An accurate parameterization of the radiative properties of water clouds suitable for use in climate models. *Journal of Climate*, **6 (4)**, 728–742.

Hudson, J. G., 2007: Variability of the relationship between particle size and cloud-nucleating ability. *Geophysical Research Letters*, **34 (8)**, hudson, James G.

Huffman, G. J. and G. A. Norman, 1988: The supercooled warm rain process and the specification of freezing precipitation. *Monthly Weather Review*, **116 (11)**, 2172–2182.

IPCC, 2007: *Climate Change 2007: The Physical Science Basis. Contribution of Working Group I to the Fourth Assessment Report of the Intergovernmental Panel on Climate Change. Solomon, S. and Qin, D. and Manning, M. and Chen, Z. and Marquis, M. Averyt, K. B. and Tignor, M. and Miller, H. L. (eds).* Cambridge University Press, Cambridge, United Kingdom and New York, NY, USA.

Isaksen, I., C. Granier., G. Myhre, and coathors, 2009: Atmospheric composition change: Climate-chemistry interactions. *Atmos. Env.*, **43**, 5138–5192.

Jensen, ., J. B., S. Lee, P. B. Krummel, J. Katzfey, and D. Gogoasa, 2000: Precipitation in marine cumulus and stratocumulus. part i: Thermodynamic and dynamic observations of closed cell circulations and cumulus bands. *Atmos. Res.*, **54**, 117–155.

Jiang, H. and G. Feingold, 2010: Effect of aerosol on the susceptibility and efficiency of precipitation in warm trade cumulus clouds. *J. Atmos. Sci.*, in press.

Jiang, H., G. Feingold, and W. R. Cotton, 2002: Simulations of aerosol-cloud dynamical feedbacks resulting from entrainment of aerosol into the marine boundary layer during ASTEX. *J. Geophys. Res.*, **107**, 4813.

Jonas, P. R., 1996: Turbulence and cloud microphysics. *Atmos. Res.*, **40**, 283–306.

Junge, C. and E. McLaren, 1971: Relationship of cloud nuclei spectra to aerosol size distribution and composition. *Journal of the Atmospheric Sciences*, **28 (3)**, 382–390.

Kajikawa, M., K. Kikuchi, Y. Asuma, Y. Inoue, and N. Sato, 2000: Supercooled drizzle formed by condensation-coalescence in the mid-winter season of the canadian arctic. *Atmospheric Research*, **52 (4)**, 293–301.

Kawa, S. R. and R. Pearson Jr., 1989: An observational study of stratocumulus entrainment and thermodynamics. *J. Atmos. Sci.*, **46**, 2649–2661.

Kessler, E., 1969: On the distribution and continuity of water substance in atmospheric circulation. *Meteorol. Monogr.*, **10**, 84pp.

Khain, A., M. Ovtchinnikov, M. Pinsky, A. Pokrovsky, and H. Krugliak, 2000: Notes on the state-of-the-art numerical modeling of cloud microphysics. *Atmospheric Research*, **55 (3-4)**, 159–224.

Khairoutdinov, M. and Y. Kogan, 2000: A new cloud physics parameterization in a large-eddy simulation model of marine stratocumulus. *J. Atmos. Sci.*, **57**, 229–243.

Kim, B. G., S. A. Klein, and J. R. Norris, 2005: Continental liquid water cloud variability and its parameterization using atmospheric radiation measurement data. *J. Geophys. Res.*, **110 (D15)**.

King, M. D. and Harshvardhan, 1986: Comparative accuracy of selected multiple scattering approximations. *J. Atmos. Sci.*, **43**, 784–801.

King, M. D., S.-C. Tsay, S. E. Platnick, M. Wang, and K.-N. Liou, 1997: Cloud retrieval algorithms for modis: Optical thickness, effective particle radius, and thermodynamic phase. MODIS Algorithm Theoretical Basis Document ATBD-MOD-05, NASA.

Klein, S. A., 1997: Synoptic variability of low-cloud properties and meteorological parameters in the subtropical trade wind boundary layer. *J. Climate*, **10**, 2018–2039.

Klein, S. A. and D. L. Hartmann, 1993: The seasonal cycle of low stratiform clouds. *J. Climate,*, **6**, 1588–1606.

Klein, S. A., D. L. Hartmann, and J. R. Norris, 1995: On the relationships among low-cloud structure, sea surface temperature, and atmospheric circulation in the summertime northeast pacific. *J. Climate*, **8**, 1140–1155.

Klein, S. A. and C. Jakob, 1999: Validation and sensitivities of frontal clouds simulated by the ecmwf model. *Mon. Wea. Rev.*, **127**, 2514–2531.

Kogan, Y. L., M. P. Khairoutdinov, D. K. Lilly, Z. N. Kogan, and Q. Liu, 1995: The simulation of a convective cloud in a 3-d model with explicit microphysics. part i: model description and sensitivity experiments. *J. Atmos. Sci.*, **52**, 2923–2940.

Kogan, Y. L. and W. J. Martin, 1994: Parameterization of bulk condensation in numerical models. *J. Atmos. Sci.*, **51**, 1728–1739.

Kollias, P., G. Tselioudis, and B. A. Albrecht, 2007: Cloud climatology at the southern great plains and the layer structure, drizzle, and atmospheric modes of continental stratus. *Journal of Geophysical Research-Atmospheres*, **112 (D9)**, 15.

Koponen, I. K., A. Virkkula, R. Hillamo, V. M. Kerminen, and M. Kulmala, 2003: Number size distributions and concentrations of the continental summer aerosols in queen maud land, antarctica. *Journal of Geophysical Research-Atmospheres*, **108 (D18)**.

Krueger, S. K., G. T. McLean, and Q. Fu, 1995a: Numerical simulation of the stratus-to-cumulus transition in the subtropical marine boundary layer. Part I: Boundary-layer structure. *J. Atmos. Sci.*, **52**, 2839–2850.

Krueger, S. K., G. T. McLean, and Q. Fu, 1995b: Numerical simulation of the stratus-to-cumulus transition in the subtropical marine boundary layer. Part II: Boundary layer circulation. *J. Atmos. Sci.*, **52**, 2851–2868.

Kubar, T. L., D. L. Hartmann, and R. Wood, 2009: On the importance of macrophysics and microphysics for precipitation in warm clouds - Part I. Satellite observations. *J. Atmos. Sci.*, submitted.

Kulmala, M., A. Laaksonen, P. Korhonen, T. Vesala, T. Ahonen, and J. C. Barrett, 1993: The effect of atmospheric nitric-acid vapor on cloud condensation nucleus activation. *Journal of Geophysical Research-Atmospheres*, **98 (D12)**, 22 949–22 958.

Kuo, H.-C. and W. H. Schubert, 1988: Stability of cloud-topped boundary layers. *Quart. J. Roy. Meteorol. Soc.*, **114**, 887–916.

Larson, V. E., K. E. Kotenberg, and N. B. Wood, 2007: An analytic longwave radiation formula for liquid layer clouds. *Monthly Weather Review*, **135 (2)**, 689–699.

Lau, N. C. and M. W. Crane, 1997: Comparing satellite and surface observations of cloud patterns in synoptic scale circulation systems. *Mon. Wea. Rev.*, **125**, 3172–3189.

Lawson, R. P., B. A. Baker, C. G. Schmitt, and T. L. Jensen, 2001: An overview of microphysical properties of arctic clouds observed in may and july 1998 during fire ace. *Journal of Geophysical Research-Atmospheres*, **106 (D14)**, 14 989–15 014.

Leaitch, W. R., et al., 1996: Physical and chemical observations in marine stratus during the 1993 north atlantic regional experiment: Factors controlling cloud droplet number concentrations. *Journal of Geophysical Research-Atmospheres*, **101 (D22)**, 29 123–29 135.

Lebsock, M. D., T. S. L'Ecuyer, and G. L. Stephens, 2010: Detecting the ratio of rain and cloud water in low-latitude shallow marine clouds. *J. Appl. Meteorol. Clim.*, in press.

Lee, S. S. and J. E. Penner, 2010: Factors determining the effect of aerosols on cloud mass and the dependence of these factors on liquid-water path. *Atmos. Chem. Phys.*, submitted.

Lee, S. S., J. E. Penner, and S. M. Saleeby, 2009: Aerosol effects on liquid-water path of thin stratocumulus clouds. *J. Geophys. Res.*, **114**, D07 204.

Lenschow, D. H. and B. B. Stankov, 1986: Length scales in the convective boundary layer. *J. Atmos. Sci.*, **43**, 1190–1209.

Lenschow, D. H., M. Y. Zhou, X. B. Zeng, L. S. Chen, and X. D. Xu, 2000: Measurements of fine-scale structure at the top of marine stratocumulus. *Boundary-Layer Meteorology*, **97 (2)**, 331–357.

Leon, D. C., Z. Wang, and D. Liu, 2008: Climatology of drizzle in marine boundary layer clouds based on 1 year of data from CloudSat and Cloud-Aerosol Lidar and Infrared Pathfinder Satellite Observations (CALIPSO). *J. Geophys. Res.*, **113 (D00A14)**, doi:10.1029/2008JD009 835.

Lewellen, D. C. and W. S. Lewellen, 1998: Large-eddy boundary layer entrainment. *J. Atmos. Sci.*, **55**, 2645–2665.

Li, J., J. W. Geldart, and P. Chylek, 1994: Solar radiative-transfer in clouds with vertical internal inhomogeneity. *Journal of the Atmospheric Sciences*, **51 (17)**, 2542–2552.

Lilly, D. K., 1968: Models of cloud-topped mixed layers under a strong inversion. *Quart. J. Roy. Meteorol. Soc.*, **94**, 292–309.

Lilly, D. K., 2002: Entrainment into mixed layers. part ii: A new closure. *Journal of the Atmospheric Sciences*, **59 (23)**, 3353–3361.

Lilly, D. K. and B. Stevens, 2008: Validation of a mixed-layer closure. i: Theoretical tests. *Quarterly Journal of the Royal Meteorological Society*, **134 (630)**, 47–55.

Liou, K.-N., 1992: *Radiation and Cloud Processes in the Atmosphere: Theory, Observation and Modeling (Oxford Monographs on Geology and Geophysics)*.

Liu, Y. and P. H. Daum, 2004: On the parameterization of the autoconversion process. Part I: Analytical formulation of the Kessler-type parameterizations. *J. Atmos. Sci.*, **61**, 1539–1548.

Locatelli, J. D., P. V. Hobbs, and K. R. Biswas, 1983: Precipitation from stratocumulus clouds affected by fall-streaks and artificial seeding. *Journal of Climate and Applied Meteorology*, **22 (8)**, 1393–1403.

Lock, A. P., 1998: The parametrization of entrainment in cloudy boundary layers. *Quart. J. Roy. Meteorol. Soc.*, **124**, 2729–2754.

Lohmann, U. and J. Feichter, 2005: Global indirect aerosol effects: A review. *Atmos. Chem. Phys.*, **5**, 715–737.

Long, A. B., 1974: Solutions to the droplet collection equation for polynomial kernels. *J. Atmos. Sci.*, **31**, 1040–1052.

Lu, M. L., W. C. Conant, H. H. Jonsson, V. Varutbangkul, R. C. Flagan, and J. H. Seinfeld, 2007: The marine stratus/stratocumulus experiment (mase): Aerosol-cloud relationships in marine stratocumulus. *Journal of Geophysical Research-Atmospheres*, **112 (D10)**, lu, Miao-Ling Conant, William C. Jonsson, Haflidi H. Varutbangkul, Varuntida Flagan, Richard C. Seinfeld, John H.

MacVean, M. K. and P. J. Mason, 1990: Cloud-top entrainment instability through small-scale mixing and its parameterization in numerical models. *J. Atmos. Sci.*, **47**, 1012–1030.

Martin, G. M., D. W. Johnson, D. P. Rogers, P. R. Jonas, P. Minnis, and D. A. Hegg, 1995: Observations of the interaction between cumulus clouds and warm stratocumulus clouds in the marine boundary layer during ASTEX. *J. Atmos. Sci.*, **52**, 2902–2922.

Martin, G. M., D. W. Johnson, and A. Spice, 1994: The measurement and parameterization of effective radius of droplets in warm stratocumulus clouds. *J. Atmos. Sci.*, **51**, 1823–1842.

McFarquhar, G. M., G. Zhang, M. R. Poellot, G. L. Kok, R. McCoy, T. Tooman, A. Fridlind, and A. J. Heymsfield, 2007: Ice properties of single-layer stratocumulus during the mixed-phase arctic cloud experiment: 1. observations. *Journal of Geophysical Research-Atmospheres*, **112 (D24)**.

McFiggans, G., et al., 2006: The effect of physical and chemical aerosol properties on warm cloud droplet activation. *Atmospheric Chemistry and Physics*, **6**, 2593–2649.

Mechem, D. B. and Y. Kogan, 2003: Simulating the transition from drizzling marine stratocumulus to boundary layer cumulus with a mesoscale model. *Monthly Weather Review*, **131**, 2342–2360.

Mellado, B., 2010: The evaporatively driven cloud-top mixing layer. *J. Fluid. Mech.*, **660**, 5–36, doi:10.1017/S0022112010002831.

Miles, N. L., J. Verlinde, and E. E. Clothiaux, 2000: Cloud droplet size distributions in low-level stratiform clouds. *J. Atmos. Sci.*, **57 (2)**, 295–311.

Miller, M. A. and B. A. Albrecht, 1995: Surface-based observations of mesoscale cumulus-stratocumulus interaction during ASTEX. *J. Atmos. Sci.*, **52**, 2809–2826.

Miller, M. A., M. P. Jensen, and E. E. Clothiaux, 1998: Diurnal cloud and thermodynamic variations in the stratocumulus transition regime: A case study using in situ and remote sensors. *Journal of the Atmospheric Sciences*, **55 (13)**, 2294–2310.

Mitchell, T. P. and J. M. Wallace, 1992: The annual cycle in equatorial convection and sea-surface temperature. *Journal of Climate*, **5 (10)**, 1140–1156.

Moeng, C. H., S. H. Shen, and D. A. Randall, 1992: Physical processes within the nocturnal stratus-topped boundary layer. *J. Atmos. Sci.*, **49**, 2384–2401.

Moeng, C. H., B. Stevens, and P. P. Sullivan, 2005: Where is the interface of the stratocumulus-topped PBL? *Journal of the Atmospheric Sciences*, **62 (7)**, 2626–2631.

Moeng, C. H., et al., 1996: Simulation of a stratocumulus-topped planetary boundary layer: Intercomparison among different numerical codes. *Bull. Am. Meteor. Soc.*, **77 (2)**, 261–278.

Mordy, W., 1959: Computations of the growth by condensation of a population of cloud droplets. *Tellus*, **11 (1)**, 16–44.

Moyer, K. A. and G. S. Young, 1994: Observations of mesoscale cellular convection from the marine stratocumulus phase of fire. *Boundary Layer Meteorol.*, **71**, 109–134.

Nakajima, T., M. D. King, J. D. Spinhirne, and L. F. Radke, 1991: Determination of the optical thickness and effective particle radius of clouds from reflected solar radiation measurements: 2. Marine stratocumulus observations. *Journal of the Atmospheric Sciences*, **48 (5)**, 728–750.

Neiburger, M., D. S. Johnson, and C. W. Chien, 1961: Studies of the structure of the atmosphere over the eastern pacific ocean in summer: Part 1. the inversion over the eastern north pacific ocean. *Univ. of Calif. Pubs. in Meteor.*, **1 (1)**, Univ. of Calif. Press.

Nenes, A., R. J. Charlson, M. C. Facchini, M. Kulmala, A. Laaksonen, and J. H. Seinfeld, 2002: Can chemical effects on cloud droplet number rival the first indirect effect? *Geophysical Research Letters*, **29 (17)**.

Nenes, A. and J. H. Seinfeld, 2003: Parameterization of cloud droplet formation in global climate models. *Journal of Geophysical Research-Atmospheres*, **108 (D14)**.

Nicholls, S., 1984: The dynamics of stratocumulus: aircraft observations and comparisons with a mixed layer model. *Quart. J. Roy. Meteorol. Soc.*, **110**, 783–820.

Nicholls, S., 1987: A model of drizzle growth in warm, turbulent, stratiform clouds. *Quart. J. Roy. Meteorol. Soc.*, **113**, 1141–1170.

Nicholls, S., 1989: The structure of radiatively driven convection in stratocumulus. *Quart. J. Roy. Meteorol. Soc.*, **115**, 487–511.

Nicholls, S. and J. Leighton, 1986: An observational study of the structure of stratiform cloud sheets: Part i. structure. *Quart. J. Roy. Meteorol. Soc.*, **112**, 431–460.

Nicholls, S. and J. D. Turton, 1986: An observational study of the structure of stratiform cloud sheets: Part II. Entrainment. *Quart. J. Roy. Meteorol. Soc.*, **112**, 461–480.

Nieuwstadt, F. T. M. and J. A. Businger, 1984: Radiative cooling near the top of a cloudy mixed layer. *Q. J. R. Meteorol. Soc.*, **110**, 1073–1078.

Nieuwstadt, F. T. M. and P. G. Duynkerke, 1996: Turbulence in the atmospheric boundary layer. *Atmos. Res.*, **40 (2-4)**, 111–142.

Norris, J. R. and S. A. Klein, 2000: Low cloud type over the ocean from surface observations. part III: Relationship to vertical motion and the regional synoptic environment. *J. Climate*, **13**, 245–256.

Norris, J. R. and C. B. Leovy, 1994: Interannual variability in stratiform cloudiness and sea-surface temperature. *Journal of Climate*, **7 (12)**, 1915–1925.

Norris, J. R. and A. Slingo, 2009: Trends in observed cloudiness and Earth's radiation budget: Whad do we not know and what do we need to know?, J. Heintzenberg and R. J. Charlson (eds.). Tech. rep., Ernst Strungmann Forum.

Norris, J. R., Y. Zhang, and J. M. Wallace, 1998: Role of low clouds in summertime atmosphere-ocean interactions over the north pacific. *J. Climate*, **11 (10)**, 2482–2490.

Nucciarone, J. J. and G. S. Young, 1991: Aircraft measurements of turbulence spectra in the marine stratocumulus-topped boundary layer. *J. Atmos. Sci.*, **48**, 2382–2392.

O'Dell, C. W., F. J. Wentz, and R. Bennartz, 2008: Cloud liquid water path from satellite-based passive microwave observations: A new climatology over the global oceans. *J. Climate*, **21**, 1721–1738.

O'Dowd, C. D., J. A. Lowe, and M. H. Smith, 1999a: Coupling sea-salt and sulphate interactions and its impact on cloud droplet concentration predictions. *Geophysical Research Letters*, **26 (9)**, 1311–1314.

Odowd, C. D., J. A. Lowe, M. H. Smith, B. Davison, N. Hewitt, and R. M. Harrison, 1997: Biogenic sulphur emissions and inferred non-sea-salt-sulphate cloud condensation nuclei in and around antarctica. *Journal of Geophysical Research-Atmospheres*, **102 (11D)**, 12 839–12 854.

O'Dowd, C. D., J. A. Lowe, M. H. Smith, and A. D. Kaye, 1999b: The relative importance of non-sea-salt sulphate and sea-salt aerosol to the marine cloud condensation nuclei population: An improved multi-component aerosol-cloud droplet parametrization. *Quarterly Journal of the Royal Meteorological Society*, **125 (556)**, 1295–1313, part B.

O'Hirok, W. and C. Gautier, 1998: A three-dimensional radiative transfer model to investigate the solar radiation within a cloudy atmosphere. part ii: Spectral effects. *Journal of the Atmospheric Sciences*, **55 (19)**, 3065–3076.

Ohtake, T., 1963: Hemispheric investigations of warm rain by radiosonde data. *J. Appl. Meteorol.*, **2**, 594–607.

Paltridge, G. W., 1974: Infrared emissivity, shortwave albedo and the microphysics of stratiform water clouds. *J. Geophys. Res.*, **79**, 4053–4058.

Paluch, I. R. and D. H. Lenschow, 1991: Stratiform cloud formation in the marine boundary layer. *J. Atmos. Sci.*, **48**, 2141–2158.

Paluch, I. R., D. H. Lenschow, S. Siems, S. McKeen, G. L. Kok, and R. D. Schillawski, 1994: Evolution of the subtropical marine boundary-layer - comparison of soundings over the eastern pacific from fire and harp. *J. Atmos. Sci.*, **51 (11)**, 1465–1479.

Park, S., C. B. Leovy, and M. A. Rozendaal, 2004: A new heuristic marine boundary layer cloud model. *J. Atmos. Sci.*, **61**, 3002–3024.

Pawlowska, H. and J. L. Brenguier, 2003: An observational study of drizzle formation in stratocumulus clouds for general circulation model (GCM) parameterizations. *J. Geophys. Res.*, **108**, 8630, doi:10.1029/2002JD002 679.

Petty, G. W., 1994: *A first course in atmospheric radiation.*

Petty, G. W., 1995: Frequencies and characteristics of global oceanic precipitation from shipboard present-weather reports. *Bull. Amer. Meteor. Soc.*, **76**, 1593–1616.

Pinnick, R. G., S. G. Jennings, P. Chylek, and H. J. Auvermann, 1979: Verification of a linear relation between ir extinction, absorption and liquid water-content of fogs. *J. Atmos. Sci.*, **36 (8)**, 1577–1586.

Pinsky, M., A. Khain, and M. Shapiro, 2001: Collision efficiency of drops in a wide range of reynolds numbers: Effects of pressure on spectrum evolution. *Journal of the Atmospheric Sciences*, **58 (7)**, 742–764.

Pinsky, M. B. and A. P. Khain, 1997: Turbulence effects on droplet growth and size distribution in clouds - a review. *J. Aerosol Sci.*, **28**, 1177–1214.

Platnick, S. and S. Twomey, 1994: Determining the susceptibility of cloud albedo to changes in droplet concentration with the Advanced Very High Resolution Radiometer. *J. Appl. Meteorol.*, **33**, 334–347.

Platt, C. M. R., 1976: Infrared absorption and liquid water content in stratocumulus clouds. *Q. J. R. Meteorol. Soc.*, **102**, 553–556.

Pruppacher, H. R. and J. D. Klett, 1997: *Microphysics of clouds and precipitation, Kluwer Academic Publishers, 976 pp.* Kluwer Academic Publishers, 976 pp.

Ramaswamy, V. and S. M. Freidenreich, 1991: Solar radiative line-by-line determination of water-vapor absorption and water cloud extinction in inhomogeneous atmospheres. *Journal of Geophysical Research-Atmospheres*, **96 (D5)**, 9133–9157.

Randall, D. A., 1980: Conditional instability of the first kind upside down. *J. Atmos. Sci.*, **37**, 125–130.

Randall, D. A., 1984: Stratocumulus cloud deepening through entrainment. *Tellus*, **36A**, 446–457.

Randall, D. A., J. A. Coakley, C. W. . Fairall, R. A. Knopfli, and D. H. Lenschow, 1984: Outlook for research on marine subtropical stratocumulus clouds. *Bull. Am. Meteor. Soc.*, **65**, 1290–1301.

Randall, D. A. and M. J. Suarez, 1984: On the dynamics of stratocumulus formation and dissipation. *J. Atmos. Sci.*, **20**, 3052–3057.

Rangno, A. L. and P. V. Hobbs, 1991: Ice particle concentrations and precipitation development in small polar maritime cumuliform clouds. *Quarterly Journal of the Royal Meteorological Society*, **117 (497)**, 207–241.

Rasmussen, R. M., I. Geresdi, G. Thompson, K. Manning, and E. Karplus, 2002: Freezing drizzle formation in stably stratified layer clouds: The role of radiative cooling of cloud droplets, cloud condensation nuclei, and ice initiation. *Journal of the Atmospheric Sciences*, **59 (4)**, 837–860.

Richter, I. and C. R. Mechoso, 2004: Orographic influences on the annual cycle of namibian stratocumulus clouds. *Geophysical Research Letters*, **31 (24)**.

Richter, I. and C. R. Mechoso, 2006: Orographic influences on subtropical stratocumulus. *Journal of the Atmospheric Sciences*, **63 (10)**, 2585–2601, richter, I. Mechoso, C. R.

Riehl, H. and J. S. Malkus, 1957: On the heat balance and maintenance of circulation in the trades. *Quart. J. Roy. Meteorol. Soc.*, **83**, 21–29.

Riehl, H., T. C. Yeh, J. S. Malkus, and N. E. LaSeur, 1951: The north-east trade of the pacific ocean. *Quart. J. Roy. Meteorol. Soc.*, **77**, 598–626.

Roach, W. T., 1961: Some aircraft observations of fluxes of solar radiation in the atmosphere. *Q. J. R. Meteorol. Soc.*, **87 (373)**, 346–363.

Roach, W. T., R. Brown, S. J. Caughey, B. A. Crease, and A. Slingo, 1982: A field-study of nocturnal stratocumulus .1. mean structure and budgets. *Quarterly Journal of the Royal Meteorological Society*, **108 (455)**, 103–123.

Roach, W. T. and A. Slingo, 1979: A high resolution infrared radiative transfer scheme to study the interaction of radiation with cloud. *Q. J. R. Meteorol. Soc.*, **105**, 603–614.

Rogers, D. P. and D. Koracin, 1992: Radiative transfer and turbulence in the cloud-topped marine atmospheric boundary layer. *J. Atmos. Sci.*, **49**, 1473–1486.

Rossow, W. B., C. Delo, and B. Cairns, 2002: Implications of the observed mesoscale variations of clouds for earth's radiation budget. *J. Climate*, **15**, 557–585.

Rossow, W. B. and W. B. Garder, 1993: Cloud detection using satellite measurements of infrared and visible radiances for ISCCP. *J. Climate*, **6**, 2341–2369.

Rothermel, J. and E. M. Agee, 1980: Aircraft investigation of mesoscale cellular convection during amtex75. *J. Atmos. Sci.*, **37**, 1027–1040.

Rozendaal, M. A., C. B. Leovy, and S. A. Klein, 1995: An observational study of the diurnal cycle of marine stratiform cloud. *J. Climate*, **8**, 1795–1809.

Rutledge, S. A. and P. V. Hobbs, 1983: The mesoscale and microscale structure and organization of clouds and precipitation in mid-latitude cyclones .8. a model for the seeder-feeder process in warm-frontal rainbands. *J. Atmos. Sci.*, **40 (5)**, 1185–1206.

Sandu, I., B. Stevens, and R. Pincus, 2010: On the transitions in marine boundary layer cloudiness. *Atmos. Chem. Phys. Disc.*, submitted.

Savic-Jovcic, V. and B. Stevens, 2008: The structure and mesoscale organization of precipitating stratocumulus. *J. Atmos. Sci.*, **65**, 1587–1605.

Schubert, W. H., 1976: Experiments with lilly's cloud-topped mixed layer model. *J. Atmos. Sci.*, **33**, 436–446.

Schubert, W. H., J. S. Wakefield, E. J. Steiner, and S. K. Cox, 1979a: Marine stratocumulus convection. Part I: Governing equations and horizontally homogeneous solutions. *J. Atmos. Sci.*, **36**, 1286–1307.

Schubert, W. H., J. S. Wakefield, E. J. Steiner, and S. K. Cox, 1979b: Marine stratocumulus convection. Part II: Horizontally inhomogeneous solutions. *J. Atmos. Sci.*, **36**, 1308–1324.

Sears-Collins, A. L., D. M. Schultz, and R. H. Johns, 2006: Spatial and temporal variability of nonfreezing drizzle in the united states and canada. *Journal of Climate*, **19 (15)**, 3629–3639.

Serpetzoglou, E., B. A. Albrecht, P. Kollias, and C. W. Fairall, 2008: Boundary layer, cloud, and drizzle variability in the southeast pacific stratocumulus regime. *Journal of Climate*, **21 (23)**, 6191–6214.

Shao, Q. and D. A. Randall, 1996: Closed mesoscale cellular convection driven by cloud-top radiative cooling. *J. Atmos. Sci.*, **53**, 2144–2165.

Sharon, T. M., B. A. Albrecht, H. Jonsson, P. Minnis, M. M. Khaiyer, T. M. VanReken, J. Seinfeld, and R. Flagan, 2006: Aerosol and cloud microphysical characteristics of rifts and gradients in maritime stratocumulus clouds. *J. Atmos. Sci.*, **63**, 983–997.

Siebert, H., K. Lehmann, and M. Wendisch, 2006: Observations of small-scale turbulence and energy dissipation rates in the cloudy boundary layer. *Journal of the Atmospheric Sciences*, **63 (5)**, 1451–1466.

Siebesma, A., et al., 2004: Cloud representation in general-circulation models over the northern Pacific Ocean: A EUROCS intercomparison study. *Quart. J. Roy. Meteorol. Soc.*, **130**, 3245–3267.

Siems, S., C. Bretherton, M. Baker, S. Shy, and R. Breidenthal, 1990: Buoyancy reversal and cloud-top entrainment instability. *Q. J. R. Meteorol. Soc.*, **116 (493)**, 705–739.

Siems, S. T., D. H. Lenschow, and C. S. Bretherton, 1993: A numerical study of the interaction between stratocumulus and the air ovserlying it. *J. Atmos. Sci.*, **50**, 3663–3676.

Slingo, A., 1989: A gcm parameterization for the shortwave properties of water clouds. *J. Atmos. Sci.*, **46**, 1419–1427.

Slingo, A., 1990: Sensitivity of the earth's radiation budget to changes is low clouds. *Nature*, **343**, 49–51.

Slingo, A., R. Brown, and C. L. Wrench, 1982a: A field-study of nocturnal stratocumulus .3. high-resolution radiative and microphysical observations. *Q. J. R. Meteorol. Soc.*, **108 (455)**, 145–165.

Slingo, A., S. Nicholls, and J. Schmetz, 1982b: Aircraft observations of marine stratocumulus during jasin. *Quart. J. Roy. Meteorol. Soc.*, **108**, 833–856.

Slingo, A. and H. M. Schrecker, 1982: On the shortwave radiative properties of stratiform water clouds. *Quart. J. Roy. Meteorol. Soc.*, **108**, 407–426.

Slingo, J. M., 1987: The development and verification of a cloud prediction scheme for the ECMWF model. *Quart. J. Roy. Meteorol. Soc.*, **113**, 899–927.

Snider, J. R., S. Guibert, J. L. Brenguier, and J. P. Putaud, 2003: Aerosol activation in marine stratocumulus clouds: 2. kohler and parcel theory closure studies. *Journal of Geophysical Research-Atmospheres*, **108 (D15)**.

Sorooshian, A., G. Feingold, M. Lebsock, H. Jiang, and G. Stephens, 2009: On the precipitation susceptibility of clouds to aerosol perturbations. *Geophys. Res. Lett.*, **36**, L13 803, doi:10.1029/2009GL038 993.

Squires, P., 1952: The growth of cloud drops by condensation. 1: General characteristics. *Aust. J. Sci. Res.*, **5**, 59–86.

Stage, S. A. and J. A. Businger, 1981: A model for entrainment into a cloud-topped marine boundary-layer .1. model description and application to a cold-air outbreak episode. *Journal of the Atmospheric Sciences*, **38 (10)**, 2213–2229.

Stephens, G. L., 1978a: Radiation profiles in extended water clouds .1. theory. *J. Atmos. Sci.*, **35 (11)**, 2111–2122.

Stephens, G. L., 1978b: Radiation profiles in extended water clouds .2. parameterization schemes. *J. Atmos. Sci.*, **35 (11)**, 2123–2132.

Stephens, G. L., S. Ackerman, and E. A. Smith, 1984: A shortwave parameterization revised to improve cloud absorption. *Journal of the Atmospheric Sciences*, **41 (4)**, 687–690.

Stephens, G. L. and T. J. Greenwald, 1991: Observations of the earth's radiation budget in relation to atmospheric hydrology. part ii: Cloud effects and cloud feedback. *J. Geophys. Res*, **96**, 15 325–15 340.

Stephens, G. L., G. W. Paltridge, and C. M. R. Platt, 1978: Radiation profiles in extended water clouds .3. observations. *J. Atmos. Sci.*, **35 (11)**, 2133–2141.

Stevens, B., 2000: Cloud-transitions and decoupling in shear-free stratocumulus topped boundary layers. *Geophys. Res. Lett.*, **27**, 2557–2560.

Stevens, B., 2002: Entrainment in stratocumulus topped mixed layers. *Quart. J. Roy. Meteorol. Soc.*, **128**, 2663–2690.

Stevens, B., 2005: Atmospheric moist convection. *Annu. Rev. Earth Planet. Sci.*, **32**, 605–643.

Stevens, B., 2010: Cloud top entrainment instability? *J. Fluid. Mech.*, **660**, 1–4, doi:10.1017/S0022112010003575.

Stevens, B., A. Beljaars, S. Bordoni, C. Holloway, M. Kohler, S. Krueger, V. Savic-Jovcic, and Y. Y. Zhang, 2007: On the structure of the lower troposphere in the summertime stratocumulus regime of the northeast pacific. *Monthly Weather Review*, **135 (3)**, 985–1005, stevens, Bjorn Beljaars, Anton Bordoni, Simona Holloway, Christopher Koehler, Martin Krueger, Steven Savic-Jovcic, Verica Zhang, Yunyan.

Stevens, B. and J.-L. Brenguier, 2008: Cloud controlling factors - low clouds, J. Heintzenberg and R. J. Charlson (eds.). Tech. rep., Ernst Strungmann Forum.

Stevens, B., W. R. Cotton, G. Feingold, and C.-H. Moeng, 1998: Large-eddy simulations of strongly precipitating, shallow, stratocumulus-topped boundary layers. *J. Atmos. Sci.*, **55**, 3616–3638.

Stevens, B., J. J. Duan, J. C. McWilliams, M. Munnich, and J. D. Neelin, 2002: Entrainment, rayleigh friction, and boundary layer winds over the tropical pacific. *Journal of Climate*, **15 (1)**, 30–44.

Stevens, B., G. Vali, K. Comstock, R. Wood, M. VanZanten, P. H. Austin, C. S. Bretherton, and D. H. Lenschow, 2005a: Pockets of open cells (POCs) and drizzle in marine stratocumulus. *Bull. Am. Meteor. Soc.*, **86**, 51–57.

Stevens, B., et al., 2003: Dynamics and Chemistry of Marine Stratocumulus - DYCOMS II. *Bull. Amer. Meteor. Soc.*, **84**, 579–593.

Stevens, B., et al., 2005b: Evaluation of large-eddy simulations via observations of nocturnal marine stratocumulus. *Monthly Weather Review*, **133 (6)**, 1443–1462.

Stewart, D. A. and O. M. Essenwanger, 1982: A survey of fog and related optical propagation characteristics. *Revs. Geophys.*, **20 (3)**, 481–495.

Sundararajan, R. and M. Tjernstrom, 2000: Observations and simulations of a non-stationary coastal atmospheric boundary layer. *Q. J. R. Meteorol. Soc.*, **126 (563)**, 445–476, part B.

Szczodrak, M., P. H. Austin, and P. B. Krummel, 2001: Variability of optical depth and effective radius in marine stratocumulus clouds. *J. Atmos. Sci.*, **58**, 2912–2926.

Taylor, J. P., J. M. Edwards, M. D. Glew, P. Hignett, and A. Slingo, 1996: Studies with a flexible new radiation code .2. comparisons with aircraft short-wave observations. *Quarterly Journal of the Royal Meteorological Society*, **122 (532)**, 839–861, part B.

Tennekes, H. and J. L. Lumley, 1972: *A first course in turbulence*. MIT Press.

Tjemkes, S. A. and P. G. Duynkerke, 1989: The nocturnal boundary-layer - model-calculations compared with observations. *J. Appl. Meteorol.*, **28 (3)**, 161–175.

Tjernstrom, M. and A. Rune, 2003: The structure of gradually transforming marine stratocumulus during the astex first lagrangian experiment. *Q. J. R. Meteorol. Soc.*, **129 (589)**, 1071–1100, part C.

Tripoli, G. J. and W. R. Cotton, 1980: A numerical investigation of several factors contributing to the observed variable density of deep convection over south florida. *J. App. Meteorol.*, **19**, 1037–1063.

Turton, J. D. and S. Nicholls, 1987: A study of the diurnal variation of stratocumulus using a multiple mixed layer model. *Q. J. R. Meteorol. Soc.*, **113**, 969–1009.

Twohy, C. H., M. D. Petters, J. R. Snider, B. Stevens, W. Tahnk, M. Wetzel, L. Russell, and F. Burnet, 2005: Evaluation of the aerosol indirect effect in marine stratocumulus clouds: Droplet number, size, liquid water path, and radiative impact. *Journal of Geophysical Research-Atmospheres*, **110 (D8)**.

Twomey, S., 1959: The nuclei of natural cloud formation. part II: The supersaturation in natural clouds and the variation of cloud droplet concentration. *Geofis. Pura. Appl.*, **43**, 243–249.

Twomey, S., 1974: Pollution and the planetary albedo. *Atmos. Env.*, **8**, 1251–1256.

Twomey, S., 1977: The influence of pollution on the shortwave albedo of clouds. *J. Atmos. Sci.*, **34**, 1149–1152.

Twomey, S. and C. F. Bohren, 1980: Simple approximations for calculations of absorption in clouds. *J. Atmos. Sci.*, **37 (9)**, 2086–2094.

Vaillancourt, P. A. and M. K. Yau, 2000: Review of particle-turbulence interactions and consequences for cloud physics. *Bulletin of the American Meteorological Society*, **81 (2)**, 285–298.

Vali, G., R. D. Kelly, J. French, H. S D. Leon, and A. McIntosh, R. E. Pazmany, 1998: Finescale structure and microphysics of coastal stratus. *J. Atmos. Sci.*, **55**, 3540–3564.

Van Zanten, M. C. and P. G. Duynkerke, 2002: Radiative and evaporative cooling in the entrainment zone of stratocumulus - the role of longwave radiative cooling above cloud top. *Boundary-Layer Meteorology*, **102 (2)**, 253–280.

Van Zanten, M. C. and B. Stevens, 2005: Observations of the structure of heavily precipitating marine stratocumulus. *J. Atmos. Sci.*, **62**, 4327–4342.

Van Zanten, M. C., B. Stevens, G. Vali, and D. Lenschow, 2005: Observations of drizzle in nocturnal marine stratocumulus. *J. Atmos. Sci.*, **62**, 88–106.

vanZanten, M. C., P. G. Duynkerke, and J. W. M. Cuijpers, 1999: Entrainment parameterization in convective boundary layers. *Journal of the Atmospheric Sciences*, **56 (6)**, 813–828.

Vohl, O., S. K. Mitra, S. Wurzler, K. Diehl, and H. R. Pruppacher, 2007: Collision efficiencies empirically determined from laboratory investigations of collisional growth of small raindrops in a laminar flow field. *Atmospheric Research*, **85 (1)**, 120–125, vohl, O. Mitra, S. K. Wurzler, S. Diehl, K. Pruppacher, H. R.

Walter, B. A., 1980: Wintertime observations of roll clouds over the bering sea. *Monthly Weather Review*, **108 (12)**, 2024–2031.

Wang, H. and G. Feingold, 2009: Modeling mesoscale cellular structures and drizzle in marine stratocumulus. Part I: Impact of drizzle on the formation and evolution of open cells. *J. Atmos. Sci.*, **66**, 3237–3255.

Wang, J. H., W. B. Rossow, T. Uttal, and M. Rozendaal, 1999: Variability of cloud vertical structure during astex observed from a combination of rawinsonde, radar, ceilometer, and satellite. *Monthly Weather Review*, **127 (10)**, 2484–2502.

Wang, Q. and B. A. Albrecht, 1994: Observations of cloud-top entrainment in marine stratocumulus clouds. *Journal of the Atmospheric Sciences*, **51 (11)**, 1530–1547.

Wang, Q. and D. H. Lenschow, 1995: An observational study of the role of penetrating cumulus in a marine stratocumulus-topped boundary layer. *J. Atmos. Sci.*, **52**, 2902–2922.

Wang, S. and B. A. Albrecht, 1986: A stratocumulus model with an internal circulation. *Journal of the Atmospheric Sciences*, **43**, 2374–2391.

Wang, S. and Q. Wang, 1994: Roles of drizzle in a one-dimensional 3rd order turbulence closure model of the nocturnal stratus-topped marine boundary layer. *J. Atmos. Sci.*, **51**, 1559–1576.

Wang, S., Q. Wang, and G. Feingold, 2003: Turbulence, condensation, and liquid water transport in numerically simulated nonprecipitating stratocumulus clouds. *Journal of the Atmospheric Sciences*, **60**, 262–278.

Wang, S. P., J. C. Golaz, and Q. Wang, 2008: Effect of intense wind shear across the inversion on stratocumulus clouds. *Geophysical Research Letters*, **35 (15)**, 6.

Warren, S. G., C. J. Hahn, J. London, R. M. Chervin, and R. L. Jenne, 1986: Global distribution of total cloud cover and cloud types over land. NCAR Technical Note NCAR/TN-273+STR 29pp+200 maps, National Center for Atmospheric Research, Boulder, CO.

Warren, S. G., C. J. Hahn, J. London, R. M. Chervin, and R. L. Jenne, 1988: Global distribution of total cloud cover and cloud types over ocean. NCAR Technical Note NCAR/TN-317+STR 42pp+170 maps, National Center for Atmospheric Research, Boulder, CO.

Weaver, C. J. and R. Pearson, 1990: Entrainment instability and vertical motion as causes of stratocumulus breakup. *Quarterly Journal of the Royal Meteorological Society*, **116 (496)**, 1359–1388.

Weaver, C. P. and V. Ramanathan, 1997: Relationships between large-scale vertical velocity, static stability, and cloud radiative forcing over northern hemisphere extratropical oceans. *Journal of Climate*, **10 (11)**, 2871–2887.

Weng, F. Z. and N. C. Grody, 1994: Retrieval of cloud liquid water using the special sensor microwave imager (ssm/i). *Journal of Geophysical Research-Atmospheres*, **99 (D12)**, 25 535–25 551.

Weng, F. Z., N. C. Grody, R. Ferraro, A. Basist, and D. Forsyth, 1997: Cloud liquid water climatology from the special sensor microwave/imager. *Journal of Climate*, **10 (5)**, 1086–1098.

Wood, R., 2005a: Drizzle in stratiform boundary layer clouds: Part I. Vertical and horizontal structure. *J. Atmos. Sci.*, **62**, 3011–3033.

Wood, R., 2005b: Drizzle in stratiform boundary layer clouds: Part II. Microphysical aspects. *J. Atmos. Sci.*, **62**, 3034–3050.

Wood, R., 2006: The rate of loss of cloud droplets by coalescence in warm clouds. *J. Geophys. Res.*, **111 (D21205)**, doi:10.1029/2006JD007 553.

Wood, R., 2007: Cancellation of aerosol indirect effects in marine stratocumulus through cloud thinning. *J. Atmos. Sci.*, **64**, 2657–2669.

Wood, R. and P. N. Blossey, 2005: Comments on "Parameterization of the autoconversion process. part I: Analytical formation of the Kessler-type parameterizations. *J. Atmos. Sci.*, **62**, 3003–3006.

Wood, R., C. Bretherton, D. Leon, A. Clarke, P. Zuidema, G. Allen, and H. Coe, 2010: An aircraft case study of the spatial transition from closed to open mesoscale cellular convection over the southeast pacific. *Atmos. Chem. Phys.*, submitted.

Wood, R. and C. S. Bretherton, 2004: Boundary layer depth, entrainment and decoupling in the cloud-capped subtropical and tropical marine boundary layer. *J. Climate*, **17**, 3576–3588.

Wood, R. and C. S. Bretherton, 2006: On the relationship between stratiform low cloud cover and lower-tropospheric stability. *J. Climate*, **19**, 6425–6432.

Wood, R., C. S. Bretherton, and D. L. Hartmann, 2002a: Diurnal cycle of liquid water path over the subtropical and tropical oceans. *Geophys. Res. Lett.*, **29**, 2092, doi:10.1029/2002GL015 371.

Wood, R., K. K. Comstock, C. S. Bretherton, C. Cornish, J. Tomlinson, D. R. Collins, and C. Fairall, 2008: Open cellular structure in marine stratocumulus sheets. *J. Geophys. Res.*, **113 (D12207)**, doi:10.1029/2007JD009 596.

Wood, R., P. R. Field, and W. R. Cotton, 2002b: Autoconversion rate bias in boundary layer cloud parameterizations. *Atmos. Res.*, **65**, 109–128.

Wood, R. and D. L. Hartmann, 2006: Spatial variability of liquid water path in marine boundary layer clouds: The importance of mesoscale cellular convection. *J. Climate*, **19**, 1748–1764.

Wood, R., M. Köhler, R. Bennartz, and C. O'Dell, 2009a: The diurnal cycle of surface divergence over the global oceans. *Q. J. R. Meteorol. Soc.*, **135**, 1484–1493.

Wood, R., T. Kubar, and D. L. Hartmann, 2009b: Understanding the importance of microphysics and macrophysics for warm rain in marine low clouds: Part ii. heuristic models of rain formation. *J. Atmos. Sci.*, **66**, 2973–2990.

Wood, R. and J. P. Taylor, 2001: Liquid water path variability in unbroken marine stratocumulus. *Quart. J. Roy. Meteorol. Soc.*, **127**, 2635–2662.

Wyant, M. C., C. S. Bretherton, J. T. Bacmeister, J. T. Kiehl, I. M. Held, Z. M. S. A. Klein, and B. A. Soden, 2006: A comparison of tropical cloud properties and their response to climate change in three agcms sorted into regimes using mid-tropospheric vertical velocity. *Clim. Dyn.*, **27 (2-3)**, 261–279.

Wyant, M. C., C. S. Bretherton, H. A. Rand, and D. E. Stevens, 1997: Numerical simulations and a conceptual model of the stratocumulus to trade cumulus transition. *J. Atmos. Sci.*, **54**, 168–192.

Wyngaard, J. C. and R. A. Brost, 1984: Top-down and bottom-up diffusion of a scalar in the convective boundary layer. *J. Atmos. Sci.*, **41**, 102–112.

Xiao, H., C.-M. Wu, and C. R. Mechoso, 2010: Buoyancy reversal, decoupling and the transition from stratocumulus-topped to trade-wind cumulus-topped marine boundary laye. *Clim. Dyn.*, in press.

Xu, H., Y. Wang, and S. P. Xie, 2004: Effects of the Andes on eastern Pacific climate: A regional atmospheric model study. *J. Climate*, **17**, 589–602.

Xue, H., G. Feingold, and B. Stevens, 2008a: Aerosol effects on clouds, precipitation, and the organization of shallow cumulus convection. *J. Atmos. Sci.*, **65**, 392–406.

Xue, Y., L. P. Wang, and W. W. Grabowski, 2008b: Growth of cloud droplets by turbulent collision-coalescence. *Journal of the Atmospheric Sciences*, **65 (2)**, 331–356, xue, Yan Wang, Lian-Ping Grabowski, Wojciech W.

Yamaguchi, T. and D. A. Randall, 2008: Large-eddy simulation of evaporatively driven entrainment in cloud-topped mixed layers. *J. Atmos. Sci.*, **65**, 1481–1504.

Yang, S. and E. A. Smith, 2006: Mechanisms for diurnal variability of global tropical rainfall observed from TRMM. *J. Climate*, **19**, 5190–5226.

Young, G. S. and T. D. Sikora, 2003: Mesoscale stratocumulus bands caused by gulf stream meanders. *Monthly Weather Review*, **131 (9)**, 2177–2191.

Yum, S. S. and J. G. Hudson, 2002: Maritime/continental microphysical contrasts in stratus. *Tellus*, **B54**, 61–73.

Yum, S. S. and J. G. Hudson, 2004: Wintertime/summertime contrasts of cloud condensation nuclei and cloud microphysics over the southern ocean. *Journal of Geophysical Research-Atmospheres*, **109 (D6)**.

Zhang, M. H. and . coauthors, 2005: Comparing clouds and their seasonal variations in 10 atmospheric general circulation models with satellite measurements. *J. Geophys. Res.*, **110**, D15S02, doi:10.1029/2004JD005 021O.

Zhang, Y., B. Stevens, B. Medeiros, and M. Ghil, 2009: Low-cloud fraction, lower-tropospheric stability, and large-scale divergence. *J. Climate*, **22**, 4827–4844.

Zhu, P., B. Albrecht, and J. Gottschalck, 2001: Formation and development of nocturnal boundary layer clouds over the southern great plains. *J. Atmos. Sci.*, **58**, 1409–1426.

Zuidema, P., F. C. E. Westwater, and D. Hazen, 2005: Ship-based liquid water path estimates in marine stratus. *J. Geophys. Res.*, in press.

Zuidema, P. and D. L. Hartmann, 1995: Satellite determination of stratus cloud microphysical properties. *J. Climate*, **8**, 1638–1656.